

MIXED MATRIX MEMBRANES

**A NEW PLATFORM FOR
ENZYMATIC REACTIONS**

This work was financially supported by The Netherlands Organization for Scientific Research (NWO).

Mixed Matrix Membranes. A new platform for enzymatic reactions

Ph.D. Thesis, University of Twente

ISBN: 978-90-365-2790-3

© João Miguel de Sousa André, Enschede (The Netherlands), 2009

No part of this work may be reproduced by print, photocopy or any other means without permission of the author.

Printed by Wöhrmann Print Service

Mixed Matrix Membranes

A new platform for enzymatic reactions

DISSERTATION

to obtain
the doctor's degree at the University of Twente
on the authority of the rector magnificus,
prof. dr. H. Brinksma
on account of the decision of the graduation committee,
to be publicly defended
on Friday 6th February 2009 at 16:45

by

João Miguel de Sousa André

Born on 15th December 1975

In Leiria, Portugal

This dissertation has been approved by:

Promoter: Prof. Dr.-Ing. M. Wessling

Assistant-promoter: Dr. Ing. Z. Borneman

Para o meu avô Zé
e para a minha avó Júlia

TABLE OF CONTENTS

CHAPTER 1 - INTRODUCTION	1
1.1 GENERAL INTRODUCTION	1
1.2 OUTLINE OF THE THESIS	5
CHAPTER 2	6
CHAPTER 3	6
CHAPTER 4	6
CHAPTER 5	7
CHAPTER 6	7
CHAPTER 7	8
REFERENCES	8
CHAPTER 2 - INTRODUCTION TO ENZYME IMMOBILIZATION	13
2.1 IMMOBILIZATION METHODS	13
2.1.1 IMMOBILIZATION VIA BINDING	14
2.1.2 IMMOBILIZATION VIA ENTRAPMENT OR ENCAPSULATION	22
2.1.3 IMMOBILIZATION VIA CROSS-LINKING	26
2.2 CARRIER TYPES	28
2.3 MIXED MATRIX MEMBRANES	30
2.4 CONCLUSIONS	31
REFERENCES	32
CHAPTER 3 - NOVEL MEMBRANES FOR ENZYMATIC CONVERSION	41
ABSTRACT	41
3.1 INTRODUCTION	43
3.2 EXPERIMENTAL	44
3.2.1 MATERIALS	44
3.2.2 PARTICLE MODIFICATION	45
3.2.3 EUPERGIT [®] CHARACTERIZATION	45
3.2.4 MIXED MATRIX MEMBRANES	46
3.2.5 TRYPSIN IMMOBILIZATION	47
3.3 RESULTS AND DISCUSSION	50
3.3.1 OXIRANE STABILITY IN EUPERGIT [®] PARTICLES	50

3.3.2 MIXED MATRIX MEMBRANE CHARACTERIZATION	51
3.3.3 STATIC MEASUREMENTS	52
3.3.4 DYNAMIC MEASUREMENTS	54
3.3.5 MMM'S CONTAINING CHEMICALLY MODIFIED EUPERGIT®	55
3.4 CONCLUSIONS	59
REFERENCES	60

CHAPTER 4 - ENZYMATIC CONVERSION
USING MIXED MATRIX HOLLOW FIBERS **63**

ABSTRACT	63
4.1 INTRODUCTION	65
4.2 EXPERIMENTAL	66
4.2.1 MATERIALS AND METHODS	66
4.2.2 PARTICLE MODIFICATION	67
4.2.3 MIXED MATRIX HOLLOW-FIBERS	68
4.2.5 TRYPSIN IMMOBILIZATION	70
4.2.6 ACTIVITY MEASUREMENTS	71
4.3 RESULTS AND DISCUSSION	72
4.3.1 FIBER PRODUCTION AND CHARACTERIZATION	72
4.3.4 DYNAMIC MEASUREMENTS	77
4.3.5 INFLUENCE OF SUPPORT ON DYNAMIC ACTIVITY	79
4.4 CONCLUSIONS	80
REFERENCES	81

CHAPTER 5 - ENZYMATIC CONVERSION
USING ION-EXCHANGE MMHF **85**

ABSTRACT	85
5.1 INTRODUCTION	87
5.2 EXPERIMENTAL	89
5.2.1 MATERIALS	89
5.2.2 FIBER SPINNING	90
5.2.3 SCANNING ELECTRON MICROSCOPY (SEM)	91
5.2.4 STATIC ADSORPTION	92
5.2.5 MODULE PREPARATION	92
5.2.6 DYNAMIC ADSORPTION	93
5.2.7 ENZYMATIC ACTIVITY	93
5.3 RESULTS AND DISCUSSION	94
5.3.1 FIBER STRUCTURE	94

5.3.2 STATIC ADSORPTION	96
5.3.3 DYNAMIC ADSORPTION	99
5.3.4 DYNAMIC ACTIVITIES	104
5.4 CONCLUSIONS	106
REFERENCES	107

CHAPTER 6 - GLUCOSE OXIDASE IMMOBILIZATION
IN COVALENT MIXED MATRIX HOLLOW-FIBERS **111**

ABSTRACT	111
6.1 INTRODUCTION	113
6.2 EXPERIMENTAL	114
6.2.1 MATERIALS	114
6.2.2 DYNAMIC IMMOBILIZATION	115
6.2.3 ENZYMATIC ACTIVITY	116
6.3 RESULTS AND DISCUSSION	117
6.3.1 MEMBRANE MORPHOLOGY	117
6.3.2 DYNAMIC IMMOBILIZATION	117
6.3.3 DYNAMIC ACTIVITY MEASUREMENTS	119
6.3.4 COMPARISON WITH MMF WITH CATION-EXCHANGE FUNCTIONALITY	120
6.4 CONCLUSIONS	122
REFERENCES	123

SUMMARY **127**

SAMENVATTING **131**

ACKNOWLEDGMENTS **135**

1

Introduction

1.1 GENERAL INTRODUCTION

Membranes have first been introduced as materials used in reaction engineering over three decades ago and have been growing in importance ever since. Membrane processes are presently used in a wide range of applications which is continuously growing. Membrane processes can be divided according to the function they perform, which permits to identify three main categories of membranes: membrane separators, membrane contactors and membrane (bio)reactors [1].

Membrane separators act, as indicated by the name, as a semipermeable barrier between two phases. Membranes are able to discriminate by size or affinity between the different components in a feed stream. In figure 1.1, a schematic representation of a membrane separator is presented.

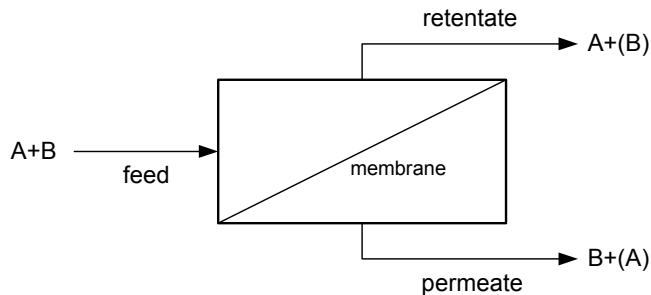


Figure 1.1 – Schematic representation of a membrane separator. A two component feed stream is separated by the membrane. The components between brackets indicate residual trace components that are left behind in the feed stream or non-selectively passed through the membrane into the permeate stream.

Membrane contactors are systems where the membrane function is to facilitate diffusive mass transport between two contacting phases avoiding dispersion of one phase into the other. The membrane acts mainly as an interface which provides a very high area per volume ratio. A schematic representation of a membrane contactor system is visualized in figure 1.2.

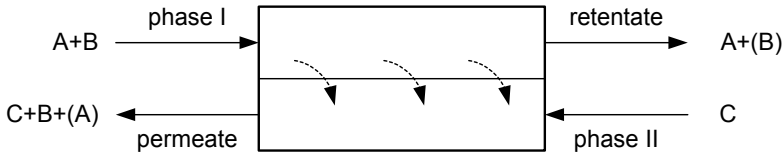


Figure 1.2 – Schematic representation of the extraction of a component from a binary mixture using a membrane contactor in counter-current mode. The components between brackets are trace components in the respective stream. The process may also be used in co-current mode.

Membrane reactors and bioreactors were introduced with the goal of coupling the separation properties of a membrane with a chemical or biochemical reaction. This coupling is made with the purpose of introducing a separation step simultaneously with the reaction in order to remove an endproduct and thus shift the reaction equilibrium in the direction of the product side. In these processes, a catalyst may be incorporated in the reaction phase, on the membrane surface or in the membrane wall. A schematic representation of a membrane (bio)reactor is depicted in figure 1.3.

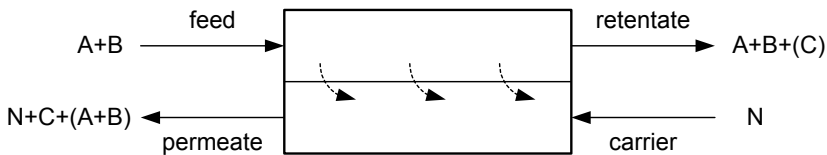


Figure 1.3 – Schematic representation of a membrane (bio)reactor in counter-current mode. The product a reaction mixture is selectively transported through a membrane in order to shift the equilibrium. In certain cases, a carrier phase N may be used to collect the product. The brackets refer to trace components in the respective stream. The process may also be used in co-current mode.

In some cases where the membrane acts as a support for a catalyst or as the catalyst itself, the feed stream is permeated through the membrane in order to promote the desired reaction and there is no retentate stream. This kind of systems is explored in this thesis. A schematic representation of such a process is presented in figure 1.4.

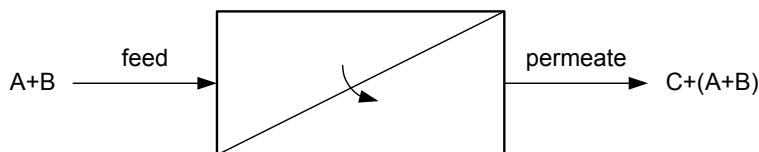


Figure 1.4 – Schematic representation of a membrane (bio)reactor where the feed is permeated through the membrane wall without recovery of retentate. The permeate stream contains both the product and the unreacted reagents.

The fact that membranes can be used to combine reaction and separation processes in a single step is what first attracted the attention and since then several different concepts of membrane (bio)reactors, also called catalytic membrane reactors (CMR's) have appeared in literature. CMR's present important advantages over alternative approaches in unit operations, such as lower investment costs, lower energy requirements (pumps, heating, cooling) and improved contact between two reagent species [2].

Initially, most applications concerning CMR's concerned the use of inorganic membranes. This was due to the fact that most reactions took place at elevated pressure and temperature [3-5]. Also the possibility of using palladium or palladium alloys as catalysts for hydrogenation and dehydrogenation reactions which can be incorporated into or coated onto the membranes [6, 7] made the use of inorganic materials highly attractive. Inorganic reactive membranes have been used in diverse applications, such as production of syngas [8], steam reforming [9, 10] or for use in refinery products [11].

The use of polymeric materials as the support for reactive membranes is justified by the higher availability of different chemistries and the low costs that polymers present compared to inorganic ceramic or metallic materials. Also the possibility to fine-tune the morphology and the easy preparation of polymeric membranes are seen as big advantages. Meanwhile, the incorporation of ceramic or metallic catalysts in polymeric membranes to achieve the catalytic characteristics of inorganic materials is still possible.

By far, the most common reactions to be applied with CMR's are hydrogenation reactions [12]. This is equally true for polymeric membranes, for which most publications concerning reactive membranes involve the incorporation or coating of palladium in a polymeric membrane for use in hydrogenation reactions [13, 14]. Also the use of homogeneous catalysts which can be heterogenized by incorporation in membranes has been reported [15]. One of the most common applications using reactive membranes are, however, those involving esterification or transesterification reactions, where the inorganic materials are incorporated in the membrane or dispersed on the surface [16, 17] or with the catalytic capacity being given by functional groups in the polymeric matrix [18-20].

The most common application of CMR's found in literature is, however, in the field of enzymatically catalyzed reactions. In this case, enzymes are initially immobilized in a membrane and then used as the catalytic medium to perform biochemical conversions [21]. Enzyme immobilization can take place using different techniques, taking advantage of readily available functional groups or physical properties from the polymeric matrix [22, 23]. Alternatively, the membrane may be chemically modified in order to provide the desired functionality needed for enzyme immobilization [24-26] or to improve the immobilization process [27]. The membrane containing the immobilized enzymes can then be directly applied in bioconversions with high yield and specificity.

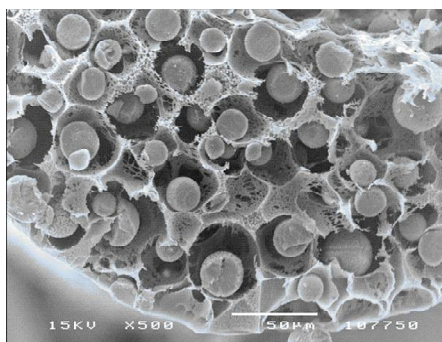


Figure 1.5 – Electron microscopic image of the cross-section of a solid porous polymer fiber with adsorptive chromatography beads embedded (SP Sepha-rose HP particles).

Mixed matrix membranes (MMM's) consist of a polymeric membrane in which functional particles are embedded. These membranes were first developed for gas transport and pervaporation, using zeolites embedded in a

dense polymeric membrane [28-31]. More recently, MMM's have been developed with a porous polymer having functional particles embedded. These new structures may find applications in the field of biotechnology, as media for protein adsorption [32, 33] and separation [34], blood purification [35, 36] and enzyme concentration [37, 38]. Figure 1.5 shows an example of a mixed matrix hollow-fiber.

A first catalytic proof-of-principle describing the incorporation of catalytic Pt/SiO₂ particles in a membrane was recently described by Radivojevic et al [39]. A schematic representation of the different fields of applications is found in figure 1.6. Due to the nature of the MMM platform technology, different types of functional particles can be incorporated in the polymeric matrix, both of which can be selected to fit specifically the desired application. This makes mixed matrix membranes uniquely suited for membrane based reactions in which the reactive sites are contained in the particles embedded in the polymeric matrix.

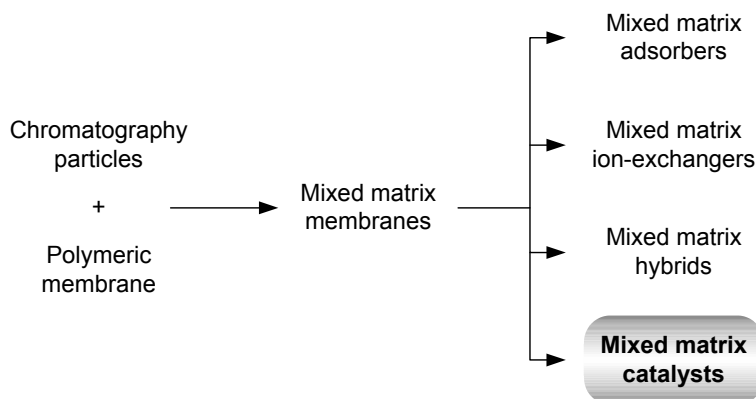


Figure 1.6 – Schematic representation of the mixed matrix membrane preparation and application concept.

1.2 OUTLINE OF THE THESIS

This thesis mainly focuses on bioconversions, where the enzymes are immobilized in mixed matrix membranes (MMM's) and then used as catalysts in bioreactions. Also the possibility of using MMM's as the bare catalyst medium for non-biological reactions is studied.

Chapter 2

An overview of the different methods used in enzyme immobilization is given. The applied techniques are explained and a discussion about the different support types is presented. Finally, the chapter contains a review on mixed matrix membranes, with the focus on factors determining the performance of these membranes.

Chapter 3

In this chapter, the preparation of a flat-sheet mixed matrix membrane is described. The membrane is prepared using EVAL₄₄ as the hydrophilic polymer and Eupergit® C and Eupergit® C250L as oxirane-based functional particles. The effect of the size reduction of the particles is investigated, as well as the influence of a chemical modification using ethylenediamine and activation with glutaraldehyde. The prepared MMM's were used for the immobilization of trypsin, which was chosen as model enzyme. The activity of immobilized trypsin was evaluated by reaction with L-Benzoyl-Arginine-Ethyl-Ester (BAEE). We demonstrated that the size reduction increases both the immobilization capacity and the enzymatic activity of immobilized trypsin. The use of MMM's showed higher enzymatic activities in all cases. MMM's containing modified Eupergit® particles show an increased immobilization capacity and a more than nine fold increase in enzymatic activity. A comparison between membrane-embedded modified Eupergit® particles and modified Eupergit® in a packed bed showed an overall better performance of the membrane based system. The highest enzymatic conversion rates were obtained with milled Eupergit® C particles that were chemically modified and embedded in a macro-porous membrane structure.

Chapter 4

The preparation of mixed matrix hollow-fiber (MMHF) membranes is described in this chapter. EVAL₄₄ is used as the polymeric matrix. Eupergit® C, chemically modified according to the reaction described in chapter 3 provides the functionality. Two particle size classes (20-40 µm and < 20 µm) were studied in order to evaluate the influence of particle size in the fiber morphology. The fiber structure was optimized by varying the solvent, additive and polymer ratio in the dope solution. Dynamic activity experiments of

immobilized trypsin proved that the prepared hollow-fibers allowed trypsin to retain a high degree of activity. The results showed a higher trypsin activity with fibers prepared with particles from the sieve fraction below 20 μm over those containing particles in the size class of 20-40 μm . Hollow-fiber MMM showed a four times increase in trypsin activity when compared to flat-sheet MMM and more than 35 times when compared to a packed bed system containing unmodified Eupergit[®] C particles.

Chapter 5

In this chapter, we prepared polyether sulfone (PES) MMHF's containing embedded strong cation-exchange Lewatit resins which were used for the physical immobilization of glucose oxidase (GOx). Static enzyme immobilization tests yielded high adsorption values at pH's below the isoelectric point (pI) of GOx. In this pH region, the adsorption followed a pseudo Langmuir-type behavior. We found that adsorption performed above the pI takes place preferentially via hydrophobic interactions. Dynamic GOx adsorption experiments resulted in the same values as those obtained in static experiments. Formation of GOx multilayers was observed for all applied pH's. Dynamic glucose conversion measurements showed that the immobilized GOx retains an appreciable activity after adsorption via both methods. GOx immobilized via hydrophobic interaction yielded the highest activity values. Enzymes immobilized via electrostatic interaction showed the highest multi-layer adsorption, resulting in a reduced enzyme-normalized enzymatic activity. The highest enzymatic activity was found for pH 5.0.

Chapter 6

In this chapter we describe the covalently binding of GOx to chemically modified Eupergit[®] C embedded in EVAL₄₄ fibers. The Eupergit[®] particle sizes were 20-40 and < 20 μm . GOx was immobilized in the fibers in dynamic mode and fibers containing the smallest particles show the highest immobilization capacity. The activity of immobilized enzyme was evaluated by dynamic conversion of glucose, with the highest glucose conversion yields being obtained for fibers with bigger particles. The results further showed that GOx covalently immobilized in EVAL/Eupergit[®] fibers has a lower enzymatic activity than GOx that is physically immobilized in Polyether Sulfone (PES) fibers containing strong cation exchange (SCIEX) resins.

Chapter 7

In this chapter, the use of mixed matrix PES hollow-fiber membranes containing Lewatit 112WS strong cation-exchange resins as a catalyst for the esterification reaction of ethanol and acetic acid is validated. The MMHF catalysis performance was compared to that resins in batch mode and incorporated in a packed bed by means of a theoretical model to describe the reaction kinetics. The results showed a more than twice increase in catalytic capacity by MMHF's when compared to those of the other systems.

REFERENCES

1. Mulder, M.H.V., *Basic Principles of Membrane Technology*. 1991, Dordrecht, The Netherlands: Kluwer.
2. Vankelecom, I.F.J., *Polymeric Membranes in Catalytic Reactors*. Chem. Rev., 2002. **102**(10): p. 3779.
3. Dong, H., et al., *Investigation on POM reaction in a new perovskite membrane reactor*. Catalysis Today, 2001. **67**(1-3): p. 3.
4. Hsieh, H.P., *Inorganic Membrane Reactors*. Catalysis Reviews, 1991. **33**(1): p. 1.
5. Ross, J.R.H. and E. Xue, *Catalysis with membranes or catalytic membranes?* Catalysis Today, 1995. **25**(3-4): p. 291.
6. Dittmeyer, R., V. Höllein, and K. Daub, *Membrane reactors for hydrogenation and dehydrogenation processes based on supported palladium*. Journal of Molecular Catalysis A: Chemical, 2001. **173**(1-2): p. 135.
7. Li, A., W. Liang, and R. Hughes, *Characterisation and permeation of palladium/stainless steel composite membranes*. Journal of Membrane Science, 1998. **149**(2): p. 259.
8. Jin, W., et al., *Experimental and simulation study on a catalyst packed tubular dense membrane reactor for partial oxidation of methane to syngas*. Chemical Engineering Science, 2000. **55**(14): p. 2617.
9. Tsuru, T., et al., *Catalytic Membrane Reaction for Methane Steam Reforming Using Porous Silica Membranes*. Separation Science and Technology, 2001. **36**(16): p. 3721.
10. Oklany, J.S., K. Hou, and R. Hughes, *A simulative comparison of dense and microporous membrane reactors for the steam reforming of methane*. Applied Catalysis A: General, 1998. **170**(1): p. 13.

11. Armor, J.N., *Applications of catalytic inorganic membrane reactors to refinery products*. Journal of Membrane Science, 1998. **147**(2): p. 217.
12. Dittmeyer, R., K. Svajda, and M. Reif, *A Review of Catalytic Membrane Layers for Gas/Liquid Reactions*. Topics in Catalysis, 2004. **29**(1): p. 3.
13. Gao, H., et al., *Catalytic polymeric hollow-fiber reactors for the selective hydrogenation of conjugated dienes*. Journal of Membrane Science, 1995. **106**(3): p. 213.
14. Bengtson, G., et al., *Catalytic membrane reactor to simultaneously concentrate and react organics*. Chemical Engineering Journal, 2002. **85**(2-3): p. 303.
15. Shimotori, T., E.L. Cussler, and W.A. Arnold, *Diffusion of mobile products in reactive barrier membranes*. Journal of Membrane Science, 2007. **291**(1-2): p. 111.
16. Gao, Z., Y. Yue, and W. Li, *Application of zeolite-filled pervaporation membrane*. Zeolites, 1996. **16**(1): p. 70.
17. Liu, Q., P. Jia, and H. Chen, *Study on catalytic membranes of H3PW12O40 entrapped in PVA*. Journal of Membrane Science, 1999. **159**(1-2): p. 233.
18. Shah, T.N. and S.M.C. Ritchie, *Esterification catalysis using functionalized membranes*. Applied Catalysis A: General, 2005. **296**(1): p. 12.
19. David, M.O., Q.T. Nguyen, and J. Néel, *Pervaporation membranes endowed with catalytic properties, based on polymer blends*. Journal of Membrane Science, 1992. **73**(2-3): p. 129.
20. López, D.E., J.J.G. Goodwin, and D.A. Bruce, *Transesterification of triacetin with methanol on Nafion® acid resins*. Journal of Catalysis, 2007. **245**(2): p. 381.
21. Prazeres, D.M.F. and J.M.S. Cabral, *Enzymatic membrane bioreactors and their applications*. Enzyme and Microbial Technology, 1994. **16**(9): p. 738.
22. Krajewska, B., *Application of chitin- and chitosan-based materials for enzyme immobilizations: a review*. Enzyme and Microbial Technology, 2004. **35**(2-3): p. 126.
23. Wang, Y., et al., *Immobilization of lipase with a special microstructure in composite hydrophilic CA/hydrophobic PTFE membrane for the chiral separation of racemic ibuprofen*. Journal of Membrane Science, 2007. **293**(1-2): p. 133.

24. Arica, M.Y., et al., *Dye derived and metal incorporated affinity poly(2-hydroxyethyl methacrylate) membranes for use in enzyme immobilization*. Polymer International, 1998. **46**(4): p. 345.
25. Pujari, N.S., et al., *Poly(urethane methacrylate-co-glycidyl methacrylate)-supported-polypropylene biphasic membrane for lipase immobilization*. Journal of Membrane Science, 2006. **285**(1-2): p. 395.
26. Pozniak, G., B. Krajewska, and W. Trochimczuk, *Urease immobilized on modified polysulphone membrane: Preparation and properties*. Biomaterials, 1995. **16**(2): p. 129.
27. Butterfield, D.A., et al., *Catalytic biofunctional membranes containing site-specifically immobilized enzyme arrays: a review*. Journal of Membrane Science, 2001. **181**(1): p. 29.
28. te Hennepe, H.J.C., et al., *Zeolite-filled silicone rubber membranes : Part 1. Membrane preparation and pervaporation results*. Journal of Membrane Science, 1987. **35**(1): p. 39.
29. te Hennepe, H.J.C., et al., *Zeolite-filled silicone rubber membranes Experimental determination of concentration profiles*. Journal of Membrane Science, 1994. **89**(1-2): p. 185.
30. Duval, J.M., et al., *Adsorbent filled membranes for gas separation. Part 1. Improvement of the gas separation properties of polymeric membranes by incorporation of microporous adsorbents*. Journal of Membrane Science, 1993. **80**(1): p. 189.
31. Duval, J.M., et al., *Preparation of zeolite filled glassy polymer membranes*. Journal of Applied Polymer Science, 1994. **54**(4): p. 409.
32. Avramescu, M.-E., Z. Borneman, and M. Wessling, *Dynamic behavior of adsorber membranes for protein recovery*. Biotechnology and Bioengineering, 2003. **84**(5): p. 564.
33. Avramescu, M.-E., et al., *Preparation of mixed matrix adsorber membranes for protein recovery*. Journal of Membrane Science, 2003. **218**(1-2): p. 219.
34. Avramescu, M.-E., Z. Borneman, and M. Wessling, *Mixed-matrix membrane adsorbers for protein separation*. Journal of Chromatography A, 2003. **1006**(1-2): p. 171.
35. Avramescu, M.E., et al., *Adsorptive membranes for bilirubin removal*. Journal of Chromatography B, 2004. **803**(2): p. 215.
36. Stamatialis, D.F., et al., *Medical applications of membranes: Drug delivery, artificial organs and tissue engineering*. Journal of Membrane Science, 2008. **308**(1-2): p. 1.
37. Saiful, Z. Borneman, and M. Wessling, *Enzyme capturing and concentration with mixed matrix membrane adsorbers*. Journal of Membrane Science, 2006. **280**(1-2): p. 406.

38. Avramescu, M.-E., Z. Borneman, and M. Wessling, *Particle-loaded hollow-fiber membrane adsorbers for lysozyme separation*. Journal of Membrane Science, 2008. **322**(2): p. 306.
39. Radivojevic, D., et al., *Frozen slurry catalytic reactor: A new structured catalyst for transient studies in liquid phase*. Applied Catalysis A: General. **In Press, Corrected Proof**.

2

Introduction to enzyme immobilization

Enzymes have been used for centuries in their native form in applications ranging from early food processes to modern applications in pharmaceutical and chemical industries. The interest to start immobilizing enzymes arose from the interest in exploiting the technical and commercial advantages of performing biochemical reactions in which isolated enzymes could be used. The immobilization of enzymes permit a better process design, due to acceptable conversion yields, low mass transfer limitations and a long-term stability of the enzymes. Enzyme immobilization can be performed using different types of carriers, ranging from particles to membranes. There is a high variety of immobilization methods available, spanning from in situ enzyme incorporation to chemical binding. The immobilization strategy is usually chosen in accordance to the application since different methods yield different conversion capacities, and require different post- and pre-treatment steps.

2.1 IMMOBILIZATION METHODS

Several different approaches for the immobilization of enzymes have been proposed. The immobilization of enzymes can be viewed as the confinement or localization of an enzyme to a certain defined position with the retention of catalytic activities which can be used repeatedly and continuously, according to the definition of Katchalski-Katzir [1]. Enzymes are typically highly specific for certain reactions, which take place in conditions present in industrial reactors. Immobilization can thus be used to permit enzymes to withstand conditions which, in any other circumstances, would be too

harsh. One further advantage of immobilization is the possibility of reusing the enzymes. The immobilization process must then be oriented in view of maintaining the active conformation of the enzyme, in order for the catalytic activity to be preserved.

Immobilization can take place via three main techniques: binding to carriers, crosslinking and entrapment [2]. For each technique, different methods can be selected (table 2.1). There is no single technique displaying the best results, with different authors usually opting for the most familiar one. The catalytic activity of the immobilized enzymes can thus vary greatly with the technique and the specific enzyme. Though some guidelines concerning the chemical structure of the enzyme can be followed, the process remains largely empirical.

Table 2.1 – Summary of immobilization methods

Binding	Crosslinking	Physical entrapment
covalent binding	cross-linked enzyme	entrapment in a matrix
ionic/electrostatic binding	crystals	encapsulation
hydrophobic binding	cross-linked enzyme	
metal binding	aggregates	
affinity binding		

2.1.1 Immobilization via binding

The immobilization of enzymes by binding consists basically on forming chemical or physical bonds to a physical carrier. Mainly five types of binding are distinguishable: covalent, ionic, adsorptive, metal and affinity.

Covalent binding yields the strongest kind of enzyme-carrier bond and is usually the most commonly adopted option for enzyme binding. One strong reason for this option lays in its capacity for preventing reversible unfolding of the immobilized enzyme [3]. However, caution should be exerted when choosing the ideal chemistry and reaction conditions to be applied, since these can cause a considerable loss in enzymatic activity. The method consists in the formation of a covalent bond using different functional groups on the carrier surface and groups belonging to amino acid residues in the enzyme. The binding is not site specific and thus does not influence the ori-

entation of the enzyme during the immobilization process. As seen in figure 2.1, the bond is established between the surface and the most readily available amino acids from the enzyme. The most often used groups are the amine of lysine or arginine, carboxyl from aspartic or glutamic acid, hydroxyl of serine or threonine and sulfhydryl of cysteine [4]. The groups from the support can originally be available at the surface of the carrier or can be incorporated by chemically activating the carrier prior to the immobilization process. Alternatively, the enzyme can react using an activation agent prior to the immobilization procedure. This method is less followed due to a higher risk of inactivation of the enzyme, since the enzyme modification is accomplished by highly reactive non-group specific chemicals which can easily alter the structure and the catalytic activity of the enzyme [2].

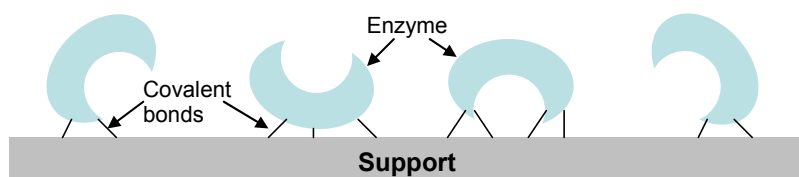


Figure 2.1 – Schematic representation of covalent immobilization of enzymes. The enzyme uses any available functional groups present in the structure to bind with the available carrier functional groups.

One of the most common types of covalent immobilization is by using aldehyde groups on the carrier which bind to the enzyme [5]. Glutaraldehyde, due to its ability to react rapidly with amines, is frequently chosen as the activation reagent for the modification of the support [6-12]. Typically, glutaraldehyde reacts with amine groups already present on the surface of the carrier [6, 7, 10, 11, 13] or added by a previous chemical modification, just as the addition of a spacer arm [12]. The resulting aldimine bonds between the enzyme and the support are relatively weak in acidic solutions and can thus be stabilized by reaction with sodium borohydride, sodium cyanoborohydride or by pyridine-borane reduction [2, 14]. Although amine groups are by far the most common targets for glutaraldehyde activation, the use of hydroxyl groups has also been reported [7]. Alternatively, other proteins, such as bovine serum albumine (BSA) have also been immobilized to provide a spacer between the surface of the support and the enzyme. In this case, the protein was activated by cross-linking with glutaraldehyde prior to enzyme immobilization [8, 9, 15]. A representation of this immobilization reaction can be found in figure 2.2.

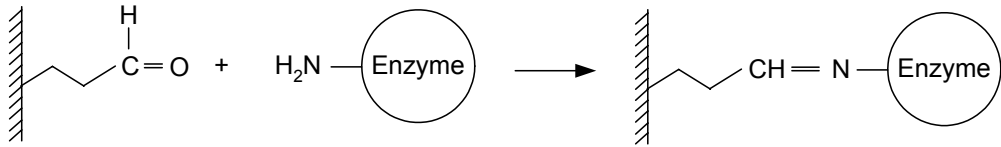


Figure 2.2 – Covalent enzyme immobilization using aldehyde groups of the support and amine groups in the enzyme.

In many cases, the direct immobilization of the enzyme by using readily available groups on the surface carrier has been pursued. One favored method is by using epoxy groups for the covalent immobilization of enzymes. The highly reactive groups bind promptly to the amine groups in the enzyme, thus forming a strong bond (figure 2.3) [1, 6, 16-19]. Epoxy groups can also be incorporated in the carrier by chemical activation using epichlorohydrin [12, 20, 21]. In this case, hydroxyl groups on the support are activated with epichlorohydrin in a basic medium to provide the epoxy groups for the subsequent enzyme immobilization process. The amino groups in the enzyme react directly to the reactive epoxy groups, thus providing a strong and stable covalent bond between the enzyme and the support.

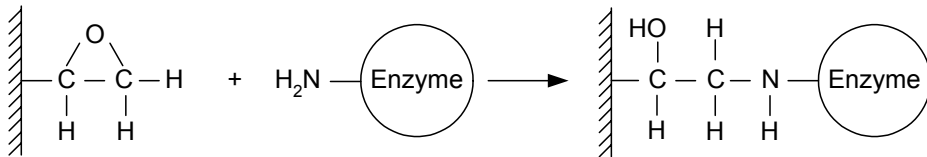


Figure 2.3 – Covalent enzyme immobilization using epoxy groups from the support and amine groups in the enzyme.

Another typical coupling method is using carbodiimide activation. This reaction takes place on the surface of the support using an activation agent containing the carbodiimide group and another functional group which can bind to the available groups of the carrier. Typically, 1-ethyl-3-(3-dimethylaminepropyl) carbodiimide hydrochloride (EDC) is used as activation agent by reacting with carboxyl groups on the surface of the carrier [22, 23] or alternatively present on spacer arms grafted to the carrier [24, 25].

Ionic binding, also referred to as electrostatic binding, makes use of ionic charges both on the surface of the carrier and of the enzyme. In typical covalent binding, the conjugate carrier-enzyme must be discarded as waste after the enzyme becomes inactivated. With the use of ion-exchange materials, the enzyme can be desorbed from the carrier after inactivation and thus permit the recovery of the used support materials, reducing the waste and the costs [26, 27]. Ionic binding takes advantage of functional groups on the carrier surface which, in solution, assume ionic form by accepting or releasing a proton. The enzyme can be induced into an ionic form by changing the pH of the medium to values above or below the isoelectric point (pI) of the protein. A pH above the pI causes the enzyme to release a proton and thus assume an anionic form whereas a pH below the protein pI causes the enzyme to accept a proton and thus becomes a cation. By choosing the pH that adjusts the characteristic of the carrier, the enzyme thus forms an ionic bond with the support and becomes immobilized. The process is dependant on several variables, such as pH value, isoelectric point, enzyme concentration, structural stability of the protein, ionic strength of the solution or domain composition. From these factors, the most commonly addressed are pH and ionic strength. After inactivation, the desorption takes place via the opposite process of adsorption, with the pH being switched to a value that permits the enzyme to assume the same charge as the carrier and thus leach out. The process of ionic binding is exemplified for both cation- and anion-exchange supports in figures 2.4a and 2.4b respectively.

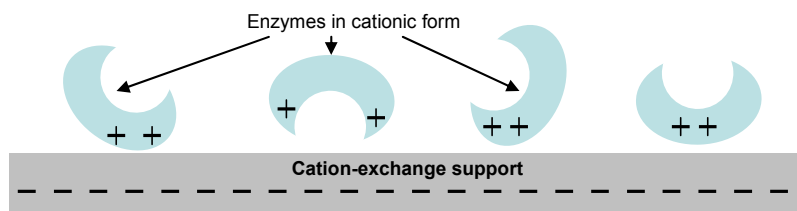


Figure 2.4a – Enzymatic immobilization on cation-exchange supports at $\text{pH} < \text{pI}$. The enzymes assume a cationic form and are attracted to the negatively charged carrier surface.

Different types of functional groups can be used for ionic binding. Polyethyleneimine (PEI) has been reported as a typical material for coating of other materials in order to provide ion-exchange capacity to the supports [6, 10, 28]. This technique can be interesting where the ideal pH for the enzy-

matic reaction is suited for the ionic binding process, as it does not cause the leaching of the enzyme from the support. The method also presents the advantage of being usually simple and cheap.

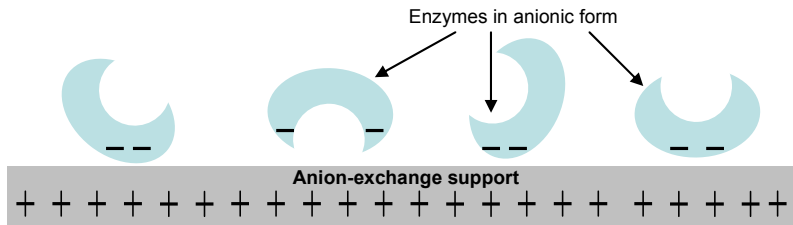


Figure 2.4b – Enzymatic immobilization on anion-exchange supports at $\text{pH} > \text{pI}$. The enzymes assume an anionic form and are attracted to the positively charged carrier surface.

Hydrophobic binding, sometimes referred to as adsorptive binding, takes place with different approaches depending on the type of carrier used. When in presence of a carrier with hydrophobic characteristics, the enzyme will adsorb on the surface, thereby changing its conformation. This type of adsorption can be difficult to handle, as the remaining activity can be enhanced [29-33] or reduced [34-37], depending on how the unfolding of the protein takes place. In situations where the active sites of the immobilized enzyme are exposed to the surrounding medium, the activity can be highly enhanced (figure 2.5I). If, on the other hand, the enzyme adsorbs using the active sites, the activity can be partial or totally lost (figure 2.5II). One other situation takes place when the unfolding of the enzyme leads to a denaturation of the enzyme thus causing a total and permanent loss of activity. The influence of the adsorption procedure in enzyme activity, however, cannot be wholly predicted and depends very much on trial and error, with situations being reported case to case.

Carriers making use of hydrophobic adsorption do not require any specific preparation, as the mechanism which is used is directly based on the intrinsic characteristics of the material. The risk of enzyme leaching from the support however is higher for adsorption binding in comparison with other methods for enzyme binding, due to the relatively weaker enzyme-carrier interactions. In contrast, adsorption methods are the simplest for enzyme immobilization, thus reducing costs. Also no chemical changes to the enzymes are required prior to the immobilization which reduces the potential damage [4].

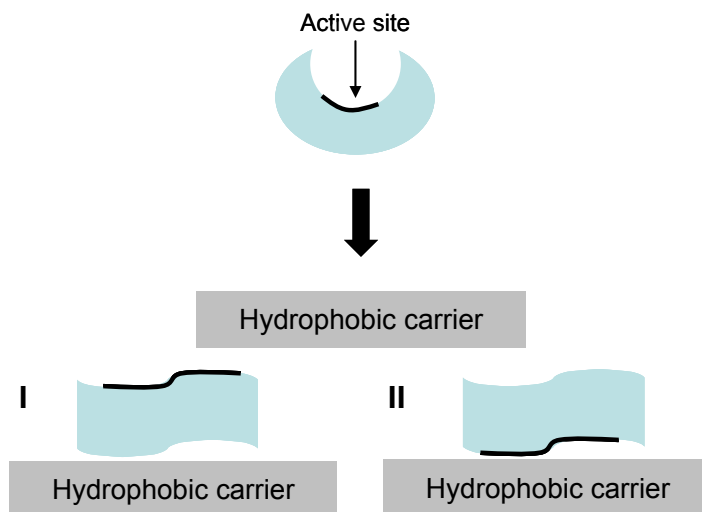


Figure 2.5 – Enzyme immobilization via hydrophobic adsorption. I – Enzymatic superactivation due to preferable orientation of active site; II – Enzymatic activity reduction due to bad orientation of active site.

Metal binding is based on the use of metal chelates for the attachment of enzymes. In this process, transition metals are used to form complexes both with the support and the enzyme. The process takes place by creating a metal chelate using hydroxyl or carboxylic groups from the support. This metal chelate is then placed in contact with an enzyme solution at near-neutral pH in order to form a second chelate between the metal and hydroxyl, carboxylic or amino groups belonging to the enzyme which will act as ligands [38]. Naturally, a symmetric approach can also be used, in which a metal chelate is first formed with the enzyme in a solution and only afterwards is the enzyme/metal chelate adsorbed onto the support. The activity of the immobilized enzyme depends on the same type of factors as in other types of bonds, like the availability of the groups in the enzyme, their proximity with the active sites of the enzyme or the proximity between immobilized enzymes. Since the immobilization depends on the chemistry of the support, both membranes [40, 41] and beads [19, 41-43] have been used for enzyme immobilization via metal binding. Direct immobilization in transition metal salts has also been reported [44].

Affinity binding can be understood as an immobilization method where the enzyme attachment to the carrier is mediated by the action of a ligand which shows a specific affinity for the target enzyme. This method is used to allow the immobilization of a specific enzyme from a mixture and to provide a higher mobility to the immobilized enzyme in order to increase activity. Affinity ligands can be classified as biospecific or pseudobiospecific. Biospecific ligands include mono- and polyclonal antibodies, whereas pseudobiospecific ligands usually refer to immobilized metals, hydrophobic amino acids and dyes [45].

Affinity interactions between enzymes and substrates and between antibody-antigen pairs are characterized by high association constants of the resulting complexes, which permits the use of recognition techniques in enzyme immobilization. Enzymes can be immobilized by first creating enzyme-anti-antibody conjugates and attaching antibody molecules to the carrier surface (figure 2.6). The antibody molecules on the carrier surface provide the specific molecular recognition which permits the immobilization of the conjugate via the specific anti-antibody molecules. This technique enables enzyme immobilization without interfering with the enzyme active sites, which permits to conserve enzymatic activity after the immobilization takes place [46-49].

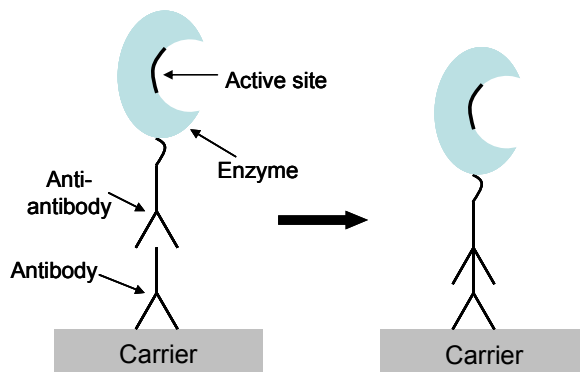


Figure 2.6 – Enzyme affinity immobilization. Antibody molecules attach to the carrier surface and specifically bind to the enzyme. By repeating the procedure, multilayers can be formed.

A different approach can also be used, in which the avidin is non-specifically adsorbed onto the carrier surface and a biotin-labeled enzyme is then attached to it [49-51]. Alternatively, biotin can be initially attached to the carrier and then bound to an avidin molecule, thus creating a strong

biotin-avidin bond. A biotin-enzyme conjugate can then be specifically immobilized onto the carrier surface retaining high activity [49, 51, 52]. Both approaches permit multilayer formation (figures 2.7.A and 2.7.B), since an avidin molecule can bind to up to four biotin molecules.

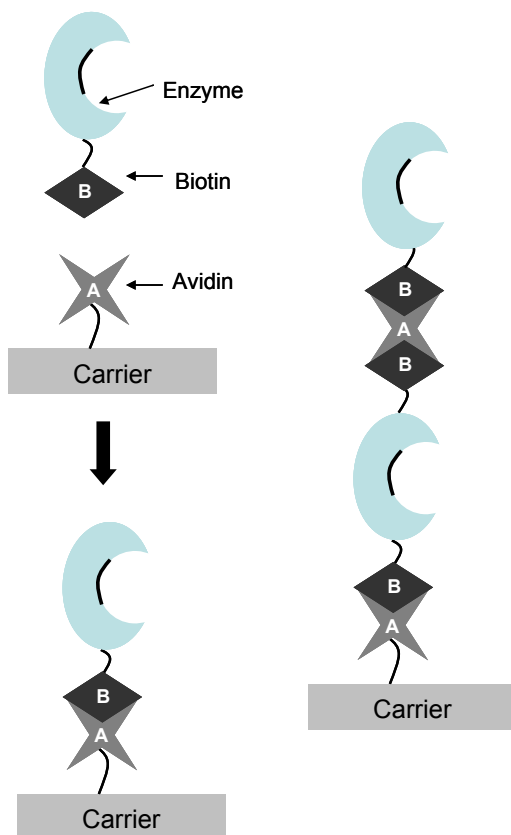


Figure 2.7.A – Enzyme affinity immobilization. Biotin molecules are immobilized to the carrier surface and specifically bind to the avidin conjugated enzyme. By repeating the procedure, multilayers can be formed.

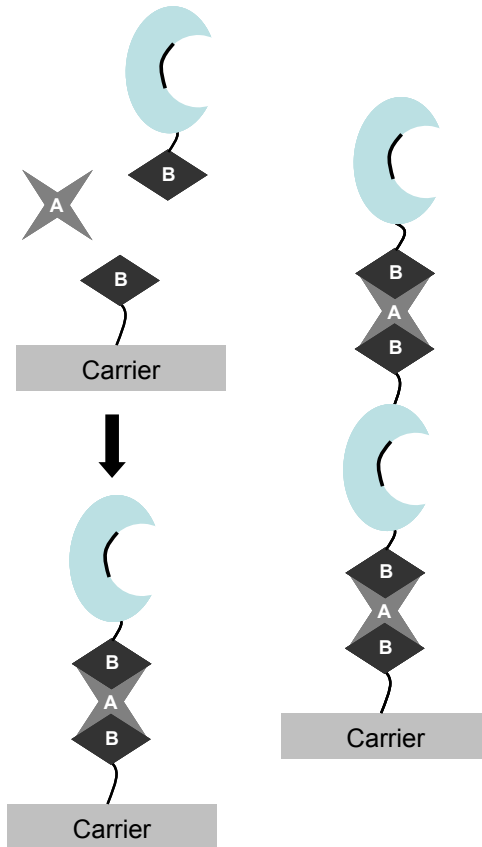


Figure 2.7.B – Enzyme affinity immobilization. Avidin molecules are adsorbed to the carrier surface and specifically bind to the biotin-labeled enzyme. By repeating the procedure, multi-layers can be formed.

2.1.2 Immobilization via entrapment or encapsulation

Entrapment or encapsulation of enzymes differs from chemical or physical binding in terms of enzyme mobility. While a bound enzyme has the mobility restricted by interactions with the support, entrapped or encapsulated enzymes are free in solution but the mobility is restricted in space by the structure of the support (entrapment) or by a form of semi permeable membrane enveloping the enzyme (encapsulation) [4].

Enzyme entrapment takes place by restricting enzyme movement within the lattice structure of the support as depicted in figure 2.8. The enzymes can thus keep a certain degree of movement within the structure, which has a finely controlled porosity in order to simultaneously avoid enzyme leaking and permit the penetration of substrate in and product out of the confined structure. The support acts as an additional resistance to mass transfer, which is a disadvantage, since it restricts the access to the immobilized enzymes. However, it can also be an advantage, since the enzyme contact with harmful or toxic compounds can be prevented.

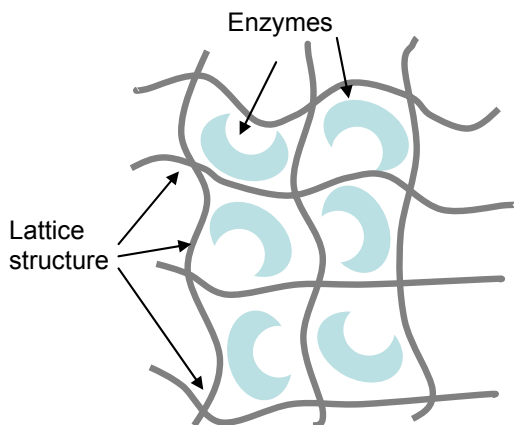


Figure 2.8 – Enzyme immobilization via physical entrapment in a lattice structure. The enzymes have full mobility inside the delimiting cells, but are unable to diffuse out of the matrix.

Physical entrapment of enzymes can be achieved by several methods. A commonly used method is by electrochemically inducing the polymerization of monomers in an aqueous solution containing enzymes. The enzymes are dissolved in a medium containing monomers to which an electrical current is applied and become entrapped in the polymeric mesh created as the polymerization reaction occurs, thus becoming immobilized. This method presents the advantage of permitting the immobilization without affecting enzymatic activity. It also allows for an easily tunable film thickness, as the polymerization process is dependant on the applied electrical charge. This technique has been extensively used in the production of biosensors as it fit for producing the support film over complex geometrical structures [51, 53].

Another approach to immobilize enzymes is using sol-gel chemistry [54-57], such as in the preparation of monoliths. The method follows a methodology

similar to that of immobilization during electrochemical polymerization, with the enzymes being entrapped in the porous structure during the sol-gel reaction. The reaction takes place in a solution containing the target enzyme, which becomes entrapped in the growing structure, becoming thus immobilized. This method is highly dependant on the materials and conditions used, with sol-gel materials being found to increase the stability and activity of the immobilized enzymes [58]. The produced enzyme-activated monoliths present frequently interconnected micropores, which can limit the transport to only small-sized substrate molecules. One main problem of the method is that typical sol-gel reactions often produce disordered structures, thus reducing the reactions that can be used [57]. Also, some degree of ionic interaction seems to be important to maintain a high enzymatic activity after entrapment [57, 59].

One other alternative for enzyme entrapment can be found using mesoporous materials. In this case the materials are readily available and do not need to be synthesized or prepared. The entrapment is achieved by allowing the solubilized enzyme to diffuse into the pores of the support, thus becoming entrapped. Since the pores are generally in the same order of magnitude as the target enzymes (10-300 Å), the entrapment process is carried in the presence of swelling agents that allow a better transport of the enzymes into the mesoporous structure. After entrapment, in the absence of the swelling agents, the enzymes become effectively immobilized [59].

One further method consists in the entrapment of the enzymes on a membrane surface by ultrafiltration. In this method, an enzyme solution is filtered in back-flush mode through a hydrophilic membrane, thus being retained in the more open spongy region on the inside of the membrane (figure 2.9). This method has been proposed for lipase immobilization using hydrophilic materials, on which the lipases are active. The concept is highly dependant on a membrane structure that must be open enough on the feed side to allow the passage of enzyme molecules but then must possess small enough pores in the inner structure, so that the enzymes can be retained [60, 61].

Gels are also a commonly used material for enzymatic entrapment. The enzyme is immobilized in the lattice-like structure of the gel, thus preventing enzyme leaching while allowing free movement of substrate and product. The immobilization can be achieved by mixing the enzyme with the desired polymer and then achieve the entrapment by cross-linking or temperature-induced gelation. Also photo polymerization of acrylic monomers can be used. Entrapment in alginate gels can be achieved by mixing the enzyme

with alginate solutions and adding divalent cations, such as calcium, thus causing the gelation and entrapping the enzyme molecules [38]. Gels have the advantage of acting as a good barrier that can prevent interaction between enzymes and harmful media or that can increase the biological compatibility of the enzymatic support [4].

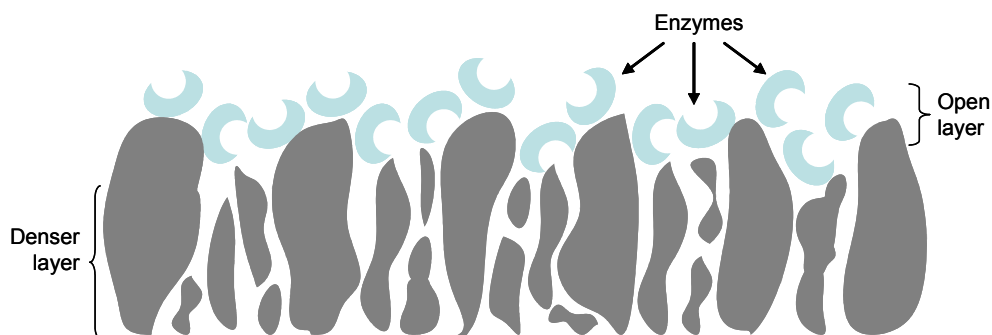


Figure 2.9 – Enzyme entrapment in a membrane by ultrafiltration. The membranes are retained in the more open and spongy top surface layer and cannot permeate through the denser ultrafiltration matrix.

Enzyme encapsulation does not depend on a static support structure. By this method, the enzymes are protected from the surrounding environment by a thin semi-permeable layer that permits the transport of smaller molecules but not larger molecules such as proteins (figure 2.10). The enzymes are in effect as mobile in the reactive medium as the capsules that encompass them.

Enzyme encapsulation follows a similar path to that of enzyme entrapment. The difference is placed mainly in changing the support from an interconnected lattice-like mesh to spherical carriers. Gels are therefore a commonly used material for enzyme encapsulation, particularly alginate gels. The main difference with enzyme entrapment lies on the process which produces enzyme-containing capsules instead of a matrix. The gelation takes place in presence of the dissolved enzyme and of a thickening agent, necessary to maintain the spherical shape of the capsules, during agitation to promote the mass transfer and control the capsule size. In order to avoid enzyme leakage or to harden the capsules, a cross-linking step of the capsule surface may be added after the encapsulation process. The capsules can then be used either in batch mode or in a packed bed column [62, 63].

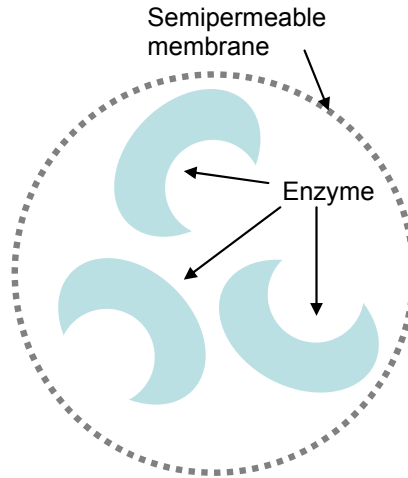


Figure 2.10 – Enzyme immobilization by encapsulation. The enzymes have full mobility inside the capsule but cannot diffuse through the semi-permeable membrane, permeable only for smaller components.

Other methods have been reported for enzyme encapsulation, by creating polymer multilayers around enzyme crystals. In this method, enzyme crystals are used as templates for the deposition of consecutive layers of cationic and anionic polymers thus covering the enzyme. When in contact with an adequate medium, the crystal solubilizes and becomes encapsulated inside the polymer layers [64].

Some other situations have been described, in which the enzyme can be immobilized into a support covalently [65] or by adsorption [58], with the conjugate enzyme-support being afterwards encapsulated for the applications.

2.1.3 Immobilization via cross-linking

This method provides the only support-free method for enzymatic immobilization. This technique is based on joining several enzyme molecules into three dimensional aggregates (figure 2.11) by means of covalent binding between active groups within the enzymes using bi- or multifunctional reagents such as glutaraldehyde or toluene diisocyanate [4]. Although this technique offers an easy path to produce insoluble cross-linked enzymes

with catalytic activity, the lack of a solid support causes the gelatinous aggregates to show low mechanical stability and to be difficult to handle. Also the reproducibility is difficult to achieve and the retained enzymatic activity rather low [39].

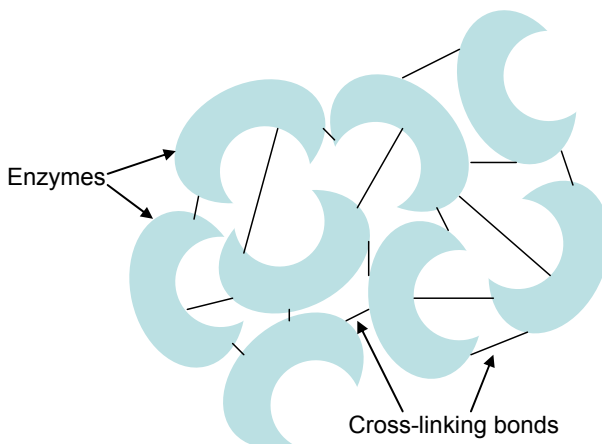


Figure 2.11 – Enzyme immobilization by cross-linking. Each enzyme stabilizes the ones it is bound to, creating a more stable group than the individual enzymes.

Two types of enzymatic cross-linking should be distinguished: cross-linked enzyme crystals (CLEC's) and cross-linked enzyme aggregates (CLEA's). CLEC's are formed by directly cross-linking enzyme crystals, thus providing additional stability. CLEC's usually present improved resistance to denaturation by heat, organic solvents and proteolysis than CLEA's. CLEC's are also easy to control in terms of particle size and are easy to recycle, thus rendering them suitable for industrial biotransformations [39]. The main problem arising from the use of CLEC's is the need to crystallize the enzyme, which can be a laborious and time-consuming step. In order to solve this problem, CLEA's could be developed. These aggregates are produced by inducing the precipitation of the enzymes and then cross-linking the resulting aggregates with the process taking place essentially in one step. This method is designed to render the enzyme aggregates insoluble while preserving the main structure and thus the activity. The main difficulty during the preparation of CLEA's resides in the activity retained by the enzyme after cross-linking, which means that most of the research has been directed to deal with this issue. Work has been developed to improve activity by means of a better understanding of the aggregate structure [66], by using

different cross-linkers [67], by combining enzymes in so-called combi-CLEA's in which a heterogeneous population of enzymes is cross-linked, thus better preserving the activity [68] or by slightly altering the precipitation/cross-linking process [69]. Since in CLEA's, like with every other enzyme immobilization method, no obvious rule can be used to predict the success of an immobilization reaction, much literature has been published on the application of the cross-linking process to different enzymes [70-72].

In the case of cross-linked enzyme crystals (CLEC's), the focus rests on a first step of enzyme crystallization, followed by the cross-linking reaction. The resulting CLEC's present a solid microporous structure, with uniform solvent-filled channels of 15-100 Å over the entire crystals. The crystallization process can take place by varying pH, temperature or protein and precipitant concentration. The step must be optimized for each enzyme, with the focus on the reproducibility of crystal size and purity. Cross-linking of the formed crystals can be achieved by bi- or multi-functional reagents, with glutaraldehyde as the typical choice. This step has to be closely controlled in order to avoid aggregation, precipitation or loss of activity due to excessive cross-linking [73]. Due to the improved structure and stability, CLEC's can withstand the shear forces associated with stirred tanks, cross-flow microfilters and pumps. Being heterogeneous catalysts, CLEC's can be isolated, recycled and reused several times [74]. Typically, CLEC's are thermally stable though with lower activities than the respective soluble enzymes [75, 76] and with a reduced activity in organic solvents. The range of applications for CLEC's can be found in synthetic chemistry, biosensor technology and biomedical applications [74].

2.2 CARRIER TYPES

As seen above, enzyme immobilization tends to take place using solid carriers as support. With the exception of cross-linking, all immobilization techniques previously described demand the existence of a surface on which the enzyme can interact or that provides a physical barrier to the free movement of the enzyme molecules. When selecting the carrier materials, some properties should be taken into consideration, either to influence the immobilization process by the presence of specific functional groups or the way the enzyme interacts with the carrier, in order to maximize its stability and activity. Therefore, some main properties should be taken into consideration [2]:

- **Functionality** – the presence and density, as well as the nature of functional groups influences decisively post-immobilization activity yields, stability and operational stability.
- **High surface area and porosity** – the carrier should have as high a surface area as possible, with high accessibility to the functional sites provided by large pores to allow enzyme diffusion into the support.
- **Hydrophilicity and hydrophobicity** – enzymes behave differently in the presence of materials of different natures. The nature of the material can cause an enhanced stability or superactivation of the immobilized enzyme.
- **Insolubility** – the carrier should be insoluble to avoid the loss of enzyme and to protect the enzyme molecules from contact with undesirable contaminants.
- **Mechanical stability** – supports should be stable enough to withstand shear forces that may be used in the chemical processes.

As mentioned, all materials present both advantages and disadvantages relatively to the necessary characteristics for a carrier suited to enzyme immobilization. Organic carriers are cheaper and provide wider variety of functionalities, but are less resistant to the medium. Inorganic carriers provide higher resistances, but less flexibility in terms of process. One other important factor are the mass transfer limitations often present in these processes. A fine balance between immobilization capacity and mass transfer limitations has to be taken into account. Supports with higher surface areas, such as porous particles, often present smaller pores and cause the process to be diffusively controlled for both the immobilization and enzymatic conversion steps, thus reducing the overall process speed. Materials which present a more open structure, like in the case of membranes, often have better mass transfer properties, with a more convectively controlled process, but usually present lower immobilization capacities. A possible solution is to fuse both support categories together to obtain the advantages inherent to both. In this case, a more open and permeable structure, such as a macroporous membrane, could be used in combination with microporous structures, such as particles, in a single material, which is named a mixed matrix material (MMM). This objective can be achieved by embedding functional particles in macroporous membranes, in which the membrane provides the structure which controls the hydrodynamics and the particles

the active sites for enzyme immobilization, thus causing a balance between the reduced diffusively controlled immobilization process and the convectively controlled mass flow through the membrane. This approach is explored in this thesis. An introduction about mixed matrix membranes is given below.

2.3 MIXED MATRIX MEMBRANES

Mixed matrix membranes (MMM) have initially been produced in dense polymeric films for the purpose of gas transport facilitation through the membrane. The embedding of hydrophobic zeolites in rubber polymers proved to improve alcohol permeability and selectivity in pervaporation processes in the presence of water [77]. Also for the pervaporation of alcohol/water mixtures MMM have been used to improve the separation of water, using hydrophilic zeolites [78, 79]. Similarly, MMM have been developed for gas separation processes in which different types of polymers and rigid filler materials were used. In this case the selectivity is achieved as a combination of the permeation rates of the desired gas through the polymer material and through the filler material. Initially, molecular sieves have been incorporated by dispersing zeolites in rubber polymers [80]. Also the dispersion of zeolites in glassy polymers has been studied [81-84]. More recently, carbon nanotubes have been used as dispersed material in the production of MMM for gas separation [85].

In recent years, however, studies have appeared with these materials in ultra- and microfiltration, both in flat-sheet form and as porous hollow fibers began to be used as a laboratory technique to isolate and concentrate specific solutes prior to chromatography processes [86, 87]. The incorporation of particles with specific functionalities into a porous membrane permits the formation of an adsorptive matrix which can be used for protein or peptide retention from multi-component mixtures [88-90]. Alternatives to conventional stationary chromatographic media have been prepared by incorporating of active carbon particles [91] and ion-exchange resins [92] to produce membrane adsorbers with enhanced separation efficiency.

Generally speaking, mixed matrix membranes used for biological separations are materials in which small functional particles are embedded in a polymeric matrix. Mixed matrix membranes present a balance between characteristics intrinsic to membranes and characteristics typical for chro-

matography in packed bed particles. MMM are characterized by high fluxes with low pressure drop, with a predominant convection-type of transport. The particles embedded in the porous matrix provide the active sites with the desired functionality and permit to obtain high capacities typical of chromatographic columns. MMM materials combine the high selectivity of the filler materials with the low costs, manufacturing ease and flow behavior of membranes [93]. By combining the two techniques, high permeabilities and selectivities can be achieved in membrane separation processes.

Mixed matrix membranes are prepared in an analogous manner to that of normal membranes. A solution containing the desired polymer, the solvent(s) and additive(s) is prepared and homogenized. Afterwards, the desired functional particles, preferably in sizes below 50 μm , are dispersed in the polymer solution using strong agitation. The dispersion can then be cast into a flat-sheet or spun into a fiber by using a dry-wet phase inversion process. The flexibility in preparing different geometries tailored for specific applications is a great advantage of the MMM platform technology. An important factor for the MMM performance is the particle loading. The particle loading controls not only the capacity, but it also greatly influences the membrane forming process and the resulting structure. A main concern when producing MMM is to guarantee that the polymer, solvents and additives are compatible with the particles, so that the functionality will not be lost in the embedding process.

2.4 CONCLUSIONS

More and more applications are using immobilized enzymes, as a means to reduce waste, energy consumption and costs and to increase enzyme stability in more aggressive reactive media. The increasing amount of processes using immobilized enzymes indicates that this technique will have the tendency to become the approach of choice in enzyme-based reactions in the future.

Most problems in enzyme immobilization are related to choosing the ideal immobilization approach and to mass-transfer limitations during processing. There is still no rule of thumb for selecting the best type of immobilization technique that guarantees the highest activity, being still necessary an approach of trial and error to determine the best option. In terms of support types, particles with different functionalities or membranes have been the

main materials of choice. Particles combine a wider possibility of functionalities with higher enzyme loadings but suffer from mass transfer limitations, are restricted in terms of operational conditions, especially in terms of applied pressure. These problems also limit the choice of geometries to be used for a reactor. Membranes present better mass transfer performances and present a much higher flexibility in terms of possible geometries. Still, the availability of different functionalities is much lower and the capacities are much reduced.

An approach to overcome these problems is the integration of both techniques by using mixed matrix materials, where different particles with different functionalities are embedded in macroporous membranes to make use of the mass transfer advantages of the porous media and to permit a wider variety of geometries. Despite some work with catalyst particles in microporous membranes to produce catalytic active membranes for nitrate reduction in water [94], most work so far in the field of Mixed Matrix Membranes has been directed to protein recovery [95], separation [96] and concentration [97] and to toxin removal [98]. This thesis proved the promising approach by embedding different particulate materials used in enzymatic processes, with different functionalities in macroporous membranes, The result is a robust and easily scalable concept that combines well controlled enzymatic conversions with high enzymatic activities.

REFERENCES

1. Katchalski-Katzir, E. and D.M. Kraemer, *Eupergit^(R) C, a carrier for immobilization of enzymes of industrial potential*. Journal Of Molecular Catalysis B-Enzymatic, 2000. **10**(1-3): p. 157.
2. Tischer, W. and F. Wedekind, *Immobilized enzymes: Methods and applications*, in *Biocatalysis - From Discovery To Application*. 1999. p. 95.
3. Mozhaev, V.V., *Mechanism-based strategies for protein thermostabilization*. Trends in Biotechnology, 1993. **11**(3): p. 88.
4. Bickerstaff, G.F., ed. *Immobilization of Enzymes and Cells*. Methods in Biotechnology. Vol. 1. 1997, Humana Press: Totowa, New Jersey.
5. Montes, T., et al., *Improved stabilization of genetically modified penicillin G acylase in the presence of organic cosolvents by co-*

- immobilization of the enzyme with polyethyleneimine*. *Advanced Synthesis & Catalysis*, 2007. **349**(3): p. 459.
6. Bolivar, J.M., et al., *Evaluation of different immobilization strategies to prepare an industrial biocatalyst of formate dehydrogenase from Candida boidinii*. *Enzyme and Microbial Technology*, 2007. **40**(4): p. 540.
 7. Foresti, M.L. and M.L. Ferreira, *Chitosan-immobilized lipases for the catalysis of fatty acid esterifications*. *Enzyme And Microbial Technology*, 2007. **40**(4): p. 769.
 8. Geng, L., et al., *The covalent immobilization of trypsin at the galleries of layered [gamma]-zirconium phosphate*. *Colloids and Surfaces B: Biointerfaces*, 2003. **30**(1-2): p. 99.
 9. Nouaimi-Bachmann, M., et al., *Co-immobilization of different enzyme activities to non-woven polyester surfaces*. *Biotechnology And Bioengineering*, 2007. **96**(4): p. 623.
 10. Lopez-Gallego, F., et al., *Stabilization of different alcohol oxidases via immobilization and post immobilization techniques*. *Enzyme and Microbial Technology*, 2007. **40**(2): p. 278.
 11. Palomo, J.M., et al., *Modulation of the enantioselectivity of lipases via controlled immobilization and medium engineering: hydrolytic resolution of mandelic acid esters*. *Enzyme and Microbial Technology*, 2002. **31**(6): p. 775.
 12. Yucel, D., N. Ozer, and V. Hasirci, *Construction of a choline biosensor through enzyme immobilization on a poly(2-hydroxyethyl methacrylate)-grafted Teflon film*. *Journal Of Applied Polymer Science*, 2007. **104**(5): p. 3469.
 13. Migneault, I., et al., *Comparison of two glutaraldehyde immobilization techniques for solid-phase tryptic peptide mapping of human hemoglobin by capillary zone electrophoresis and mass spectrometry*. *Electrophoresis*, 2004. **25**(9): p. 1367.
 14. Petro, M., F. Svec, and J.M.J. Frechet, *Immobilization of trypsin onto "molded" macroporous poly(glycidyl methacrylate-co-ethylene dimethacrylate) rods and use of the conjugates as bioreactors and for affinity chromatography*. *Biotechnology And Bioengineering*, 1996. **49**(4): p. 355.
 15. Avramescu, M.E., W.F.C. Sager, and M. Wessling, *Functionalised ethylene vinyl alcohol copolymer (EVAL) membranes for affinity pro-*
-

- tein separation*. Journal of Membrane Science, 2003. **216**(1-2): p. 177.
16. Arroyo, M., J.M. Sanchez-Montero, and J.V. Sinisterra, *Thermal stabilization of immobilized lipase B from Candida antarctica on different supports: Effect of water activity on enzymatic activity in organic media*. Enzyme and Microbial Technology, 1999. **24**(1-2): p. 3.
 17. Boller, T., C. Meier, and S. Menzler, *EUPERGIT oxirane acrylic beads: How to make enzymes fit for biocatalysis*. Organic Process Research & Development, 2002. **6**(4): p. 509.
 18. Mateo, C., et al., *Increase in conformational stability of enzymes immobilized on epoxy-activated supports by favoring additional multi-point covalent attachment*. Enzyme And Microbial Technology, 2000. **26**(7): p. 509.
 19. Mateo, C., et al., *Multifunctional Epoxy Supports: A New Tool To Improve the Covalent Immobilization of Proteins. The Promotion of Physical Adsorptions of Proteins on the Supports before Their Covalent Linkage*. Biomacromolecules, 2000. **1**(4): p. 739.
 20. Arica, M.Y., N.G. Alaeddinoglu, and V. Hasirci, *Immobilization of glucoamylase onto activated pHEMA/EGDMA microspheres: properties and application to a packed-bed reactor*. Enzyme and Microbial Technology, 1998. **22**(3): p. 152.
 21. Arica, M.Y., V. Hasirci, and N.G. Alaeddinoglu, *Covalent immobilization of [α]-amylase onto pHEMA microspheres: preparation and application to fixed bed reactor*. Biomaterials, 1995. **16**(10): p. 761.
 22. Williams, R.A. and H.W. Blanch, *Covalent immobilization of protein monolayers for biosensor applications*. Biosensors and Bioelectronics, 1994. **9**(2): p. 159.
 23. Hong, J., et al., *Covalent binding of alpha-chymotrypsin on the magnetic nanogels covered by amino groups*. Journal Of Molecular Catalysis B-Enzymatic, 2007. **45**(3-4): p. 84.
 24. Kang, E.T., et al., *Surface Modification and Functionalization of Polytetrafluoroethylene Films*. Macromolecules, 1996. **29**(21): p. 6872.
 25. Kulik, E.A., et al., *Trypsin immobilization on to polymer surface through grafted layer and its reaction with inhibitors*. Biomaterials, 1993. **14**(10): p. 763.
 26. Katchalski-Katzir, E., *Immobilized enzymes -- learning from past successes and failures*. Trends in Biotechnology, 1993. **11**(11): p. 471.
-

27. Mateo, C., et al., *Reversible enzyme immobilization via a very strong and nondistorting ionic adsorption on support-polyethylenimine composites*. *Biotechnology and Bioengineering*, 2000. **68**(1): p. 98.
28. Torres, R., et al., *Reversible Immobilization of Invertase on Sepabeads Coated with Polyethyleneimine: Optimization of the Biocatalyst's Stability*. *Biotechnol. Prog.*, 2002. **18**(6): p. 1221.
29. Bryjak, J. and A.W. Trochimczuk, *Immobilization of lipase and penicillin acylase on hydrophobic acrylic carriers*. *Enzyme and Microbial Technology*, 2006. **39**(4): p. 573.
30. Geluk, M.A., et al., *Adsorption of lipase from *Candida rugosa* on cellulose and its influence on lipolytic activity*. *Enzyme and Microbial Technology*, 1992. **14**(9): p. 748.
31. Nouredini, H. and X. Gao, *Characterization of sol-gel immobilized lipases*. *Journal of Sol-Gel Science and Technology*, 2007. **41**(1): p. 31.
32. Palomo, J.M., et al., *Interfacial adsorption of lipases on very hydrophobic support (octadecyl-Sepabeads): immobilization, hyperactivation and stabilization of the open form of lipases*. *Journal of Molecular Catalysis B: Enzymatic*, 2002. **19-20**: p. 279.
33. Bastida, A., et al., *A single step purification, immobilization, and hyperactivation of lipases via interfacial adsorption on strongly hydrophobic supports*. *Biotechnology and Bioengineering*, 1998. **58**(5): p. 486.
34. Knezevic, Z., L. Mojovic, and B. Adnadjevic, *Palm oil hydrolysis by lipase from *Candida cylindracea* immobilized on zeolite type Y*. *Enzyme and Microbial Technology*, 1998. **22**(4): p. 275.
35. Marin-Zamora, M.E., et al., *Direct immobilization of tyrosinase enzyme from natural mushrooms (*Agaricus bisporus*) on d-sorbitol cinnamic ester*. *Journal of Biotechnology*, 2006. **126**(3): p. 295.
36. Petkar, M., et al., *Immobilization of lipases for non-aqueous synthesis*. *Journal of Molecular Catalysis B: Enzymatic*, 2006. **39**(1-4): p. 83.
37. Rojas-Melgarejo, F., et al., *Cinnamic carbohydrate esters show great versatility as supports for the immobilization of different enzymes*. *Enzyme and Microbial Technology*, 2006. **38**(6): p. 748.
38. Woodward, J., ed. *Immobilised cells and enzymes: a practical approach*. The Practical Approach Series. 1985, IRL Press: Oxford.

39. Sheldon, R.A., *Enzyme Immobilization: The Quest for Optimum Performance*. Advanced Synthesis & Catalysis, 2007. **349**(8-9): p. 1289.
40. Arica, M.Y., et al., *Dye derived and metal incorporated affinity poly(2-hydroxyethyl methacrylate) membranes for use in enzyme immobilization*. Polymer International, 1998. **46**(4): p. 345.
41. Krajewska, B., *Application of chitin- and chitosan-based materials for enzyme immobilizations: a review*. Enzyme and Microbial Technology, 2004. **35**(2-3): p. 126.
42. Ardao, I., et al., *One step purification-immobilization of fuculose-1-phosphate aldolase, a class II DHAP dependent aldolase, by using metal-chelate supports*. Enzyme and Microbial Technology, 2006. **39**(1): p. 22.
43. Pessela, B.C.C., et al., *One-Step Purification, Covalent Immobilization, and Additional Stabilization of a Thermophilic Poly-His-Tagged β -Galactosidase from Thermus sp. Strain T2 by using Novel Heterofunctional Chelate-Epoxy Sepabeads*. Biomacromolecules, 2003. **4**(1): p. 107.
44. Yang, W.Y., et al., *Immobilization and characterization of laccase from Chinese Rhus vernicifera on modified chitosan*. Process Biochemistry, 2006. **41**(6): p. 1378.
45. Kawai, T., K. Saito, and W. Lee, *Protein binding to polymer brush, based on ion-exchange, hydrophobic, and affinity interactions*. Journal of Chromatography B, 2003. **790**(1-2): p. 131.
46. Bourdillon, C., et al., *A fully active monolayer enzyme electrode derivatized by antigen-antibody attachment*. J. Am. Chem. Soc., 1993. **115**(26): p. 12264.
47. Bourdillon, C., et al., *Step-by-Step Immunological Construction of a Fully Active Multilayer Enzyme Electrode*. J. Am. Chem. Soc., 1994. **116**(22): p. 10328.
48. Bourdillon, C., et al., *From Homogeneous Electroenzymatic Kinetics to Antigen-Antibody Construction and Characterization of Spatially Ordered Catalytic Enzyme Assemblies on Electrodes*. Acc. Chem. Res., 1996. **29**(11): p. 529.
49. Willner, I. and E. Katz, *Integration of Layered Redox Proteins and Conductive Supports for Bioelectronic Applications*. Angewandte Chemie International Edition, 2000. **39**(7): p. 1180.
50. Anzai, J.i., et al., *Layer-by-Layer Construction of Enzyme Multilayers on an Electrode for the Preparation of Glucose and Lactate Sensors*:

- Elimination of Ascorbate Interference by Means of an Ascorbate Oxidase Multilayer.* Anal. Chem., 1998. **70**(4): p. 811.
51. Cosnier, S., *Biomolecule immobilization on electrode surfaces by entrapment or attachment to electrochemically polymerized films. A review.* Biosensors and Bioelectronics, 1999. **14**(5): p. 443.
 52. Pantano, P., T.H. Morton, and W.G. Kuhr, *Enzyme-modified carbon-fiber microelectrodes with millisecond response times.* J. Am. Chem. Soc., 1991. **113**(5): p. 1832.
 53. Bidan, G., *Electroconducting conjugated polymers: New sensitive matrices to build up chemical or electrochemical sensors. A review.* Sensors and Actuators B: Chemical, 1992. **6**(1-3): p. 45.
 54. Barsan, M.M., et al., *Design and application of a flow cell for carbon-film based electrochemical enzyme biosensors.* Talanta, 2007. **71**(5): p. 1893.
 55. Lin, C.L., C.L. Shih, and L.K. Chau, *Amperometric L-Lactate sensor based on sol-gel processing of an enzyme-linked silicon alkoxide.* Analytical Chemistry, 2007. **79**(10): p. 3757.
 56. Pauliukaite, R., et al., *Characterisation of poly(neutral red) modified carbon film electrodes; application as a redox mediator for biosensors.* Journal of Solid State Electrochemistry, 2007. **11**(7): p. 899.
 57. Han, Y.-J., et al., *Catalytic activity of mesoporous silicate-immobilized chloroperoxidase.* Journal of Molecular Catalysis B: Enzymatic, 2002. **17**(1): p. 1.
 58. Gill, I., E. Pastor, and A. Ballesteros, *Lipase-Silicone Biocomposites: Efficient and Versatile Immobilized Biocatalysts.* J. Am. Chem. Soc., 1999. **121**(41): p. 9487.
 59. Takahashi, H., et al., *Immobilized enzymes in ordered mesoporous silica materials and improvement of their stability and catalytic activity in an organic solvent.* Microporous and Mesoporous Materials, 2001. **44-45**: p. 755.
 60. Long, W.S., A. Kamaruddin, and S. Bhatia, *Chiral resolution of racemic ibuprofen ester in an enzymatic membrane reactor.* Journal of Membrane Science, 2005. **247**(1-2): p. 185.
 61. Wang, Y., et al., *Immobilization of lipase with a special microstructure in composite hydrophilic CA/hydrophobic PTFE membrane for the chiral separation of racemic ibuprofen.* Journal of Membrane Science, 2007. **293**(1-2): p. 133.

62. Ates, S., et al., *Production of l-DOPA using Cu-alginate gel immobilized tyrosinase in a batch and packed bed reactor*. *Enzyme and Microbial Technology*, 2007. **40**(4): p. 683.
63. Jiang, Z., et al., *Encapsulation of β -Glucuronidase in Biomimetic Alginate Capsules for Bioconversion of Baicalin to Baicalein*. *Ind. Eng. Chem. Res.*, 2007. **46**(7): p. 1883.
64. Caruso, F., et al., *Enzyme Encapsulation in Layer-by-Layer Engineered Polymer Multilayer Capsules*. *Langmuir*, 2000. **16**(4): p. 1485.
65. Zou, J.-l. and X.-l. Chen, *Using silica nanoparticles as a catalyst carrier to the highly sensitive determination of thiamine*. *Microchemical Journal*, 2007. **86**(1): p. 42.
66. Schoevaart, R., et al., *Preparation, optimization, and structures of cross-linked enzyme aggregates (CLEAs)*. *Biotechnology and Bioengineering*, 2004. **87**(6): p. 754.
67. Mateo, C., et al., *A new, mild cross-linking methodology to prepare cross-linked enzyme aggregates*. *Biotechnology and Bioengineering*, 2004. **86**(3): p. 273.
68. Dalal, S., M. Kapoor, and M.N. Gupta, *Preparation and characterization of combi-CLEAs catalyzing multiple non-cascade reactions*. *Journal of Molecular Catalysis B: Enzymatic*, 2007. **44**(3-4): p. 128.
69. López-Serrano, P., et al., *Cross-linked enzyme aggregates with enhanced activity: application to lipases*. *Biotechnology Letters*, 2002. **24**(16): p. 1379.
70. Cao, L., F. van Rantwijk, and R.A. Sheldon, *Cross-Linked Enzyme Aggregates: A Simple and Effective Method for the Immobilization of Penicillin Acylase*. *Org. Lett.*, 2000. **2**(10): p. 1361.
71. Tyagi, R., R. Batra, and M.N. Gupta, *Amorphous enzyme aggregates: stability toward heat and aqueous-organic cosolvent mixtures*. *Enzyme and Microbial Technology*, 1999. **24**(5-6): p. 348.
72. van Langen, L.M., et al., *Cross-Linked Aggregates of (R)-Oxynitrilase: A Stable, Recyclable Biocatalyst for Enantioselective Hydrocyanation*. *Org. Lett.*, 2005. **7**(2): p. 327.
73. Govardhan, C.P., *Crosslinking of enzymes for improved stability and performance*. *Current Opinion in Biotechnology*, 1999. **10**(4): p. 331.
74. Jegan Roy, J. and T. Emilia Abraham, *Strategies in Making Cross-Linked Enzyme Crystals*. *Chem. Rev.*, 2004. **104**(9): p. 3705.

75. Abraham, T.E., et al., *Crosslinked enzyme crystals of glucoamylase as a potent catalyst for biotransformations*. Carbohydrate Research, 2004. **339**(6): p. 1099.
76. Ayala, M., et al., *Cross-linked crystals of chloroperoxidase*. Biochemical and Biophysical Research Communications, 2002. **295**(4): p. 828.
77. te Hennepe, H.J.C., et al., *Zeolite-filled silicone rubber membranes Experimental determination of concentration profiles*. Journal of Membrane Science, 1994. **89**(1-2): p. 185.
78. Guan, H.-M., et al., *Poly(vinyl alcohol) multilayer mixed matrix membranes for the dehydration of ethanol-water mixture*. Journal of Membrane Science, 2006. **268**(2): p. 113.
79. te Hennepe, H.J.C., et al., *Zeolite-filled silicone rubber membranes : Part 1. Membrane preparation and pervaporation results*. Journal of Membrane Science, 1987. **35**(1): p. 39.
80. Duval, J.M., et al., *Adsorbent filled membranes for gas separation. Part 1. Improvement of the gas separation properties of polymeric membranes by incorporation of microporous adsorbents*. Journal of Membrane Science, 1993. **80**(1): p. 189.
81. Li, Y., et al., *The effects of polymer chain rigidification, zeolite pore size and pore blockage on polyethersulfone (PES)-zeolite A mixed matrix membranes*. Journal of Membrane Science, 2005. **260**(1-2): p. 45.
82. Pechar, T.W., et al., *Preparation and characterization of a glassy fluorinated polyimide zeolite-mixed matrix membrane*. Desalination, 2002. **146**(1-3): p. 3.
83. Suer, M.G., N. Bac, and L. Yilmaz, *Gas permeation characteristics of polymer-zeolite mixed matrix membranes*. Journal of Membrane Science, 1994. **91**(1-2): p. 77.
84. Duval, J.M., et al., *Preparation of zeolite filled glassy polymer membranes*. Journal of Applied Polymer Science, 1994. **54**(4): p. 409.
85. Kim, S., T.W. Pechar, and E. Marand, *Poly(imide siloxane) and carbon nanotube mixed matrix membranes for gas separation*. Desalination, 2006. **192**(1-3): p. 330.
86. Lensmeyer, G.L., et al., *Use of particle-loaded membranes to extract steroids for high-performance liquid chromatographic analyses improved analyte stability and detection*. Journal of Chromatography A, 1995. **691**(1-2): p. 239.

87. Lingeman, H. and S.J.F. Hoekstra-Oussoren, *Particle-loaded membranes for sample concentration and/or clean-up in bioanalysis*. Journal of Chromatography B: Biomedical Sciences and Applications, 1997. **689**(1): p. 221.
88. Baxter-International, *Composite membranes and methods to make such membranes*. 1999, Patent WO0002638. p. 58.
89. Millipore, *Cast membrane structures for sample preparation*. 2000, Patent US6048457.
90. Tokuyama-Soda-Kabushiki-Kaisha, *Microporous shaped article and process for preparation thereof*. 1993, Patent US5238735.
91. Ballinas, L., et al., *Factors influencing activated carbon-polymeric composite membrane structure and performance*. Journal of Physics and Chemistry of Solids, 2004. **65**(2-3): p. 633.
92. Avramescu, M.-E., et al., *Preparation of mixed matrix adsorber membranes for protein recovery*. Journal of Membrane Science, 2003. **218**(1-2): p. 219.
93. Vu, D.Q., W.J. Koros, and S.J. Miller, *Mixed matrix membranes using carbon molecular sieves: I. Preparation and experimental results*. Journal of Membrane Science, 2003. **211**(2): p. 311.
94. Ludtke, K., et al., *Nitrate removal of drinking water by means of catalytically active membranes*. Journal of Membrane Science, 1998. **151**(1): p. 3.
95. Avramescu, M.-E., Z. Borneman, and M. Wessling, *Dynamic behavior of adsorber membranes for protein recovery*. Biotechnology and Bioengineering, 2003. **84**(5): p. 564.
96. Avramescu, M.-E., Z. Borneman, and M. Wessling, *Mixed-matrix membrane adsorbers for protein separation*. Journal of Chromatography A, 2003. **1006**(1-2): p. 171.
97. Saiful, Z. Borneman, and M. Wessling, *Enzyme capturing and concentration with mixed matrix membrane adsorbers*. Journal of Membrane Science, 2006. **280**(1-2): p. 406.
98. Avramescu, M.E., et al., *Adsorptive membranes for bilirubin removal*. Journal of Chromatography B, 2004. **803**(2): p. 215.

3

Novel membranes for enzymatic conversion

ABSTRACT

Particle-loaded mixed matrix membranes (MMM's) for enzymatic conversions have been prepared by covalently binding trypsin molecules on Eupergit® particles embedded in a macroporous EVAL matrix. The MMM's performance was studied to determine the dynamic trypsin immobilization capacity and the dynamic trypsin enzymatic activity after immobilization. Modification with ethylenediamine and activation with glutaraldehyde increases the enzymatic activity of the Eupergit® particles. The MMM's containing modified Eupergit® particles show an increased immobilization capacity and a more than nine fold increase in enzymatic activity. A comparison between membrane-embedded modified Eupergit® particles and modified Eupergit® in a packed bed showed an overall better performance of the membrane based system. The highest enzymatic conversion rates were obtained with milled Eupergit® C particles that were chemically modified and embedded in a macro-porous membrane structure.

3.1 INTRODUCTION

Enzymes have been used in pharmaceutical and chemical industries for decades. In recent years, the demands for more selective and enantiomerically pure chemicals for pharmaceutical and biochemical applications are increasing. Biotransformations tend to be simpler than normal chemical processes, eliminating the need for many other chemicals and reducing the amount of waste involved in the reactions [1].

Due to the rapid growth of this area, the need for more economical enzyme use is desired. Therefore, enzyme immobilization in solid supports has been widely spread in biotechnology. With this technique it is possible to reuse enzymes, an option which is unavailable when enzymes are applied in the free form. Besides this, immobilization also prolongs enzyme lifetime due to increased stability, which permits the use of the enzyme in a larger array of conditions [2].

Several enzyme immobilization techniques have been applied, such as crosslinking, adsorption, adsorption with subsequent crosslinking, covalent binding, entrapment or enzyme crystallization [3]. Two types of solid support have been mainly used for enzyme immobilization: particles and membranes. Particles provide high capacities and selectivities and can be selected according to the chromatographic application [4]. Membranes provide higher dynamic capacities and are less susceptible to bed compression [5] being easily scaled-up [6].

In recent years, a synergistic match between the two approaches was reported [4, 7-9] for protein isolation and concentration based on electrostatic interaction. This platform technique, named mixed matrix membrane, consists out of a macro-porous polymeric structure in which functionalized particles are embedded in order to selectively isolate or concentrate proteins. The platform is also used for enzyme purification and concentration, maintaining the enzymatic activity after desorption [9].

In this study, a new approach for enzyme immobilization is introduced. Two types of Eupergit® beads, Eupergit® C (average pore size of 10 nm) and Eupergit® C250L (average pore size of 100 nm), both containing oxirane functional groups and widely used in enzyme immobilization [3], were embedded in a macro-porous membrane where the enzymes are afterwards covalently bound. A summary with the Eupergit® particles' characteristics can be found in table 3.1. The influence of the embedding process on the beads oxirane density was studied, as well as the morphology of the fabricated

membranes. Trypsin, chosen as the model enzyme in the immobilization studies, was dynamically immobilized via covalent binding on embedded Eupergit® particles. The activity of the immobilized trypsin was measured by the L-Benzoyl-Arginine-Ethyl-Ester (BAEE) conversion. The Eupergit® particles were chemically modified to improve the immobilization and conversion processes.

Table 3.1 – Eupergit® characteristics as supplied by the producer.

Type of Eupergit® particle	Oxirane density		Average pore size	Particle size
	($\mu\text{mol/g}$)	(wt. %)	(nm)	(μm)
Eupergit® C250L	331	0.53	100	100-250
Eupergit® C	802	1.28	10	100-250

3.2 EXPERIMENTAL

3.2.1 Materials

Eval (a random copolymer of ethylene and vinyl alcohol) with an average ethylene content of 44 mol% was purchased from Aldrich and used without further modification. Hydrochloric acid (Merck) and sodium thiosulfate (Merck) were used in the Eupergit® characterization. Dimethylsulfoxide (DMSO, Merck) was employed as solvent and 1-Octanol (Fluka) as non-solvent additive. Water was used as non-solvent in the coagulation bath. Ethylenediamine (Acros) and glutaraldehyde (Acros) were used in the chemical modification of the particles. Ethanol was used for washing the Eupergit® particles after the chemical modification. Potassium phosphate (mono- and dibasic, Acros) and Tris-HCl (Sigma) were used for preparing buffer solutions. Trypsin from porcine pancreas (Sigma) with an activity of 1500 BAEE units/mg was used as enzyme and L-Benzoyl-Arginine-Ethyl-Ester (BAEE, Sigma) as substrate. Calcium chloride (Acros) was added to the enzyme solutions to prevent trypsin self-digestion. Eupergit® C and Eupergit® C250L beads were kindly provided by Degussa (Germany). Ultrapure water was prepared using a Millipore purification unit Milli-Q plus.

3.2.2 Particle modification

Prior to embedding, in order to improve the active area, provide a better embedding and reduce the diffusive path, the Eupergit® particles were grinded and fractionated to 20-40 μm size class. A Fritsch analysette shaker with 20 and 40 μm sieves stacked was used. Glass beads were added during sieving to provide impact. In order to improve the immobilization and conversion processes, chemical modification of the Eupergit® particles was carried out as described by Petro *et al* [10]. To protect the chemically active groups, the beads were modified by reacting with ethylenediamine at 80 °C for 72 hours in order to change the oxirane functionality into more stable amine groups. After the reaction was terminated, the beads were washed consecutively with abundant ethanol, water and 0.1 M phosphate buffer pH 6.9 while stirring gently. Each washing solution was then removed by using a Buchner funnel. The modified beads were activated as depicted in figure 3.1 by using a 10% solution of glutaraldehyde in phosphate buffer pH 6.9 at 30 °C for 3 hours. Finally, prior to use, the beads were washed with abundant water, acetone and dried under vacuum at room temperature for one week.

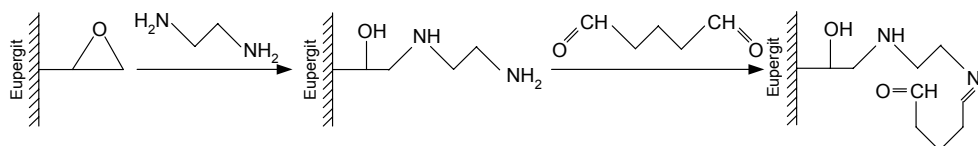


Figure 3.1 – Schematic representation of the chemical modification of Eupergit®. The oxirane group of the Eupergit® particles reacts with ethylenediamine, followed by an activation step using glutaraldehyde.

3.2.3 Eupergit® characterization

Oxirane density

The particle oxirane density was determined by the method as described by Sundberg and Porath [11] according to the scheme shown in figure 3.2.

The thiosulfate ions present in the solution open the oxirane ring thus producing hydroxyl ions in a 1:1 proportion. The amount of produced OH^- was determined by a back titration with hydrochloric acid. For this, 300 mg (600 mg for mixed matrix membranes) of particles were suspended under gentle swirling in deionized water and the pH was adjusted to 7.0. 15 ml of a

$\text{Na}_2\text{S}_2\text{O}_3$ 1.3 M solution was added and the suspension was shaken for two hours in order to allow the reaction to complete. The OH^- ions were then back titrated with a 0.01 M HCl solution to determine the oxirane density.

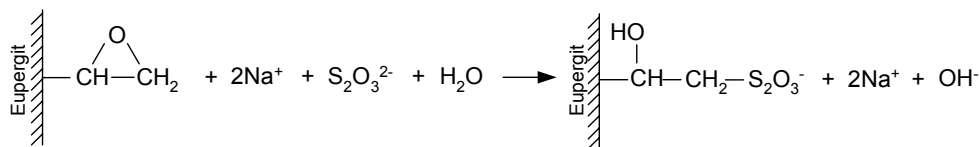


Figure 3.2 – Schematic representation of the reaction of $\text{Na}_2\text{S}_2\text{O}_3(\text{aq})$ with Eupergit® particles to determine oxirane density.

Solvent influence

To assess the influence of the membrane preparation process in oxirane density, Eupergit® particles were dispersed in DMSO, 1-octanol and water and stirred overnight at 45 °C. Afterwards, the particles were washed with abundant cold water, ethanol and acetone and dried under vacuum for one week before determining the oxirane density. Parallel control tests proved that cold water, ethanol and acetone had no influence in oxirane density.

3.2.4 Mixed matrix membranes

The membranes were prepared according to the method as published by Avramescu *et al* [4] using EVAL as the polymeric matrix. A dope solution was prepared by dissolving overnight at 45 °C 10 wt% EVAL, in a solution containing 1 part 1-Octanol and 8 parts DMSO. After the solution was homogenized, milled Eupergit® particles, either modified or unmodified, with an equivalent weight to EVAL, were added. The mixture was left under strong stirring for over 24 hours to break down any particle clusters. The solution was cast at room temperature on a glass plate using a 0.47 mm casting knife. The glass plate with the polymer solution was then immersed in a water bath at 40-45 °C to promote polymer precipitation. The formed membrane was then washed continuously with water for over 72 hours to remove all 1-octanol traces. Finally, the membrane was air dried and cut into disks of 2.5 cm in diameter.

SEM characterization

The membrane morphology was investigated by scanning electron microscopy (SEM). To expose cross-section areas, fresh wetted membrane pieces were frozen in liquid nitrogen and fractured. After drying, the samples were gold coated using a Balzers Union SCD 040 coater and examined using a Jeol JSM-5600 LV Scanning Electron Microscope.

Clean water fluxes

The membrane clean water flux was determined using a nitrogen pressurized stirred dead-end ultrafiltration cell. The filtration experiments were carried out at room temperature with a transmembrane pressure of 0.5 bar. The pure water flux was determined after steady state condition was obtained.

3.2.5 Trypsin immobilization

Static immobilization

Trypsin was dissolved in a 0.02 M solution of CaCl_2 in Tris-HCl buffer, pH 7.0 to a concentration of 1 mg/mL. CaCl_2 was added to minimize trypsin self-digestion by the action of the Ca^{2+} ions in solution [12, 13]. 500 mg of particles were suspended in a 20 mL trypsin solution and kept for 72 hours at 4 °C and shaken occasionally. The immobilized amount was determined by measuring the trypsin depletion in the supernatant solution through monitoring the UV absorbance at $\lambda=280$ nm using a Cary 300 Varian photometer.

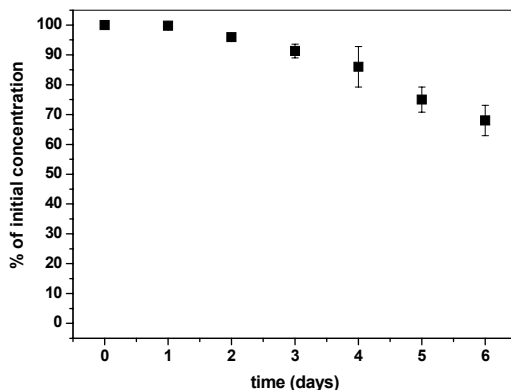


Figure 3.3 – Decrease in trypsin concentration over time at 4 °C in presence of CaCl_2 .

Due to a tendency from trypsin to self-digestion, trypsin stability over time was assessed. Solutions of trypsin were prepared to which no Eupergit® was added. The remaining trypsin concentration in the solution was periodically evaluated by UV monitoring after filtering using 0.45 µm Spartan filter units from Schleicher&Schuell. The trypsin concentration decline can be seen in figure 3.3.

Dynamic immobilization

Five MMM disks were stacked in a stainless steel flow cell. The membranes were initially equilibrated by continuously permeating the CaCl₂-containing Tris-HCl buffer under UV absorbance (λ=280 nm) and conductivity monitoring using an Äkta Prime liquid chromatography system. After equilibration was achieved, a trypsin solution of 1 mg/mL in the same buffer was eluted at 0.1 mL/min, equivalent to a residence time of 6.5 minutes, through the stack. The UV signal monitored the trypsin depletion from the system. At the end of the immobilization step, the process was terminated by eluting buffer through the stack in order to remove all unbound trypsin. The amount of trypsin immobilized onto the membrane was measured continuously and calculated according to the following equation:

$$I = \sum i_j \quad (3.1)$$

$$i = \frac{\left(1 - \frac{C'}{C_0}\right) \times C_0 \times V'}{W} \quad (3.2)$$

in which I is the total amount of immobilized trypsin in the membrane (mg/g), i is the fraction of trypsin immobilized in the membrane (mg/g), C' the fractional concentration in the permeate side (mg/mL), C_0 is the initial concentration (mg/mL), V' is the fraction volume (mL) and W is the dry weight of membrane (g).

Activity measurements

The free trypsin activity in aqueous solutions is determined in the cuvette of an UV spectrometer using the standard method [14] at 25 °C with BAEE as substrate [15].

The activity of immobilized trypsin was determined by modifying the standard method, by flowing at 20 °C BAEE solution at different flow rates through the MMM stack containing immobilized trypsin [10, 16-18]. The permeate UV absorbance ($\lambda=254$ nm) was monitored to determine the substrate conversion. The flow rate was changed and the absorbance under steady-state was measured. The absorbance is then plotted against the different residence times as illustrated in figure 3.4.

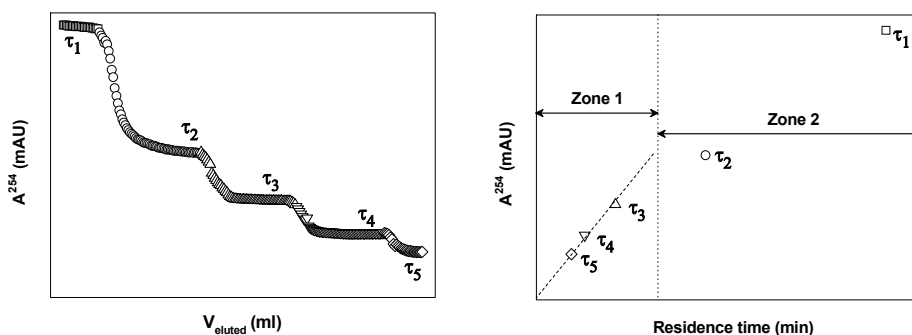


Figure 3.4 – Schematic representation of the activity calculation procedure. $\tau_1 - \tau_5$ represent the different residence times. Zone 1 denotes the enzyme-limiting conversion area and zone 2 denotes the BAEE-limiting conversion area.

The activity of the immobilized trypsin was determined as the slope of the linear increase (zone 1) of the UV signal at 254 nm at different residence times [16] and related to the dry weight of membrane using the following expression:

$$Act = \frac{\Delta A^{254} / \Delta \tau}{m_{MMM}} \quad (3.3)$$

where Act denotes the activity (U/g), $\Delta A^{254} / \Delta \tau$ (mAU/min) is the slope of the linear increase of absorbance and m_{MMM} is the dry mass of MMM used in the experiment (g).

3.3 RESULTS AND DISCUSSION

3.3.1 Oxirane stability in Eupergit® particles

The influence of the different process steps in the MMM preparation on the particles oxirane density was studied. Table 3.2 shows that particle milling does not affect the oxirane density in neither of the particles used. The overall change in oxirane density before and after particle milling in both Eupergit® C and Eupergit® C250L is less than 2%. The results clearly show that the milling process can be safely used for preparing smaller sized particles for embedding in a macroporous structure. Table 3.3 shows the stability in oxirane density as function of the contacting solvents that are applied in the MMM preparation process.

Table 3.2 – Influence of milling on the oxirane density of Eupergit®

Eupergit® C250L	Oxirane density (µmol/g)	Oxirane loss (%)
Normal size (200µm)	331	-
20-40 µm fraction size	325	1.8
Eupergit® C	Oxirane density (µmol/g)	Oxirane loss (%)
Normal size (200µm)	802	-
20-40 µm fraction size	810	-

Table 3.3a – Influence of different solvents on the oxirane density of Eupergit® C250L

Eupergit® C250L	Oxirane density (µmol/g)	Oxirane loss (%)
DMSO	297	10.3
1-Octanol	264	20.2
Water	199	39.9
Mixed matrix membrane	114	65.6

Table 3.3b – Influence of different solvents on the oxirane density of Eupergit® C

Eupergit® C	Oxirane density ($\mu\text{mol/g}$)	Oxirane loss (%)
DMSO	742	7.5
1-Octanol	726	9.5
Water	505	37.0
Mixed matrix membrane	468	41.6

The largest oxirane density decrease can be attributed to the hydrolysis of the functional groups by water. It was found that the oxirane groups of Eupergit® C particles are less affected by the applied solvents. This may be resultant from the smaller pore size and the higher initial oxirane density of Eupergit® C.

3.3.2 Mixed matrix membrane characterization

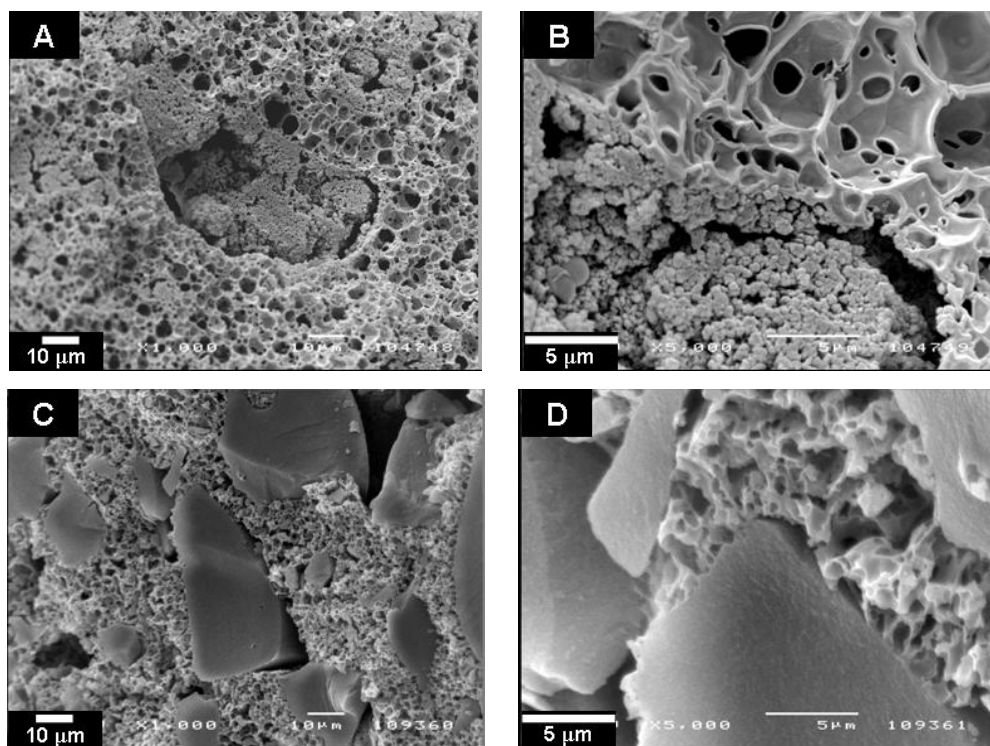


Figure 3.5 – SEM micrographs of Mixed matrix membranes. A and B: membrane ML₅₀. C and D: Membrane MC₅₀. Images A and C, magnification of 1000 \times , the size bar indicates 10 μm . Images B and D, magnification of 5000 \times , the size bar indicates 5 μm .

Mixed matrix membranes were prepared using both available types of Eupergit® particles: Eupergit® C250L (ML₅₀) and Eupergit® C (MC₅₀). The prepared membranes were characterized in terms of morphology, geometric dimensions and clean water flux. The morphology is visualized by Scanning Electron Micrography.

The SEM images of the membranes (figure 3.5) show a highly interconnected structure that allows enzyme and substrate molecules easy access to the active groups located on the embedded particles in the matrix. Both membranes show a high permeability with clean-water fluxes of about 600 L/(m².h.bar).

3.3.3 Static measurements

Before immobilization, trypsin activities were evaluated in static mode in a cuvette using the standard method. The measured activities confirmed the value given by the supplier.

Eupergit® particles

Trypsin was immobilized on original sized particles as well as on milled particles with a size of 20-40 µm. The amount of immobilized trypsin was determined by measuring the trypsin depletion from the supernatant and the obtained results were normalized for the trypsin self-digestion. The results are summarized in table 3.4.

Table 3.4 – Immobilization capacity and enzymatic activity of milled and unmilled Eupergit®

Type of Particle	Immobilized trypsin	Activity
	(mg/g _{dry particle})	(U/g _{dry particle})
Eupergit® C250L (100-250 µm)	9.3	174
Eupergit® C250L (20-40 µm)	11.3	286
Eupergit® C (100-250 µm)	13.0	297
Eupergit® C (20-40 µm)	13.1	407

Milling of Eupergit[®] C250L particles slightly increases the trypsin immobilization. The amount of trypsin immobilized in Eupergit[®] C is higher than in the case of Eupergit[®] C250L, but does not change significantly by milling. This means that trypsin has access to the binding sites located in the pores of Eupergit[®] particles. A much stronger milling effect can be seen by measuring the static activities. The activity is increased by over 60% in the case of Eupergit[®] C250L and by almost 40% in Eupergit[®] C particles. The higher increase in enzymatic activity on Eupergit[®] C250L over Eupergit[®] C particles can be explained by each particle type characteristics. Eupergit[®] C250L, with a lower density of functional groups and larger pores (100 nm), allows for a higher enzyme immobilization on the inside of the pore structure, meaning a more diffusive controlled process and reduced accessibility to the substrate by the immobilized trypsin.

In the case of milled particles, more functional groups are exposed, which increases the immobilized enzymes accessibility to the substrate medium. In the case of Eupergit[®] C, the pore size (10 nm) reduces the enzyme mobility after immobilization, as exemplified in figure 3.6, which means that conversion will take place preferably at the outer particle surface. After milling, the higher surface area increases the access to the active sites, thereby increasing enzymatic activity. Results for both types of particles indicate that substrate is converted mainly on the outer surface and that the internal area of the particles is not effectively contributing to the enzymatic activity.

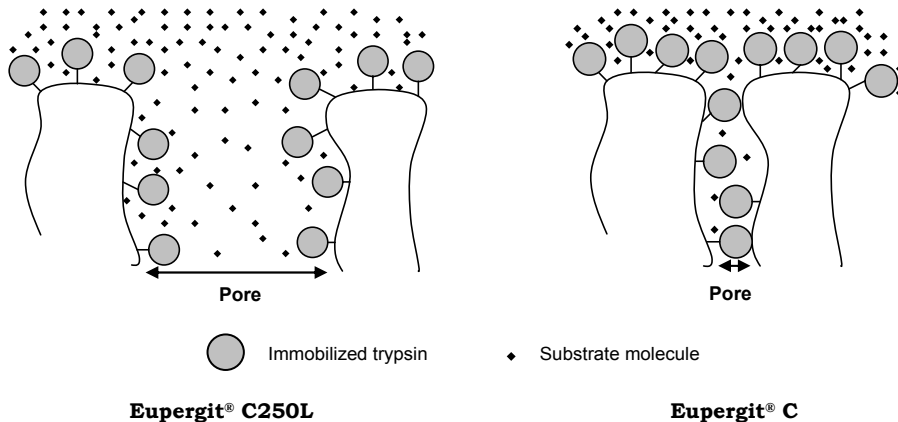


Figure 3.6 – Accessibility to immobilized trypsin inside Eupergit[®] pores.

3.3.4 Dynamic measurements

Dynamic immobilization

Trypsin was immobilized by permeating a solution containing 1 mg trypsin/mL at a flow rate of 0.1 mL/min, equivalent to a residence time of 6.5 minutes, through the membrane stack. The immobilization dynamics are presented in figure 3.7. All experiments were repeated a minimum of three times.

As can be seen in table 3.5, both membranes show a similar enzyme loading capacity. Trypsin immobilization in ML₅₀ is faster than in MC₅₀. This is likely due to the fact that in the case of Eupergit® C, particles with a higher density of oxirane groups, trypsin tends to have a higher immobilization on the external surface of the particles, thus partly blocking access to the pore structure. Furthermore, the high oxirane density can cause bound trypsin on the surface to rearrange the orientation, due to steric hindrance, thus reducing immobilization speed. In the case of embedded Eupergit® C250L particles, this effect is less pronounced, due to the much larger pore sizes which present no significant hindrance to the enzyme diffusion into the internal particle structure.

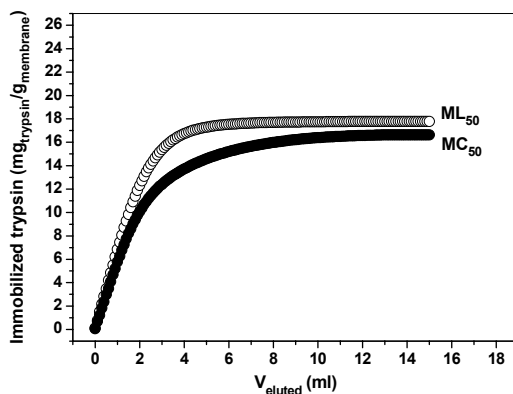


Figure 3.7 – Dynamic immobilization of trypsin in the prepared membranes.

Table 3.5 – Total amount of immobilized trypsin in membranes with unmodified Eupergit®

Membrane	Immobilized trypsin (mg/g _{membrane})
ML ₅₀	17.8 ± 1.5
MC ₅₀	16.6 ± 1.3

For both types of particles, the embedding process causes a significant increase in immobilization capacity. The differences are explained by the immobilization methods followed in each case. In static immobilization, trypsin molecules need to diffuse into a particle bed and attach to the surface in a diffusion-controlled process. In dynamic immobilization, there is a clear intrusion into the particles due to convection, which improves the immobilization process.

Dynamic activities

The dynamic activity of the prepared MMM's was evaluated by flowing BAEE in Tris-HCl buffer pH 7.6 at different flow rates ranging from 0.1 to 5 mL/min. The permeate UV absorbance was monitored to evaluate the enzymatic activities. The results are presented on table 3.6.

Table 3.6 – Enzymatic activity of membranes containing unmodified Eupergit®

Membrane	Activity (U/g_{membrane})
ML ₅₀	103 ± 2.4
MC ₅₀	224 ± 23.2

The enzymatic activity of the Eupergit® C-containing membranes proved to be higher than the Eupergit® C250L-containing MMM's. This can be attributed to the fact that trypsin binds preferably on the external surface in the case of Eupergit® C more than on Eupergit® C250L particles. These factors cause Eupergit® C to present a more convective-controlled mechanism. In case of Eupergit® C250L, trypsin is also strongly immobilized on the inner surface, with large enough pores to allow a strong contribution of these enzyme molecules to the overall activity. This leads to a partially diffusive-controlled mechanism, thus reducing the conversion rate.

3.3.5 MMM's containing chemically modified Eupergit®

Dynamic immobilization

The chemically modified Eupergit® C and Eupergit® C250L particles (chemical reaction depicted in figure 3.1) were milled and fractioned to obtain a

size class of 20-40 μm and embedded in EVAL₄₄ macroporous membranes. The membranes showed similar structures and the same clean-water fluxes of 600 l/(m².h.bar) as the ones containing milled unmodified particles. The trypsin immobilization results are presented in figure 3.8 and table 3.7.

Membranes containing chemically modified Eupergit[®] C particles showed a much higher immobilization capacity for trypsin than the ones containing chemically modified Eupergit[®] C250L. The reason is probably related to the higher density of active functional groups at the outer surface of the Eupergit[®] C particles and the fact that the added aldehyde functionality is less prone to be lost during the embedding process. The increase in immobilization capacity between membranes containing unmodified Eupergit[®] C and membranes containing modified particles supports this possibility. Also, the addition of a spacer allows a better organization of the immobilized trypsin due to a lower steric hindrance between the molecules, which results in a higher immobilization per surface area.

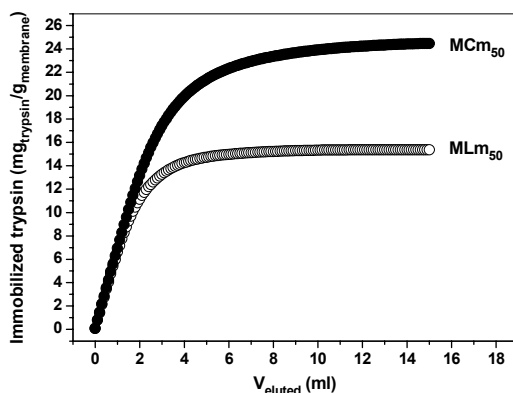


Figure 3.8 – Dynamic immobilization of trypsin in the prepared membranes.

Table 3.7 – Total amount of immobilized trypsin in membranes containing chemically modified Eupergit[®]

Membrane	Immobilized trypsin (mg/g _{membrane})
MLm ₅₀	15.4 ± 0.03
MCm ₅₀	24.5 ± 2.9

A representation of this effect can be seen in figure 3.9. The increase in active functional groups on the outer surface of the Eupergit® C250L particles after chemical modification explains the slightly lower (17.8 vs. 15.4 mg/g_{membrane}) trypsin immobilization due to pore blocking.

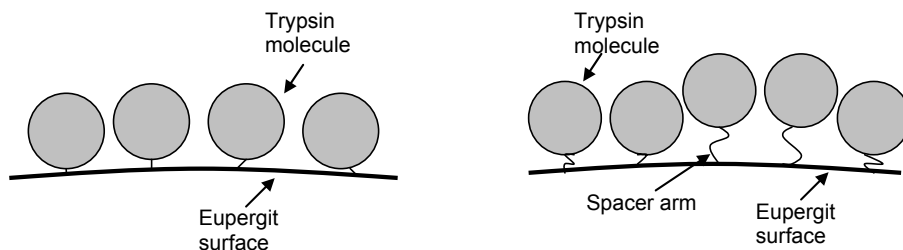


Figure 3.9 – Increase in immobilization due to spacer addition.

Dynamic activities

The membranes containing chemically modified Eupergit® particles were also tested in terms of enzymatic activity with the results presented in table 3.7.

Table 3.8 – Enzymatic activity of membranes containing modified Eupergit®

Membrane	Activity (U/g_{membrane})
MLm ₅₀	325 ± 1.4
Mcm ₅₀	1835 ± 58.6

Both membranes show a strong increase in enzymatic activity compared to membranes containing chemically unmodified particles. Membranes containing modified Eupergit® C250L show a three-fold increase in activity, whereas membranes containing modified Eupergit® C improve nine times their activity. Noting that in the case of Mcm₅₀, the increase in activity is much higher than the increase in trypsin immobilization, the activity improvement is contributed to the spacer arm, which reduces steric hindrance effects between the immobilized enzyme molecules, while provides better accessibility to the substrate. In the case of MLm₅₀, the same effect is also visible, although less pronounced due to a lower density of functional groups on the particle surface, which causes an increase in the distance between adjacent immobilized enzyme molecules, thus reducing the advantage provided by the spacer arm.

Packed bed particles

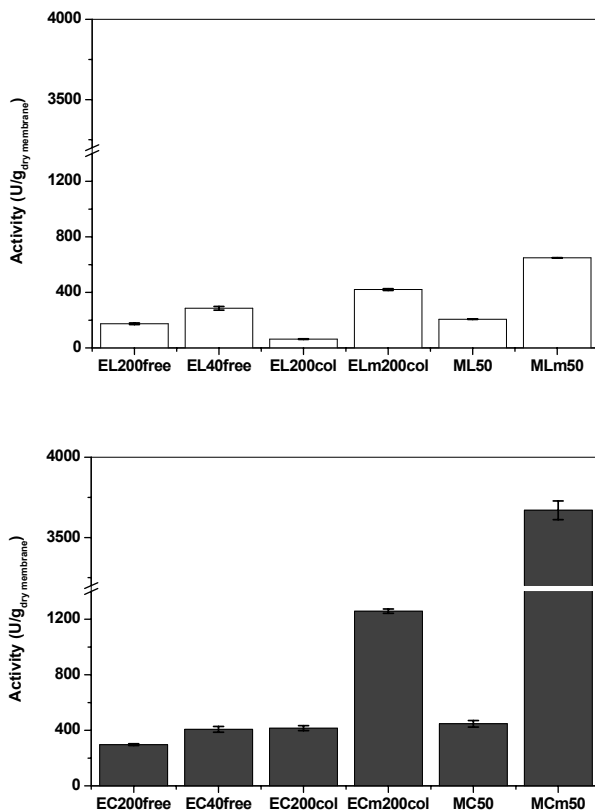


Figure 3.10 – Enzymatic activity of trypsin immobilized on Eupergit® C250L and Eupergit® C particles in different situations. Activities related to weight of dry particles. For MMM's, the activities were recalculated for the particle loading of 50% (w/w). The results represent the median value of at least three experiments.

Legend:

- EL200free** – Unmodified Eupergit® C250L particles (200 μm) in suspension
- EL40free** – Unmodified Eupergit® C250L particles (20-40 μm) in suspension
- EL200col** – Unmodified Eupergit® C250L particles (200 μm) in a packed bed column
- ELm200col** – Modified Eupergit® C250L particles (200 μm) in a packed bed column
- ML50** – MMM containing unmodified Eupergit® C250L particles (20-40 μm)
- MLm50** – MMM containing modified Eupergit® C250L particles (20-40 μm)
- EC200free** – Unmodified Eupergit® C particles (200 μm) in suspension
- EC40free** – Unmodified Eupergit® C particles (20-40 μm) in suspension
- EC200col** – Unmodified Eupergit® C particles (200 μm) in a packed bed column
- ECm200col** – Modified Eupergit® C particles (200 μm) in a packed bed column
- MC50** – MMM containing unmodified Eupergit® C particles (20-40 μm)
- MCm50** – MMM containing modified Eupergit® C particles (20-40 μm)

For comparison purposes, the enzymatic activity of particles in a packed bed was studied. Figure 3.10 illustrates that Eupergit® C particles, containing a lower pore size and a higher density of functional groups, provide generally higher activities than Eupergit® C250L particles. This is due to the fact that trypsin preferably immobilizes on the external surface of Eupergit® C, thus causing substrate conversion to be more convectively controlled. In the case of Eupergit® C250L, trypsin also tends to use the internal surface area, causing the conversion to be diffusive controlled and thus reducing the enzymatic activity of the activated particles. The chemical modification of the particles improves the activity of the particles in two ways, by protecting the functionality during the embedding process due to the presence of less reactive groups and by adding a short molecular spacer which imparts the immobilized enzymes with a better mobility. The effect is more visible on Eupergit® due to the high density of functional groups. In the absence of a spacer arm, trypsin molecules cause steric hindrance to each other, while after chemical modification, the spacer arm improves mobility and reduces the steric hindrance effects.

The embedding of the particles in a membrane structure improves the activity in all situations, due to lower bed compression and higher flow convection between the particles. Comparing 100-250 μm sized Eupergit® particles packed in a column with the MMM equivalent, the activity gain is approximately three fold for all cases, thus confirming the higher efficiency of the mixed matrix platform.

3.4 CONCLUSIONS

This work presents a new type of platform technology for enzymatic conversions, based on macro-porous membranes as a structured support for enzymatically activated particles. Eupergit® C250L and Eupergit® C particles are sized down and chemically modified before embedding to prepare particle loaded membranes applicable for enzymatic conversions. During the milling and embedding processes, about 40 and 65% of the original oxirane density was retained for Eupergit® C250L and Eupergit® C, respectively. This loss is overcompensated by the increase in enzymatic activity compared to Eupergit® particles in packed bed columns. Chemically modifying Eupergit® significantly increases the enzymatic activity of the particles both in packed beds and embedded in membranes. Due to a more convectively controlled mechanism, Eupergit® C proves to be more effective than Eupergit® C250L. This is proven by trypsin immobilization and enzymatic conversion of BAEE.

The advantage compared to conventional packed bed systems is the lower diffusion resistance and higher capacity because of the use of smaller particles without the unavoidable pressure increase that promotes bed compression and enzyme denaturation. Furthermore, the technology offers high industrial potential by the use of scaling-up.

Acknowledgments

The authors acknowledge The Netherlands Organization for Scientific Research (NWO) for the financial support of this project. The authors are also grateful to Degussa Specialty Polymers for providing the Eupergit® particles used in the studies.

REFERENCES

1. Boller, T., C. Meier, and S. Menzler, EUPERGIT oxirane acrylic beads: How to make enzymes fit for biocatalysis. *Organic Process Research & Development*, 2002. 6(4): p. 509.
2. Tischer, W. and F. Wedekind, Immobilized enzymes: Methods and applications, in *Biocatalysis - From Discovery To Application*. 1999. p. 95.
3. Katchalski-Katzir, E. and D.M. Kraemer, Eupergit (R) C, a carrier for immobilization of enzymes of industrial potential. *Journal Of Molecular Catalysis B-Enzymatic*, 2000. 10(1-3): p. 157.
4. Avramescu, M.E., et al., Preparation of mixed matrix adsorber membranes for protein recovery. *Journal Of Membrane Science*, 2003. 218(1-2): p. 219.
5. Ghosh, R., Protein separation using membrane chromatography: opportunities and challenges. *Journal Of Chromatography A*, 2002. 952(1-2): p. 13.
6. Borneman, Z., Particle loaded membrane chromatography. 2006, University of Twente: Enschede.
7. Avramescu, M.E., Z. Borneman, and M. Wessling, Mixed-matrix membrane adsorbers for protein separation. *Journal Of Chromatography A*, 2003. 1006(1-2): p. 171.

8. Avramescu, M.E., et al., Adsorptive membranes for bilirubin removal. *Journal Of Chromatography B-Analytical Technologies In The Biomedical And Life Sciences*, 2004. 803(2): p. 215.
9. Saiful, Z. Borneman, and M. Wessling, Enzyme capturing and concentration with mixed matrix membrane adsorbers. *Journal of Membrane Science*, 2006. 280(1-2): p. 406.
10. Petro, M., F. Svec, and J.M.J. Frechet, Immobilization of trypsin onto molded macroporous poly(glycidyl methacrylate-co-ethylene dimethacrylate) rods and use of the conjugates as bioreactors and for affinity chromatography. *Biotechnology and Bioengineering*, 1996. 49(4): p. 355.
11. Sundberg, L. and J. Porath, Preparation Of Adsorbents For Biospecific Affinity Chromatography .1. Attachment Of Group-Containing Ligands To Insoluble Polymers By Means Of Bifunctional Oxiranes. *Journal Of Chromatography*, 1974. 90(1): p. 87.
12. Muller, O.H. and I. Yamanouchi, Stable solutions of trypsin. *Archives of Biochemistry and Biophysics*, 1958. 76(2): p. 328.
13. Nord, F.F., M. Bier, and L. Terminiello, On the mechanism of enzyme action. LXI. The self digestion of trypsin, calcium-trypsin and acetyl-trypsin. *Archives of Biochemistry and Biophysics*, 1956. 65(1): p. 120.
14. Rick, W., ed. Trypsin. 1st ed. *Methods of enzymatic analysis*, ed. H.U. Bergmeyer. 1965, Verlag Chemie: Weinheim. 807.
15. Barman, T.E., *Enzyme Handbook*. Vol. 2. 1969, Berlin: Springer. 618.
16. Bencina, K., et al., Enzyme immobilization on epoxy- and 1,1 '-carbonyldiimidazole-activated methacrylate-based monoliths. *Journal Of Separation Science*, 2004. 27(10-11): p. 811.
17. Peterson, D.S., et al., Enzymatic microreactor-on-a-chip: Protein mapping using trypsin immobilized on porous polymer monoliths molded in channels of microfluidic devices. *Analytical Chemistry*, 2002. 74(16): p. 4081.
18. Xie, S., F. Svec, and J.M.J. Frechet, Design of reactive porous polymer supports for high throughput bioreactors: Poly(2-vinyl-4,4-dimethylazlactone-co-acrylamide-co-ethylene dimethacrylate) monoliths. *Biotechnology and Bioengineering*, 1999. 62(1): p. 30.

4

Enzymatic conversion using mixed matrix hollow fibers

ABSTRACT

Mixed matrix hollow-fibers (MMHF) containing embedded Eupergit® C particles were developed for enzymatic conversions. The Eupergit® C particles were chemically modified with ethylenediamine and activated with glutaraldehyde, milled and sieved into two different size classes, 20-40 μm and $< 20 \mu\text{m}$, before embedding in the fibers. The fiber structure was optimized by varying the solvent, additive and polymer ratio in the dope solution. Dynamic activity experiments of immobilized trypsin proved that the prepared hollow-fibers allowed trypsin to retain a high degree of activity. The results showed a higher trypsin activity with fibers prepared with particles from the sieve fraction below 20 μm over those containing particles in the size class of 20-40 μm . MMHF showed a four times increase in trypsin activity when compared to flat-sheet mixed matrix membranes and more than 35 times when compared to a packed bed system containing unmodified Eupergit® C particles.

4.1 INTRODUCTION

Membrane chromatography has been developed in the last few decades as an alternative to traditional chromatography. Chromatography tends to be carried out using packed beds, which present problems in terms of high pressure drop, diffusion limitations, channeling and possible existence of radial and axial dispersion limitations. All these transport limitations cause that scale-up of chromatography packed-bed processes is difficult [1].

One solution to overcome this problem has been presented in the form of membrane chromatography [2]. In this process, micro- or macroporous synthetic membranes are used as chromatographic media. In membrane systems, solute transport to binding sites takes place predominantly by convection, which reduces transport time and elution volumes and minimizes diffusion limitations. Due to much lower pressure drop through the column, the process permits the use of high flow-rates. One major advantage of membrane chromatographic systems over packed bed columns is the easy scale-up of the processes. Furthermore, membrane chromatographic systems are cheaper and simpler to produce, which makes possible the existence of disposable membrane modules that could be replaced when the life-time of the membranes is over, thus eliminating the need for costly cleaning procedures [1, 3].

One of the main disadvantages from traditional, chemically activated, membrane chromatographic processes is the lower capacity of membrane based systems when compared to packed bed columns, especially in the case of smaller sized protein molecules that have complete access to the entire particle pore structure. Due to higher surface areas, porous particles provide more binding sites and have therefore higher binding capacities. In the case of larger molecules, which are not able to diffuse into the particle pore structure, membrane chromatography has advantages due to less diffusion limitations [1, 4].

Membrane chromatography is available for a large array of different interactions such as ion-exchange, hydrophobic, reverse-phase and affinity. In terms of geometry, mainly flat-sheet and hollow-fiber systems have been reported [1]. Membranes have been attractive mainly in the field of preparative chromatography, with an especial regard to hollow-fiber membranes [5].

Recently, a new platform technology has been reported aiming at the synergistic merge of traditional chromatographic particles and membrane technology for protein adsorption and separation. The technology, called mixed

matrix membrane (MMM) consists on the entrapment of particulate functional material in a porous matrix. In this method, the particulate material is dispersed in a mixture consisting of dissolved polymers and additives that are cast or spun and precipitated by a dry-wet phase inversion process to obtain a flat-sheet or a fiber membrane. The prepared membranes can then be incorporated in porous beds or fibrous modules without functionality loss. Reported applications consist of steroid extraction [6], protein adsorption [7], protein separation [8] and enzyme concentration [9]. Alternatively, MMM containing particles with ion-exchange functionality have been used for protein adsorption which, after cross-linking, could be used as a ligand for toxin removal [10].

In this work, mixed matrix hollow-fibers were prepared containing particles with covalent functionality that are used for enzyme immobilization and enzymatic substrate conversion. Trypsin, an enzyme with proteolytic activity and widely used in proteomics was used as test enzyme. Trypsin activity was measured by $N\alpha$ -benzoyl-L-arginine-Ethyl Ester (BAEE) conversion. As functional material, Eupergit® C particles, widely used in enzyme immobilization [11, 12], were used, where the original oxirane functionality was replaced by reaction with ethylenediamine and activation with glutaraldehyde. The modified particles were ground and fractionated into two size classes, 20-40 μm and $< 20 \mu\text{m}$ before embedding in a hollow-fiber with ethylene vinyl alcohol as the porous polymeric matrix. The produced fibers were evaluated by single-fiber modules with a shell-in-tube configuration. The hollow-fiber modules were characterized in terms of dynamic enzyme immobilization, enzymatic conversion and compared with stacked flat-sheet MMM and packed bed systems.

4.2 EXPERIMENTAL

4.2.1 Materials and methods

EVAL₄₄ (a random copolymer of ethylene and vinyl alcohol) with an average ethylene content of 44 mol% was purchased from Aldrich and used without further modification. Dimethylsulfoxide (DMSO, Merck) was employed as solvent and 1-Octanol (Fluka) as non-solvent additive. Water was used in the coagulation bath. Ethylenediamine (Acros) and glutaraldehyde (Acros) were used in the chemical modification of the particles. Ethanol (Merck) was used for washing the Eupergit® particles after the chemical modification and

the produced fibers after spinning. Potassium phosphate (mono- and dibasic, Acros) and Tris-HCl (Sigma) were used for preparing the buffer solutions. To prevent trypsin self-digestion, calcium chloride (Acros) was added to the enzyme solutions. Trypsin from porcine pancreas (Sigma) was used as enzyme and $N\alpha$ -benzoyl-L-arginine-Ethyl Ester (BAEE, Sigma) as substrate. Eupergit® C beads were kindly provided by Degussa (Germany) and used as received. Ultrapure water was prepared using a Millipore purification unit Milli-Q plus.

4.2.2 Particle modification

Chemical modification

Prior to embedding, in order to improve the immobilization and conversion processes, chemical modification of the Eupergit® C particles was carried out as described by Petro *et al.* [13]. To protect the chemically active groups, the beads were modified by reacting with ethylenediamine at 80 °C for 72 hours in order to change the oxirane functionality into more stable amine groups. After the reaction was terminated, the beads were washed consecutively with abundant ethanol, water and 0.1 M phosphate buffer pH 6.9 while stirring gently. Each washing solution was then removed by using a Buchner funnel. The modified beads were activated as depicted in figure 4.1 by using a 10% solution of glutaraldehyde in a phosphate buffer of pH 6.9 at 30 °C for 3 hours. Finally, the beads were washed with abundant water, acetone and dried under vacuum at room temperature for one week prior to use.

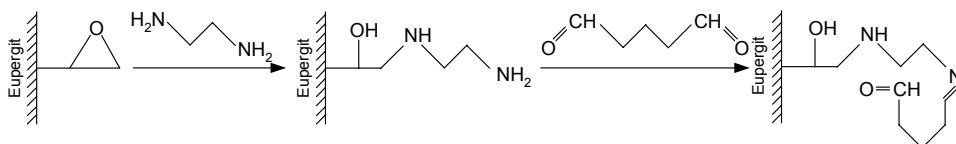


Figure 4.1 – Schematic representation of the chemical modification of Eupergit® C.

Milling and sieving

In order to increase the active surface area and to provide a better embedding, Eupergit® C particles were ground and sieved to 20-40 and < 20 μm size classes. For this a Fritsch analysette shaker attached with a stack of 40

and 20 μm sieves was used. Glass beads were added to provide impact to grind the particles during the process.

4.2.3 Mixed matrix hollow-fibers

The fibers were prepared by a dry-wet phase-inversion process using EVAL₄₄ as the polymeric matrix. A dope solution was prepared by dissolving overnight different amounts of EVAL₄₄, 1-Octanol and DMSO at 45 °C. After the solution was homogenized, milled, chemically modified, Eupergit® C particles equivalent to 2/3 in weight of polymer, were added. The mixture was left under strong stirring for over 24 hours to break down any particle clusters. The mixture was transferred into the storage tank and allowed to degas overnight.

In order to avoid particle loss and to provide a better elasticity to the produced fibers, a particle-free external layer was co-spun. The solution used for the co-spinning layer was prepared by mixing 10% EVAL₄₄, 10% 1-Octanol and 80% DMSO (weight percentages) at 45 °C. After homogenization, the solution was allowed to degas overnight prior to use. The applied bore liquid was a mixture of 30% (w/w) DMSO and 70% (w/w) water.

The spinning took place by extruding the different solutions through a triple layered spinneret into a water containing coagulation bath (Figure 4.2). The prepared fibers were left in water for 72 hours to wash out DMSO and 1-Octanol and then placed in ethanol for 24 hours to remove the final traces of the 1-Octanol. The fibers were stored in wet state to preserve flexibility and dried only before module preparation.

To calculate the total fiber particle loading, the co-spinning layer must be taken into account. The total Eupergit® loading can be determined by equation 4.1.

$$E_L^T = \frac{F_D \cdot E_C}{F_D \cdot E_C + F_D \cdot P_D + F_{CS} \cdot P_{CS}} \quad (4.1)$$

where E_L^T is the total Eupergit® loading in the fiber (%), F_D the dope solution flow rate (ml/min), P_D the polymer concentration in the dope solution (%), F_{CS} the co-spinning flow rate (ml/min), P_{CS} the polymer concentration in the co-spinning solution (%) and E_C the particle concentration in the dope solution.

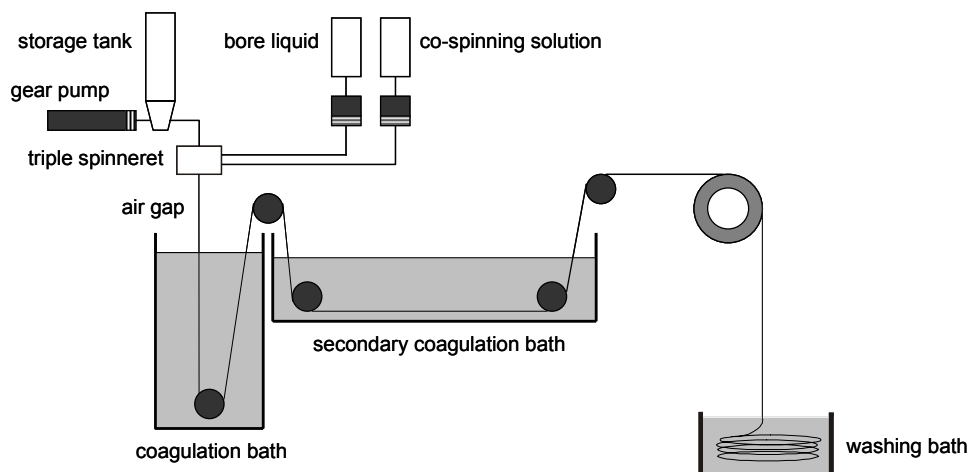


Figure 4.2 – Schematic representation of the fiber spinning process.

SEM characterization

The morphology of the fibers was investigated by scanning electron microscopy (SEM). Wetted pieces of the membranes were frozen in liquid nitrogen and fractured to expose cross-section areas. After drying, the samples were coated with gold using a Balzers Union SCD 040 coater and examined using a Jeol JSM-5600 LV Scanning Electron Microscope. The effective fiber volume, taken as the fiber wall volume is determined by the following equation:

$$V_L = \pi \cdot (R_T^2 - R_L^2) \quad (4.2)$$

where V_L represents the active fiber volume per unit length (ml/cm), R_T is the total fiber radius (cm) and R_L the fiber lumen radius (cm).

For the effective fiber surface area, taken as the fiber lumen surface area, the area can be obtained from equation 4.3.

$$S_L = 2 \cdot \pi \cdot R_L \quad (4.3)$$

with S_L as the active surface area per unit length (cm²/cm) and R_L the fiber lumen radius (cm).

Module construction

Modules were prepared following a tube-in-shell configuration containing one single fiber as exemplified in figure 4.3. The fibers were air-dried before being inserted in the module and potted with polyurethane.

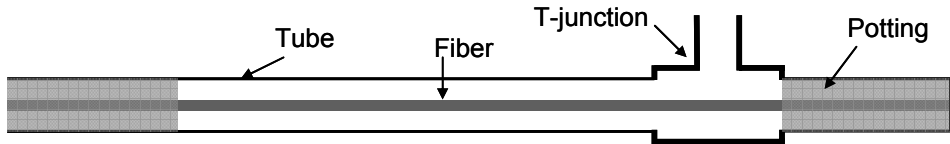


Figure 4.3 – Schematic representation of a single fiber module in shell-in-tube configuration as used for dynamic immobilization and dynamic activity measurements.

Clean water fluxes

The fibers clean water flux was determined in dead-end mode, by connecting the module to a nitrogen pressurized feed container. The filtration experiments were carried out at room temperature and a transmembrane pressure of 0.5 bar. The clean water flux was determined after steady state conditions were reached.

4.2.5 Trypsin immobilization

Dynamic Immobilization

Initially, CaCl_2 in Tris-HCl buffer at pH 7.0 was continuously pumped through the module-enclosed fiber to permit equilibration while monitoring of UV absorbance ($\lambda=280$ nm) and conductivity using an Äkta Purifier liquid chromatographic system. After membrane equilibration was achieved, a 1 mg/ml trypsin solution in the equilibration buffer was permeated through the fiber walls with a residence time of 1.4 minutes. The trypsin depletion from eluted solutions was monitored by measuring the UV absorbance. After the immobilization was completed, an elution buffer was permeated through the system to remove the unbound trypsin. The continuous immobilization of trypsin in the fiber was measured according to the following equation.

$$I = \sum i_j \quad (4.4)$$

$$i = \frac{\left(1 - \frac{C'}{C_0}\right) \times C_0 \times V'}{W} \quad (4.5)$$

with I the total amount of immobilized trypsin in the membrane (mg/g), i as the fraction of trypsin immobilized in the membrane (mg/g), C' the fractional concentration in the permeate side (mg/ml), C_0 the initial concentration (mg/ml), V' the fraction volume (ml) and W as the dry weight of membrane (g).

4.2.6 Activity measurements

The activity of trypsin in aqueous solutions was determined in the cuvette of an UV spectrometer using the at 25 °C with BAEE as substrate [14]. The activity of immobilized trypsin was determined by modifying the standard method [15], by flowing the substrate BAEE solution at different flow rates through the fiber containing immobilized trypsin [13, 16-18]. The permeate UV absorbance ($\lambda=254$ nm) was monitored to measure the substrate conversion. The flow rate was changed and the UV absorbance under steady-state was measured. The absorbance is then plotted against the different residence times.

The activity of the immobilized trypsin was determined as the slope of the linear increase in UV signal at 254 nm at different residence times [16] and related to the dry weight of membrane using the following expression:

$$Act = \frac{\Delta A^{254} / \Delta \tau}{m_{MMHF}} \quad (4.6)$$

where Act denotes the activity (U/g), $\Delta A^{254} / \Delta \tau$ (mAU/min) is the slope of the linear increase of absorbance and m_{MMHF} is the dry mass of MMHF used in the experiment (g).

4.3 RESULTS AND DISCUSSION

4.3.1 Fiber production and characterization

Fibers were spun using a dope solution containing DMSO as solvent, EVAL₄₄ as polymer and 1-Octanol both as non-solvent and pore forming agent. After the dope solution was homogenized, milled, chemically modified Eupergit® C particles were dispersed. Two different particle size classes were used in the fiber preparation. One batch was prepared containing particles with average sizes between 20 and 40 μm and another with particle sizes below 20 μm . The particle:polymer ratio was 2:5 for all dope formulations. A second solution free of particles was prepared to be used for the co-spinning layer. The dope formulations are given in table 4.1.

Table 4.1 – Composition of polymer solutions applied in the spinning experiments. The air gap used was of 5 cm.

Solution	DMSO (wt. %)	1-Octanol (wt. %)	EVAL₄₄ (wt. %)	Eupergit® Cm (% loading)
Dope (sizes 20-40 μm)	66	15	19	40
Dope (sizes < 20 μm)	66	15	19	40
Co-spinning	80	10	10	-

The following flow rates were used in the spinning process:

Dope flow rate (ml/min)	19.2
Co-spinning flow rate (ml/min)	3.6
Bore flow rate (ml/min)	9.6

The prepared fibers were characterized in terms of morphology, geometric dimensions and clean water flux. Scanning Electron Micrography is used to visualize the fiber morphology.

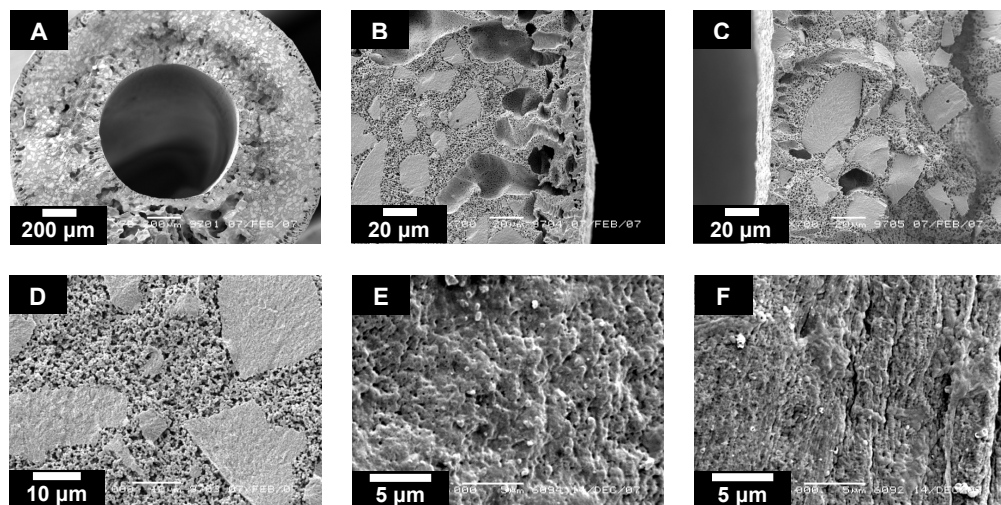


Figure 4.4 – SEM micrographs of mixed matrix hollow-fibers containing modified Eupergit® C particles with a size class of 20-40 µm, batch 1. **A** – General fiber overview, the magnification is of 70×; **B** – External surface cross-section with co-spinning layer, the magnification is of 700×; **C** – Lumen surface cross-section, the magnification is of 700×; **D** – Wall cross-section structure, the magnification is of 2000×; **E** – External (co-spinning) surface, the magnification is of 5000×; **F** – Internal (lumen) surface, the magnification is of 5000×.

The SEM images presented in figure 4.4 (A-D) show a highly interconnected pore structure with open lumen and surface. The particles are well embedded in the porous structure providing easy access of both enzyme and substrate molecules to the active sites. The fiber cross-sections show the presence of voids in the centre of the substructure. The void formation is well explained by the low miscibility of 1-Octanol in water, which leads to formation of alcohol drops, volumes without polymer.

All fibers show a considerable brittleness, especially in dry-state. When a particle-free external layer is co-spun, the mechanical strength of the fiber is much improved, due to the absence of particles in the external layer, which confer a higher elasticity to the fiber. There is no strong transition interface between the particle-containing structure and the co-spinning layer and no delamination takes place. The produced fibers show clean-water fluxes of about 20 l/(m².h.bar). Since fibers without co-spinning layer proved too fragile for practical handling, only fibers containing co-spinning layer were considered for further testing.

The fiber dimensions can be calculated (figure 4.4).

Total radius (μm)	890
Lumen radius (μm)	390
Wall thickness (μm)	500
Volume per length (ml/cm)	0.020 (eq. 4.2)
Area per length (cm^2/cm)	0.245 (eq. 4.3)
Particle loading (%)	37.6 (eq. 4.1)

As can be seen in figure 4.5, fibers prepared with particles smaller than 20 μm show a closed and deformed structure. The use of particles smaller than 20 μm causes a viscosity increase of the dope solution, leading to a condensed structure. All prepared fibers are too brittle to handle in dry state, making them unsuitable for testing.

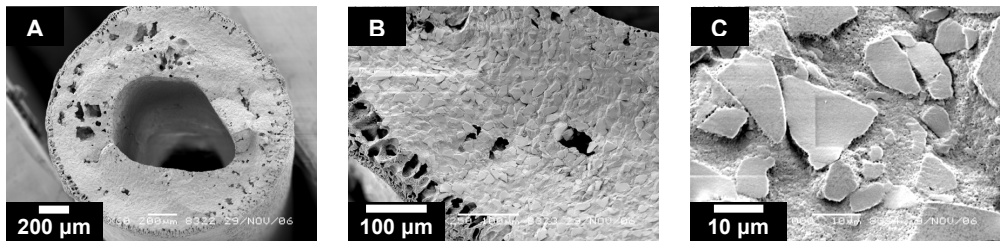


Figure 4.5 – SEM micrographs of mixed matrix hollow-fibers containing modified Eupergit® C particles with a size class < 20 μm , batch 1. **A** – General fiber overview, the magnification is of 60 \times ; **B** – Fiber wall, the magnification is of 250 \times ; **C** – Wall cross-section detail, the magnification is of 2000 \times .

In order to improve the fiber structure and to increase the mechanical strength, new dope solutions were prepared, mainly by reducing the 1-Octanol concentration and increasing the polymer concentration. The new dope compositions are given in table 4.2.

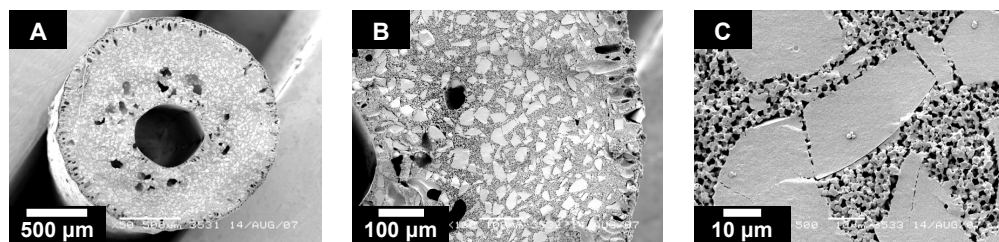
Table 4.2 – composition of polymer solutions used in spinning experiments. The air gaps used were of 10 and 20 cm.

Solution	DMSO (wt. %)	1-Octanol (wt. %)	EVAL₄₄ (wt. %)	Eupergit® Cm (% loading)
Dope (sizes 20-40 μm)	68	10	22	40
Dope (sizes < 20 μm)	70	8	22	40
Co-spinning	80	10	10	-

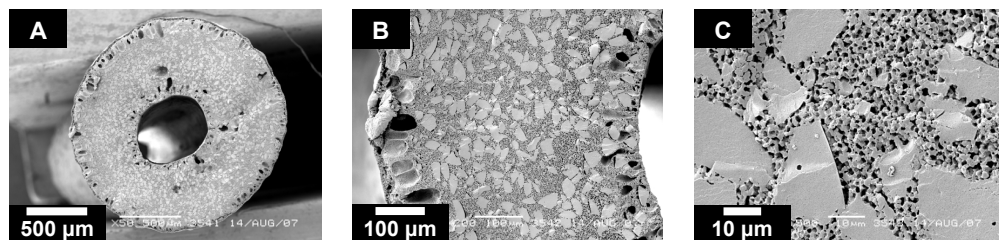
The following flow rates were used in the spinning process for both air gaps (10 and 20 cm):

Dope flow rate (ml/min)	20.4
Co-spinning flow rate (ml/min)	4.5
Bore flow rate (ml/min)	9.0

The morphology of newly prepared fibers was visualized by SEM as presented in figure 4.6.



Air Gap 20 cm

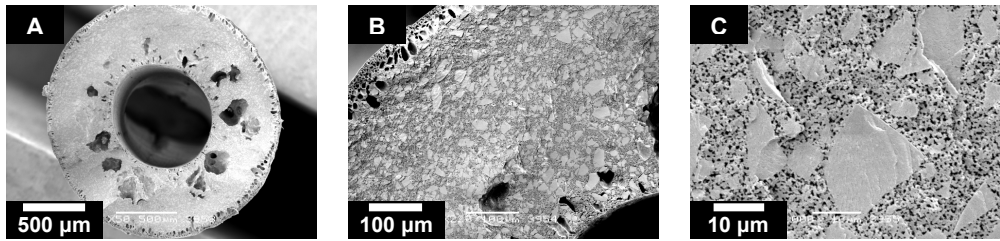


Air Gap 10 cm

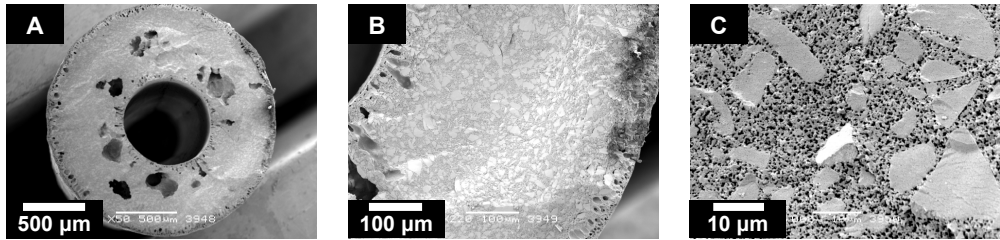
Figure 4.6 – SEM micrographs of mixed matrix hollow-fibers containing modified Eupergit® C particles with a size class of 20-40 μm , batch 2. **A** – General fiber overview, the magnification is of 50 \times ; **B** – Fiber wall, the magnification is of 180 \times for air gap 20 cm and 200 \times for air gap 10 cm; **C** – Wall cross-section detail, the magnification is of 1500 \times .

The SEM pictures of the fibers prepared with a low 1-Octanol content in the dope show almost no voids while maintaining the highly interconnected structure with easy access to the embedded particles. The interface between the co-spinning layer and the structure is unaffected by the change in dope composition. The clean-water fluxes were similar to that of previous membranes, with values of about 20 $\text{l}/(\text{m}^2\cdot\text{h}\cdot\text{bar})$.

The morphology of the newly prepared fibers containing particle sizes below 20 μm was visualized with SEM, as presented in figure 4.7.



Air Gap 20 cm



Air Gap 10 cm

Figure 4.7 – SEM micrographs of mixed matrix hollow-fibers containing modified Eupergit® C particles with a size class < 20 μm , batch 2. **A** – General fiber overview, the magnification is of 50 \times ; **B** – Fiber wall, the magnification is of 220 \times ; **C** – Wall cross-section detail, the magnification is of 2000 \times .

Fibers containing smaller sized particles show a structural improvement when lower 1-Octanol concentrations are used in the dope. The increase in solvent concentration compensates the increase in polymer concentration when compared with the previous batch, preventing the structure from becoming too close. The SEM images in figure 4.7 show a highly interconnected structure, with open pores and easy access to the embedded particles. The lower particle size in FC_{m20} fibers, when compared to that in FC_{m40} fibers, causes an increase in the viscosity of the dope solution due to the higher particle surface area. This in turn causes the structure to become slightly more closed, resulting in smaller pores. Still, the fibers show permeabilities similar to that of fibers containing bigger particles. This is due to the fiber lumen surface structure, where the highest flow resistance is present. This structure is controlled by the bore liquid, which remained the same in all batches. The lumen structure is then similar for all prepared fibers, which accounts for the similarities in permeabilities, even with slightly different dope compositions. The void formation can be reduced by decreasing the 1-Octanol concentration in the dope solution, but this is not favorable since this 1-Octanol also promotes pore formation and interconnectivity.

4.3.4 Dynamic measurements

Fibers containing particles with a size class of 20-40 μm , batch 1.

Trypsin was immobilized by permeating a solution of 1 mg/ml through the fiber with a residence time of 1.3 minutes. The flow rates were adjusted for different module lengths in order to keep a constant residence time. Activities were evaluated by permeating in dead-end mode a solution of BAEE substrate in Tris-HCl buffer at pH 7.6 through the fiber walls. The product formation was measured online by monitoring the UV signal at 254 nm. After achieving steady-state conditions, the flow rate was changed in order to obtain different residence times. The steady-state values were plotted against the correspondent residence times as previously described in chapter 3, and the activity was calculated from the slope of the linear part.

The results of dynamic immobilization and activities for the first batch of fibers are presented in table 4.3. The results are average values of at least three experiments.

Table 4.3 – Dynamic immobilization and activities of the first batch.

Fiber	Immobilization (mg/g_{fiber})	Activity (U/g_{fiber})
FCm ₄₀ (Air gap 5 cm)	38.8 ± 2.7	3017 ± 92

Fibers containing particles with a size class of 20-40 μm (FCm40) show a high immobilization capacity, with values of approximately 103 mg/g when normalized for the particle loading.

Fibers containing particles with a size class of 20-40 μm , batch 2.

Trypsin immobilization was also performed with the fibers produced with the modified dope, as depicted in table 4.2. The results for the second batch of experiments are presented in tables 4.4 and 4.5.

Table 4.4 – Dynamic immobilization and activities of the second batch.

Fiber	Immobilization (mg/g_{fiber})	Activity (U/g_{fiber})
FCm ₄₀ (Air gap 10 cm)	47.9 ± 6.9	4858 ± 746
FCm ₄₀ (Air gap 20 cm)	44.0 ± 6.3	2621 ± 395

The results show a clear influence of the air gap used in fiber spinning in the enzymatic activity of immobilized trypsin while the immobilization capacity remains approximately the same. The difference between the two sets of fibers can be explained by channeling effects due to a higher prevalence of voids in the structure of FCm₄₀ fibers prepared with a 20 cm air gap. Due to this effect, the substrate permeates preferably through these voids without contacting part of the immobilized trypsin. The effect is not visible during the trypsin immobilization due to the longer residence times used in the immobilization process. Dynamic trypsin immobilization takes place at lower flow rates (0.12 to 0.20 ml/min), leaving more time for diffusively controlled immobilization processes. In dynamic conversion processes, the flow rates are higher (0.5 and 5.0 ml/min), which implies a more convectively controlled process, which results on a stronger dependence on channeling.

The results clearly show a highly relation between fiber structure and dynamic enzymatic conversion by immobilized trypsin when compared to dynamic trypsin immobilization. Furthermore, the results confirm the hypothesis that dynamic enzymatic conversion processes in MMHF are convectively controlled as opposed to the more diffusively controlled processes in packed bed columns.

Fibers containing particles with a size class < 20 μm batch 2.

In order to study the influence of particle size on dynamic trypsin immobilization, a 1 mg/ml trypsin solution was permeated through a MMHF containing particles with sizes below 20 μm in a similar procedure to that taken for MM fibers containing 20-40 μm sized particles. The results summarized in table 4.5 are average values from at least three experiments.

Table 4.5 – Dynamic immobilization and activities of the second batch.

Fiber	Immobilization (mg/g_{fiber})	Activity (U/g_{fiber})
FCm20 (Air gap 10 cm)	44.1 ± 5.8	3609 ± 419
FCm20 (Air gap 20 cm)	44.9 ± 4.8	5118 ± 410

The results demonstrate similar immobilization capacities for fibers containing the same particle loading, both for particles with 20-40 and < 20 μm size classes. The dynamic conversion difference between the two batches

can be attributed to structure imperfections. Fibers prepared with longer air gaps possess a more homogeneous structure and therefore a better flow distribution, which permits a better contact by the substrate solution with the immobilized trypsin increasing overall conversion values.

The embedding of smaller particles ($< 20 \mu\text{m}$) into the fibers does not give a noticeable increase in immobilization capacity or dynamic activity of immobilized trypsin. Particle size reduction implies a higher available active surface area.

A reduction in particle size from $250 \mu\text{m}$ to $20\text{--}40 \mu\text{m}$ greatly increases the total particle surface area, whereas a further reduction to particle sizes below $20 \mu\text{m}$ gives a less pronounced increase in available surface area, which implies that the particle size reduction is less beneficial. In this case, porous Eupergit[®] particles with a size class of $20\text{--}40 \mu\text{m}$ already provide the maximum available surface area possible, which means a further size reduction has no additional advantages in terms of dynamic enzyme immobilization or dynamic enzymatic conversion.

4.3.5 Influence of support on dynamic activity

For comparison purposes, the dynamic activity of immobilized trypsin in Eupergit[®] C particles in packed bed columns and embedded in flat-sheet membranes, both from the original particles as after chemical modification, was compared with the presented results from the fiber experiments. Dynamic activities were normalized by relating the activities to the dry amount of embedded Eupergit[®] C particles. The results are summarized in figure 4.8.

From figure 4.8, it becomes obvious that mixed matrix hollow-fibers present a much more effective configuration for enzymatic conversion compared to flat-sheet mixed matrix membranes and packed bed systems. The advantage of both mixed matrix geometries over packed bed columns is due to a combination of particle size reduction, lower bed compression and a predominantly convective-controlled process. These factors combined proved that mixed matrix membranes, whether in flat-sheet or hollow-fiber geometries, are superior to packed bed systems in dynamic enzymatic conversion processes.

Mixed matrix fibers show a much higher dynamic enzymatic activity than flat-sheet MMM. This is a result of the higher clean-water fluxes in the flat-sheet systems. Values in the order of $600 \text{ l}/(\text{m}^2\cdot\text{h}\cdot\text{bar})$ for flat sheet mem-

branes and $20 \text{ l}/(\text{m}^2 \cdot \text{h} \cdot \text{bar})$ for hollow-fiber membranes confirms this, since the smaller pores in hollow-fibers provide a more pronounced contact between immobilized enzyme and substrate. Also the flow profile, which is radially homogeneous in the case of fibers, has advantages when compared to a more localized feed point in the case of flat-sheet membrane stack.

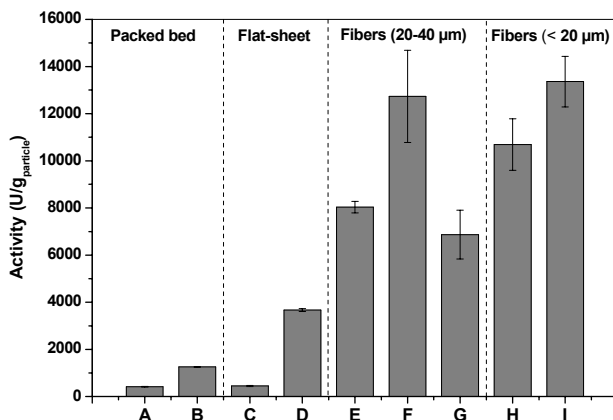


Figure 4.8 – Enzymatic activity of trypsin immobilized on Eupergit® C particles in different supports. A-D are data presented in chapter 3. Activities normalized to dry weight of embedded particles. The results represent the average value of at least three experiments.

Legend

- A** – Original particles in a packed bed column
- B** – Chemically modified particles in a packed bed column
- C** – Original particles milled in a flat-sheet membrane
- D** – Chemically modified particles milled in a flat-sheet membrane
- E** – Chemically modified particles (20-40 μm) in a MMF, batch 1, air gap 5 cm
- F** – Chemically modified particles (20-40 μm) in a MMF, batch 2, air gap 10 cm
- G** – Chemically modified particles (20-40 μm) in a MMF, batch 2, air gap 20 cm
- H** – Chemically modified particles (< 20 μm) in a MMF, batch 2, air gap 10 cm
- I** – Chemically modified particles (< 20 μm) in a MMF, batch 2, air gap 20 cm

4.4 CONCLUSIONS

In this chapter, new mixed matrix membranes with hollow-fiber geometry were prepared. It was possible to produce hollow-fibers containing modified Eupergit® C particles in two size classes, 20-40 μm and below 20 μm. The fiber morphology becomes more homogeneous by reducing the amount of

1-Octanol as additive. The fibers present clean-water fluxes of about 20 l/(m².h.bar), a relatively low value which is caused by the higher polymer concentration used in the dope when compared to the flat-sheet dope solutions and by a dense lumen surface. The fiber wall presents an open and well interconnected fine porous structure, allowing full access to the embedded particles. There is no visible interface between the sub-layer and the co-spinning layer, which prevents particle loss and provides higher flexibility to the whole fiber.

Trypsin, dynamically immobilized in all prepared fibers, presents considerably higher activities when compared to packed bed columns or flat-sheet mixed matrix membranes. Mixed matrix hollow-fibers show an activity increase up to four times compared to flat-sheet membranes. The improvement is due to a more defined flow profile, originating from a finer pore structure which allows a better usage of the embedded particles in fibers when compared to flat-sheet membranes.

Fibers prepared with smaller sized particles (< 20 μm) showed no activity increase over particles in size classes of 20-40 μm, which means that all available active sites in the embedded particles can be reached within the experimental time frame. Furthermore, as in typical membrane processes, mixed matrix hollow-fibers are more easily scaled-up.

Acknowledgments

The authors acknowledge The Netherlands Organization for Scientific Research (NWO) for the financial support of this project. The authors are also grateful to Degussa Specialty Polymers for providing the Eupergit® particles used in this study.

REFERENCES

1. Ghosh, R., Protein separation using membrane chromatography: opportunities and challenges. *Journal of Chromatography A*, 2002. 952(1-2): p. 13.
2. Klein, E., Affinity membranes: a 10-year review. *Journal Of Membrane Science*, 2000. 179(1-2): p. 1.

3. Boi, C., Membrane adsorbers as purification tools for monoclonal antibody purification. *Journal of Chromatography B*, 2007. 848(1): p. 19.
4. Przybycien, T.M., N.S. Pujar, and L.M. Steele, Alternative bioseparation operations: life beyond packed-bed chromatography. *Current Opinion in Biotechnology*, 2004. 15(5): p. 469.
5. Charcosset, C., Membrane processes in biotechnology: An overview. *Biotechnology Advances*, 2006. 24(5): p. 482.
6. Lensmeyer, G.L., et al., Use of particle-loaded membranes to extract steroids for high-performance liquid chromatographic analyses improved analyte stability and detection. *Journal of Chromatography A*, 1995. 691(1-2): p. 239.
7. Avramescu, M.-E., et al., Preparation of mixed matrix adsorber membranes for protein recovery. *Journal of Membrane Science*, 2003. 218(1-2): p. 219.
8. Avramescu, M.-E., Z. Borneman, and M. Wessling, Mixed-matrix membrane adsorbers for protein separation. *Journal of Chromatography A*, 2003. 1006(1-2): p. 171.
9. Saiful, Z. Borneman, and M. Wessling, Enzyme capturing and concentration with mixed matrix membrane adsorbers. *Journal of Membrane Science*, 2006. 280(1-2): p. 406.
10. Avramescu, M.E., et al., Adsorptive membranes for bilirubin removal. *Journal of Chromatography B*, 2004. 803(2): p. 215.
11. Boller, T., C. Meier, and S. Menzler, EUPERGIT oxirane acrylic beads: How to make enzymes fit for biocatalysis. *Organic Process Research & Development*, 2002. 6(4): p. 509.
12. Katchalski-Katzir, E. and D.M. Kraemer, Eupergit (R) C, a carrier for immobilization of enzymes of industrial potential. *Journal Of Molecular Catalysis B-Enzymatic*, 2000. 10(1-3): p. 157.
13. Petro, M., F. Svec, and J.M.J. Fréchet, Immobilization of trypsin onto molded macroporous poly(glycidyl methacrylate-co-ethylene dimethacrylate) rods and use of the conjugates as bioreactors and for affinity chromatography. *Biotechnology and Bioengineering*, 1996. 49(4): p. 355.
14. Barman, T.E., *Enzyme Handbook*. Vol. 2. 1969, Berlin: Springer. 618.

15. Rick, W., ed. Trypsin. 1st ed. Methods of enzymatic analysis, ed. H.U. Bergmeyer. 1965, Verlag Chemie: Weinheim. 807.
16. Bencina, K., et al., Enzyme immobilization on epoxy- and 1,1'-carbonyldiimidazole-activated methacrylate-based monoliths. Journal Of Separation Science, 2004. 27(10-11): p. 811.
17. Peterson, D.S., et al., Enzymatic microreactor-on-a-chip: Protein mapping using trypsin immobilized on porous polymer monoliths molded in channels of microfluidic devices. Analytical Chemistry, 2002. 74(16): p. 4081.
18. Xie, S., F. Svec, and J.M.J. Frechet, Design of reactive porous polymer supports for high throughput bioreactors: Poly(2-vinyl-4,4-dimethylazlactone-co-acrylamide-co-ethylene dimethacrylate) monoliths. Biotechnology and Bioengineering, 1999. 62(1): p. 30.

5

Enzymatic conversion using ion-exchange MMHF

ABSTRACT

This chapter reports the adsorption of glucose oxidase (GOx) in mixed matrix hollow-fibers (MMHF) using polyethersulfone as matrix and Lewatit® strong cation-exchange resins as the functional support. Static enzyme immobilization tests yielded high adsorption values at pH's below the isoelectric point (pI) of GOx, where the enzyme assumes the cationic form and adsorbs via electrostatic interaction. This adsorption by electrostatic interactions followed a Langmuir-type isotherm at pH values below the pI of GOx. Adsorption performed above the pI takes place preferentially via hydrophobic interactions. Dynamic GOx adsorption experiments resulted in the same values as those obtained in static experiments. Below the pI of the enzyme, the adsorption was found to be pH dependent. Above the pI of GOx, the adsorption was lower and independent of the pH. Formation of GOx multilayers was observed for all applied pH's. Dynamic glucose conversion measurements showed that the immobilized GOx retains an appreciable activity after adsorption via both methods. GOx immobilized via hydrophobic interaction yielded the highest activity values. Enzymes immobilized via electrostatic interaction showed multilayer adsorption, resulting in a reduced enzyme-normalized enzymatic activity. The highest enzymatic activity was found for pH 5.0.

5.1 INTRODUCTION

The use of enzymes in food, chemical and pharmaceutical industries has steadily been growing over the years. The growing demand for enantiomerically pure compounds has driven this increase, mainly in the pharmaceutical and agrochemical industries. Bioconversions can be regarded as an environmentally friendly with very high specificity and selectivity, which can dispense with chemical additives and thus reduce waste [1].

In the pursuit of more economically interesting processes, enzymes started being immobilized in solid supports in place of being used in the soluble form in a solution. Two main reasons can be considered for the immobilization of enzymes: the need for an easy separation from the product, which can be time and resources-consuming; and the reutilization of the enzyme [2]. Immobilized enzymes tend to retain a long-term stability and show an increase in chemical resistance against the action of surrounding environment, characteristics which add to the economical advantages of enzyme immobilization [3-5].

As addressed in chapter 2, enzyme immobilization can take place using several methods. Binding the enzymes to a support, crosslinking of enzymes or by physically entrapping or encapsulating the enzymes are the methods in use today for enzyme immobilization [2, 4]. Of these methods, enzyme binding has been most extensively reported, due to high flexibility in available techniques, good stability and relatively high residual activity of the immobilized enzymes. In enzyme binding, a few different techniques can be distinguished. Covalent immobilization, based on the chemical bonding of the enzyme to a support; ionic binding, in which the enzyme, in ionic form, attaches to the support's charged surface; adsorptive binding, where van der Waals and hydrophobic interactions play a role in adsorbing the enzyme to the support; and metal binding, in which a metal chelate provides the binding between the support and the enzyme.

Different types of support systems have been studied throughout the years for enzyme immobilization. Mainly two types can be identified: functional particles that are suspended in the target solution inside stirred-tank reactors or used in packed- or fluidized bed reactors; and membranes in which enzymes can be bound or entrapped [6]. In the case of functional particles, different functionalities and higher immobilization loadings can be achieved. With affinity membranes, it is possible to reach higher throughputs than in

packed or fluidized bed reactors resulting in more convective controlled reactions.

In recent years, a new platform for membrane chromatography has been introduced in which chromatography beads and membranes are fused together in order to explore the advantages of both technologies. This platform, dubbed mixed matrix membrane, makes use of a membrane's macroporous structure in which small, functional chromatography particles, with the desired functionality, can be embedded. The preparation follows an analogue procedure to typical membrane production processes, using a polymer solution in which the particles are dispersed with the resulting mix being cast or spun and solidified by a dry-wet phase-inversion process into a flat-sheet or a fiber membrane. These materials carry the advantages of membranes, such as high throughputs and low bed compression and of chromatography packed beds, like high capacities and a high range of functionalities [7-9]. They have been proved to be suitable for protein adsorption, protein separation, enzyme concentration and blood purification [10-13].

In previous chapters, mixed matrix membranes have already been shown to be suitable for enzymatic immobilization using covalent binding. In order to prove the flexibility of the concept, new functionalities and enzymes are explored. In this chapter, a different type of functionality for enzymatic immobilization using mixed matrix membranes with cation-exchange functional particles, is evaluated. Ion-exchange particles can be used for enzyme immobilization by forcing the enzyme to assume an ionic form which is complementary to the type of ion-exchange functionality present in the particles. An enzyme can switch between cationic and anionic form by changing the solution pH under or above its isoelectric point (pI). Via this route, an enzyme can be immobilized on a cation- or anion-exchange support as long as the enzyme-containing solution pH is controlled. This method has advantages over covalent immobilization in terms of support regeneration, due to the fact that a no longer active enzyme can be desorbed from the support by a pH swing around the pI value, thus permitting support regeneration. This is much more difficult to achieve in covalent immobilization. In figure 5.1, a schematic representation of enzyme immobilization on a cation-exchange support is shown.

In this chapter, mixed matrix hollow-fibers prepared with strong cation-exchange resins embedded in polyethersulfone (PES) were prepared for immobilization of glucose oxidase. Glucose oxidase (GOx), an enzyme with an isoelectric point (pI) of 4.2 frequently used in sensors [14-17], converts glucose into hydrogen peroxidase and gluconic acid in the presence of oxygen.

The enzyme immobilization was evaluated by varying the solution pH from values below the pI, region where the enzyme assumes a cationic form, to values above the pI, region where the enzyme assumes an anionic form. Dynamic activity experiments were performed at the same pH as that of the immobilization. The pH influence was evaluated, both on the immobilization capacity and in the dynamic activities of adsorbed GOx.

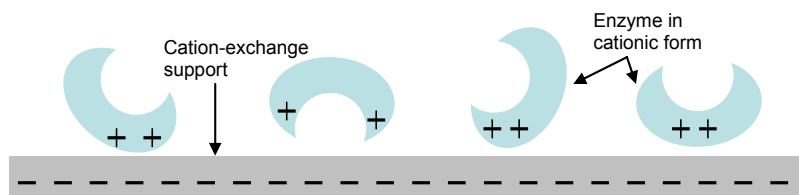


Figure 5.1 – Schematic representation of enzyme immobilization in a cation-exchange support.

5.2 EXPERIMENTAL

5.2.1 Materials

Polyethersulfone (PES, Ultrason E6020P) with a Mw of 50 kDa was kindly supplied by BASF-Nederland and used without further modification as the slightly hydrophilic polymer matrix for the fibers. Polyvinylpyrrolidone (PVP, Fluka) with three different molecular weights (K13, K30 and K90) was used as a polymeric additive. Polyethyleneglycol (PEG400, Merck) and glycerol (Merck) were used as non-solvent additives in the dope solution. N-methylpyrrolidone (NMP, 99% pure, Acros Organics) was employed as a solvent. Water was used as the non-solvent in the coagulation bath. Lewatit 112WS (strong cationic exchange resins, properties summarized in table 5.1) kindly supplied by Caldic, Belgium, were used for providing the ion-exchange functionality. The particles were milled and air classified to obtain a fraction with an average particle size of 7.9 μm and an average surface area of 1.79 m^2/g . Glucose oxidase from *aspergillus niger* (Fluka, major data summarized in table 5.2) was used as the adsorbed enzyme. Glucose (Merck) was used as the enzyme substrate. Phenol (Acros Organics), 4-Amino-Antypyrene (Acros Organics) and Horse Radish Peroxidase with an activity of 224 U/mg (Sigma) were used in the activity measurements. For the buffer preparation in the 3.5 to 7.0 pH range, Potassium phosphate (mono- and dibasic, Acros), Acetic Acid (Merck) and Formic Acid (Acros Or-

ganics) were employed. Ultrapure water was prepared using a Millipore purification unit Milli-Q plus.

Table 5.1 – Properties of Lewatit® 112WS resins as provided by the supplier.

Property	Data
Ionic form	Na ⁺
Matrix type	Cross-linked polystyrene
Bead size	0.65 mm
Density	1.24 g/ml
BET area	38.8 m ² /g
Pore diameter	28.8 nm

Table 5.2 – Relevant data of glucose oxidase as provided by the supplier.

Property	Data
Isoelectric point (pI)	4.2
Molecular weight	186 × 10 ³ g/mol
pH activity range	4-7
pH optimum	5.5
Enzymatic activity	159 U/mg

5.2.2 Fiber spinning

The prepared fibers were produced by a phase-inversion process. The dope solution was prepared by dissolving at 60 °C 14.5% PES and 8.7% PVP (in equal proportions of K13, K30 and K90) in 43.7% NMP with 8.7% glycerol and stirring overnight. After cooling of the solution, a suspension of 24.3% PEG400 containing ion-exchange particles equivalent in weight to the amount of PES used were added. All values are given as weight percentages to the final dope solution. The mixture was stirred for over 16 hours to break up any particle aggregates and then transferred into the storage tank. The dope solution was degassed for 24 hours before spinning. The hollow-fiber was prepared using a triple layered spinneret, through which the bore liquid consisting of 70% NMP and 30% water (wt. %), the dope solution and

a co-extrusion solution are extruded into a water containing coagulation bath. After solidification and winding of the fibers, these were left in water to remove any remaining traces of solvents and additives. The fibers were then immersed in a 4000 ppm NaOCl solution for 24 h to remove any remaining PVP. The fibers particle load was calculated as the weight of particles divided by the total weight of the dry fiber, consisting of particles and matrix polymer (equation 5.1).

$$P_{loading} = \left(\frac{W_R}{W_R + W_P} \right) \times 100 \quad (5.1)$$

with $P_{loading}$ as the particle loading in the membrane (wt. %), W_R the dry weight of particles added (g) and W_P as the dry weight of PES, the matrix polymer, added to the dope solution (g).

5.2.3 Scanning electron microscopy (SEM)

Samples of fiber cross-sections were prepared by cryogenic breaking of wet fibers in liquid nitrogen. The samples were dried overnight under vacuum at room temperature and coated with a thin gold layer using a Balzers Union SCD 040 coater. The characterization of cross-sectional samples took place using a Scanning Electron Microscope JEOL JSM 5600LV. The effective fiber volume, taken as the fiber wall volume is determined by the following equation:

$$V_L = \pi \cdot (R_T^2 - R_L^2) \quad (5.2)$$

where V_L represents the active fiber volume per unit length (ml/cm), R_T is the total fiber radius (cm) and R_L the fiber lumen radius (cm).

Since the fibers are used in the inside-out mode, the surface area was calculated using the fiber lumen radius (eq. 5.3).

$$S_L = 2 \cdot \pi \cdot R_L \quad (5.3)$$

with S_L as the active surface are per unit length of fiber (cm²/cm).

5.2.4 Static adsorption

The determination of the static adsorption capacity of the prepared hollow fibers was achieved by measuring the depletion of glucose oxidase (GOx) in a solution. GOx was dissolved in buffers with different pH's and a known amount of dry adsorber fibers was immersed. The depletion of GOx from the solution determined the amount of adsorbed enzyme was related to the dry weight of fibers. The concentration in the solution was determined by measuring the UV absorbance at a wavelength of 280 nm using a Varian Cary 300 spectrophotometer. The initial concentration of enzyme in the buffer solutions was set at 1 mg/ml. The adsorption tests were carried at room temperature and the solutions were agitated using a shaking machine.

Adsorption isotherm

The adsorption isotherm of GOx in the fibers was determined by incubating equal amounts of mixed matrix fibers with different amounts of enzyme in order to reach different equilibrium concentrations. The adsorption of a protein onto an ion-exchange support has often been assumed to follow a Langmuir-type isotherm [11, 18, 19] of which equation 5.4 presents the linear form:

$$\frac{1}{q^*} = \frac{1}{q_m} + \frac{K_d}{q_m} \times \frac{1}{C^*} \quad (5.4)$$

with q^* as the enzyme concentration in the adsorber membrane, q_m the maximum adsorption capacity, K_d the dissociation constant and C^* the enzyme concentration in the bulk solution. Only the q^* and C^* are equilibrium experimental data, which means that the values of $1/q^*$ versus $1/C^*$ needs to be plotted in order to determine K_d and q_m using a linear curve fitting.

5.2.5 Module preparation

Fibers prepared as previously described were air-dried before incorporation in a module. The module consists of a tube-in-shell configuration with a single hollow fiber potted using polyurethane.

5.2.6 Dynamic adsorption

The dynamic adsorption capacity of the fibers was determined by evaluating the breakthrough curves. Solutions of GOx in different buffers (concentration of 50 mM for all cases) were prepared. The module was connected to a Akta Purifier chromatography unit. The solutions were pumped into the module in dead-end mode at 1 ml/min and the GOx concentration was determined by UV-absorbance using an in-line spectrophotometer at 280 nm. The breakthrough curve was determined from the permeated volume and GOx depletion. To evaluate the best adsorption conditions, different pH's, ranging from 3 to 6, were used. In order to increase the process data resolution, the GOx concentration was set at 0.25 mg/ml.

5.2.7 Enzymatic activity

GOx activity was calculated for the free and adsorbed enzyme. The method was based on the work by Rauf *et al.* [20], using glucose as the substrate. Glucose is converted in the presence of water and oxygen to hydrogen peroxide and gluconic acid. In a second reaction, hydrogen peroxide reacts with phenol and 4-Amino-Antipyrine (4-AAP) in the presence of Horse Radish Peroxidase (HRP) to produce water and quinoneimine. The activity of GOx was then measured by recording the production of quinoneimine in time, which could be measured using a spectrophotometer at 505 nm. The two-step reaction is presented in figure 5.2.

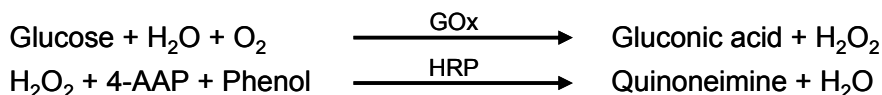


Figure 5.2 – Two-step reaction used for GOx activity measurements.

Static activity

The activity of free GOx in static mode was measured using solutions of 8.5 mM of glucose, 41.5 mM phenol, 0.06 mM 4-AAP and 0.08 U/ml of HRP in buffers at different pH's. 3 ml of the solution were placed in a 10 mm quartz cuvette, to which 20 μ l of a 200 U/ml GOx solution were added. After homogenization, the increase in signal at 505 nm in time was recorded using a Varian Cary 300 spectrophotometer. The values were then plotted against time and the activity was taken from the linear portion of the curve and related to the dry weight of enzyme.

Dynamic activity

Dynamic activity of the adsorbed GOx was evaluated by adapting the static method. After GOx adsorption, the fiber was washed with buffer to remove all unbound enzyme molecules. In order to evaluate the conversion to quinoneimine, a solution with the same pH as that used in the immobilization step, containing 50 mM glucose, 50 mM phenol, 0.08 mM 4-AAP and 0.1 U/ml HRP was permeated through the fiber walls with different flow rates. The conversion to quinoneimine in the permeate was monitored by the absorbance at 505 nm to evaluate quinoneimine conversion. For each flow rate, the reaction was given time to achieve steady-state conditions, at which the absorbance value was registered. By using different flow rates was possible to achieve different absorbance values for different residence times. The values were plotted against the different residence times and the activity was taken from the linear portion of the curve and related to the dry weight of used fiber or to the dry weight of adsorbed enzyme. In order to find the optimal conditions, different pH values were used to obtain different activities.

5.3 RESULTS AND DISCUSSION

5.3.1 Fiber structure

Mixed matrix hollow-fibers were spun using a dope solution of PES with NMP as solvent, PVP, PEG400 and glycerol were employed as additives and Lewatit 112WS resins were embedded to provide the cation-exchange functionality. The prepared fibers were characterized in terms of morphology, geometric dimensions and flow resistance. Morphology is visualized by Scanning Electron Microscopy.

Images in figure 5.3 show a very open structure with a good particle embedding and high interconnectivity. Some finger-like macrovoids are visible along the fiber wall, which may result in preferential flow. The external surface is open enough to allow a good flow, but is dense enough to avoid significant particle loss. The lumen surface is extremely open, which may result in some level of particle loss, but permits a fast convective flow to the fiber wall.

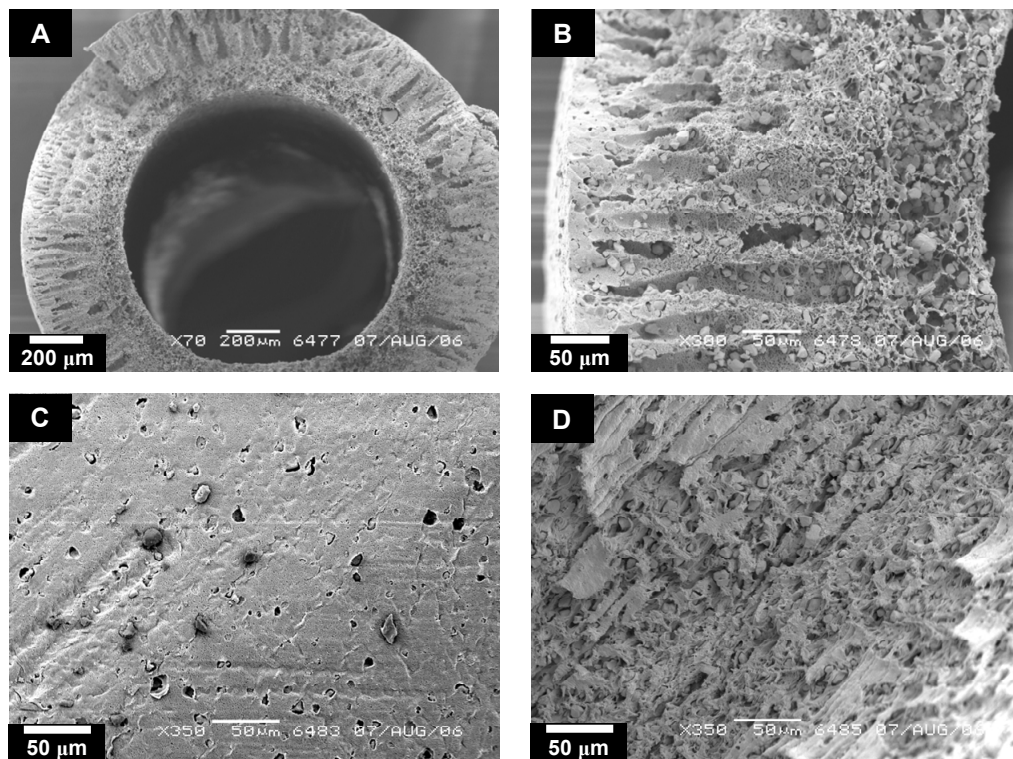


Figure 5.3 – SEM micrographs of PES hollow fibers containing strong cation-exchange resins. **A** – general view, the magnification is of 70×; **B** – fiber wall and structure, the magnification is of 300×; **C** – external surface, the magnification is of 350×; **D** – lumen surface, the magnification is of 350×.

By using the pictures in figure 5.3, the fiber dimensions can be established. A summary is found below.

Total radius (μm)	910
Lumen radius (μm)	650
Wall thickness (μm)	260
Volume per length (ml/cm)	0.013 (eq. 5.2)
Area per length (cm^2/cm)	0.408 (eq. 5.3)

For calculating the total active fiber volume for each prepared module, the volume per length value is multiplied by the active fiber length.

5.3.2 Static adsorption

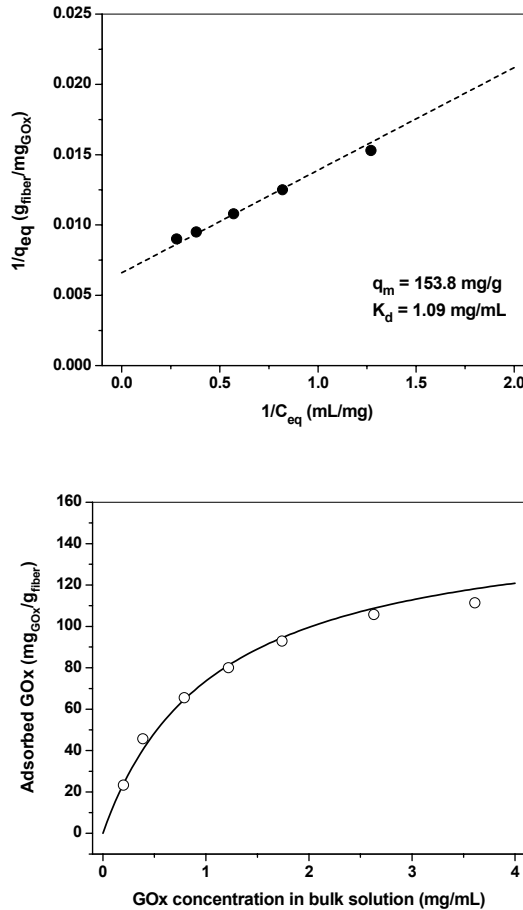


Figure 5.4 – Langmuir fittings for glucose oxidase adsorption at pH 4.0. The dashed line indicates the linear fitting. The solid line in the right hand side graph is the best fit with the Langmuir isotherm.

The static adsorption capacity of the prepared fibers was determined by measuring glucose oxidase (GOx) depletion experiments. Known amounts of mixed matrix hollow-fibers (MMHF) were placed in solutions containing GOx in different buffers at different pH's and the enzyme depletion was measured. Different initial GOx concentrations were used to obtain different adsorption equilibria. To guarantee complete equilibrium, samples were taken after 96 hours for the Langmuir fittings.

The results were used to plot the amount of adsorbed GOx in the fibers against the GOx equilibrium concentrations in the solution. In figure 5.4, the results obtained for pH 4.0 are presented. The graph shows a clear Langmuir-like adsorption behavior with a maximum adsorption capacity over 150 $\text{mg}_{\text{GOx}}/\text{g}_{\text{fiber}}$. The fact that the adsorption behavior can be fitted with a Langmuir-type isotherm is in accordance with previously published articles for protein adsorption in materials with ion-exchange functionality [21-24]. The same behavior can be observed for adsorption taking place at pH's below the enzyme pI, region where GOx molecules assume the cationic form. The Langmuir-type isotherms for pH's 3.5-4.5 are summarized in figure 5.5.

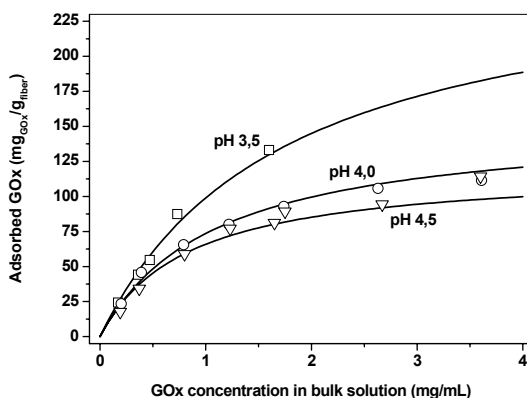


Figure 5.5 – Langmuir fittings for glucose oxidase adsorption at pH 3.5-4.5. The lines indicate the best fit with the Langmuir-type isotherm for each pH.

Even though the pI value given by the supplier for native glucose oxidase is 4.2, publications frequently refer values between 4.0 and 4.7 [22, 23, 25-28]. This explains why GOx still shows considerable adsorption capacity on cation-exchange particles at pH (4.5) values where it should assume the anionic form. Since the formation of GOx cations follows equilibrium, this also contributes for the cation adsorption on the particles, further increasing GOx immobilization. At the lower pH of 3.5, GOx assumes mainly cationic form, being thus more likely to be adsorbed by the cation-exchange resins, as can be observed in figure 5.5. The calculated values for q_{max} and K_d are given in table 5.3.

Table 5.3 – q_{\max} and K_d values for pH's 3.5-4.5 as calculated from equation (5.4).

pH	q_{\max} (mg/g _{fiber})	K_d (mg/ml)
3.5	270.3	1.73
4.0	153.8	1.09
4.5	120.5	0.83

As expected, the maximum GOx adsorption capacity increases with decreasing pH, reaching a q_{\max} of 270.3 mg/g_{fiber} at pH 3.5. Since GOx has a stability interval between pH 4.0 and pH 7.0, no measurements were performed at pH below 3.5.

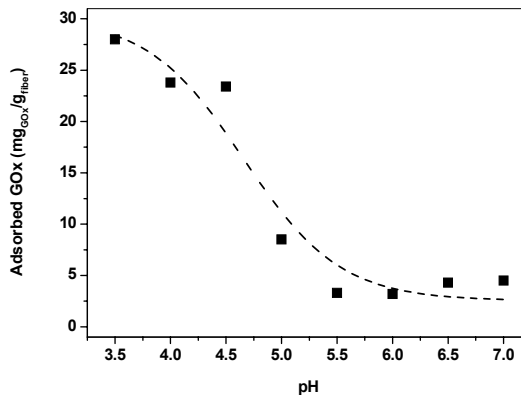


Figure 5.6 – Static adsorption of GOx in the fibers with an equilibrium concentration of 0.2 mg/ml. At pH 3.5-4.5, the adsorption was calculated as the q^* from the Langmuir equation with the respective q_{\max} and K_d values. For the 5.0-7.0 pH range, the values were taken directly from the experimental results.

At higher pH's, the glucose oxidase molecules assume anionic form, thus being unable to adsorb onto the particles via electrostatic interactions. This does not necessarily imply that adsorption is excluded, since the Lewatit 112WS ion-exchange resins embedded in the fiber do contain a hydrophobic matrix, being suitable for protein adsorption via hydrophobic interactions. The adsorption experiments, however, did not yield Langmuir-type adsorption in the pH range 5.0-7.0. This means that for this system Langmuir-type behavior is not present when the adsorption takes place via hydropho-

bic interactions. In figure 5.6, an overview of the static GOx adsorption capacity in the 3.5-7.0 pH range is presented.

The graph in figure 5.6 clearly shows the much higher GOx adsorption capacity displayed by the fibers in the 3.5-4.5 pH range. The adsorption capacity at pH 3.5 shows the highest value, due to being the furthest from the enzyme pI. At pH 4.0 and 4.5, glucose oxidase adsorption capacity is about the same due to the proximity of the enzyme pI. At higher pH, the adsorption capacity strongly decreases, due to the decrease in contribution by electrostatic interactions to the adsorption process. At pH 5.5 through to 7.0, the adsorption stays approximately constant, due to the adsorption mechanism that is completely controlled by hydrophobic interactions, which are much less dependant on the pH.

5.3.3 Dynamic adsorption

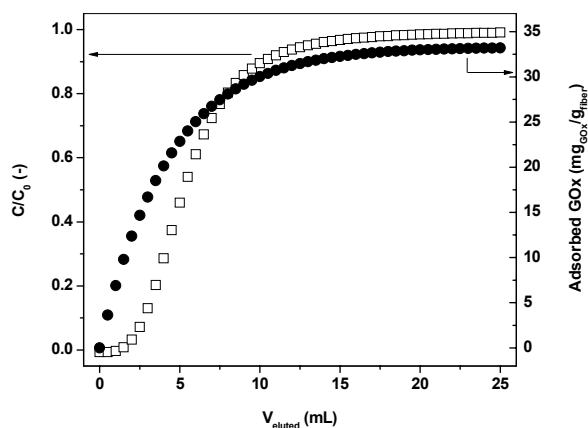


Figure 5.7 – GOx breakthrough and immobilization curves at pH 4.0. A flow rate of 1 ml/min and a GOx concentration of 0.25 mg/ml were used in the experiments. The presented results are average values of two experiments.

In order to study the effectiveness of the support in GOx immobilization, dynamic adsorption measurements were performed both at pH's where the adsorption is due to electrostatic interactions and at pH's where the adsorption takes place using hydrophobic interactions. For the dynamic measurements, glucose oxidase solutions in different buffers at different pH's, with a 0.25 mg/ml concentration were permeated at 1 ml/min through the fiber wall and the GOx permeate concentration was monitored by measur-

ing the UV absorbance inline at 280 nm. The results for adsorption due to electrostatic interactions are presented in figures 5.7 and 5.8 for pH's 4.0 and 4.5 respectively. Since GOx is not very stable at pH's below 4.0, these results are not presented.

Using the Langmuir fitting parameters from table 5.3, it is possible to predict the GOx immobilization in dynamic mode for pH 4.0 and 4.5 using a feed concentration of 0.25 mg/ml. The obtained results can then be compared with the experimental data in order to evaluate the usage of adsorption sites in dynamic mode. The comparison is valid due to the continuous feed of fresh GOx solution that guarantees the concentration equilibrium. The results are summarized in table 5.4.

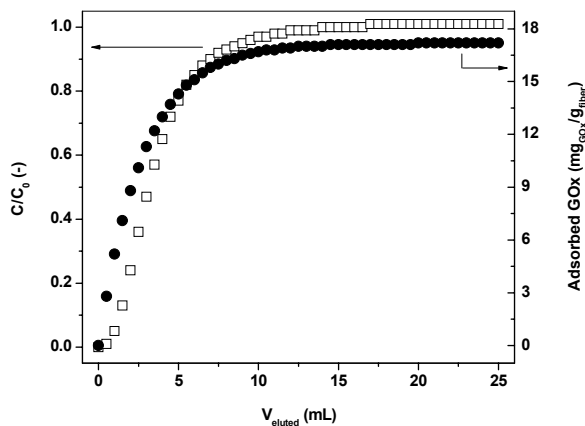


Figure 5.8 – GOx breakthrough and immobilization curves at pH 4.5. A flow rate of 1 ml/min and a GOx concentration of 0.25 mg/ml were used in the experiments. The results show an average of two experiments.

Table 5.4 – Immobilization capacities calculated from the Langmuir equation. q^* denotes the calculated (eq. 5.4) and Imm the measured GOx immobilization capacities.

pH	q^* (mg _{GOx} /g _{fiber})	Imm (mg _{GOx} /g _{fiber})
4.0	28.7	33.2
4.5	27.9	17.2

The experimental results at pH 4.0 show good agreement with the expected values as calculated from the Langmuir equation obtained for GOx adsorption for an equilibrium concentration of 0.25 mg/ml. The small variation between the two values can be attributed to an experimental error in the

lower part of the Langmuir-type isotherm curve. At pH 4.5, the variation is much more pronounced, which means that at lower concentrations the Langmuir-type isotherm does not adequately predict the adsorption behavior. This is probably due to a less dominant electrostatic adsorption mechanism at this pH due to the proximity to the pI of GOx. The fact that adsorption in the pH range of 5.0-7.0 does not follow a Langmuir-type behavior seems to support this assertion.

In figure 5.9, an overview of GOx loading relatively to the operational pH in dynamic mode is presented.

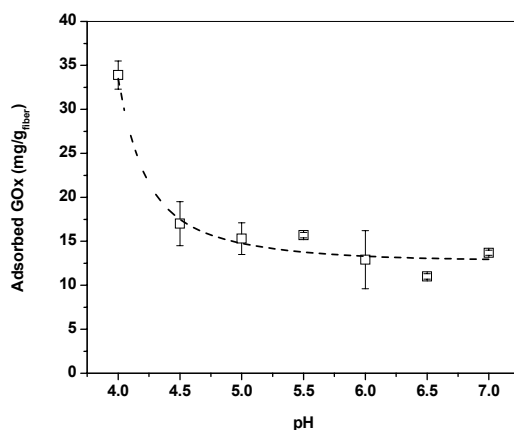


Figure 5.9 – Total GOx adsorbed in dynamic mode vs pH. The dashed line is present to guide the eye.

As expected, higher total GOx adsorption values are found at pH's below the enzyme pI, with the highest value at pH 4.0. As mentioned before, GOx is occasionally referred to possess a pI of 4.5, which explains the high adsorption. The fact that a pH value of 4.5 is higher than the typical pI, contributes for the lower stability due to weaker electrostatic interactions responsible for GOx adsorption, causing a lower total loading capacity under dynamic mode, when compared to static measurements.

At higher pH's, GOx adsorption in dynamic mode shows a similar trend as that of adsorption performed in static mode, as displayed in the graph of figure 5.6. As in static mode, hydrophobic interactions are responsible for GOx adsorption at the pH range 5.0-7.0. The higher adsorption capacities

displayed by the fibers in this pH area in dynamic mode when compared to static mode are explained by the adsorption process. In static mode, the enzyme diffuses into the fiber, being then adsorbed via short-range hydrophobic interactions by the resins embedded in the fiber wall. In dynamic mode, a constant flow of fresh enzyme is convectively permeated through the fiber wall, being thus capable of reaching the binding sites in order to be adsorbed. This causes an increased adsorption capacity of the fibers in dynamic compared to static mode. At pH's 4.0 and 4.5, the immobilization takes place mainly via faster electrostatic interactions which means that this effect is less pronounced.

Estimation of number of adsorbed glucose oxidase layers

In order to determine whether GOx adsorption takes place via multilayer formation, the area that adsorbed GOx molecules occupy per unit area must be determined. This can be done using equation 5.5, adapted from [29] and [30]

$$P_{ideal} = \frac{M_w}{\pi \cdot a \cdot b \cdot N_a} \quad (5.5)$$

where P_{ideal} denotes the ideal area covered by unit mass of GOx (ng/mm²), M_w denotes the molecular mass of GOx (ng/mol), a and b denote respectively the short and long axis of the ellipse formed by the glucose oxidase molecules (mm) and N_a is the Avogadro Number. From equation 5.5, using the values of 186×10^{12} ng/mol for M_w , 8×10^{-6} and 5.5×10^{-6} mm for a and b , respectively [31] and 6.022×10^{23} mol⁻¹ for N_a , a value of 2.23 ng/mm² for the GOx ideal coverage is obtained.

In order to calculate of the used surface coverage of the adsorbed GOx, the measured surface area resulting from the particle milling, with a value of 1.79 m²/g, is used. Since the resins possess some surface roughness, a non-uniformity factor of 1.4 is applied to the surface area [11], resulting in an active surface area of 2.51 m²/g. By using this surface area, the intraparticle volume is not taken into account as used for enzyme adsorption. This is due to the small Lewatit pore size (28.8 nm) and the high dimensions for the GOx molecules ($7 \times 5.5 \times 8$ nm [31]). This means that even a monolayer of GOx molecules adsorbed on the pore wall would effectively hinder further molecular diffusion of GOx to the intraparticle volume (fig-

ure 5.10) and a double layer would block the pore. It is therefore assumed that the internal surface area of the Lewatit particles is not contributing to the adsorption of GOx.

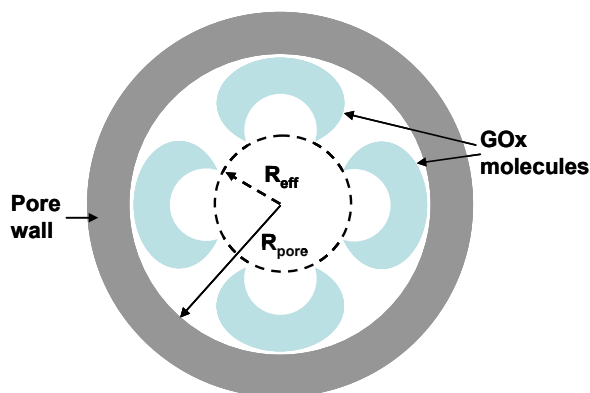


Figure 5.10 – Schematic representation of the reduction in pore diffusion area due to the adsorption of GOx molecules on the pore wall. R_{pore} denotes the pore radius and R_{eff} denotes the effective pore radius after adsorption of GOx molecules.

The total GOx surface coverage obtained during the dynamic immobilization experiments can be calculated using equation 5.6.

$$S_{coverage} = \frac{I_{GOx} \times P_{loading}}{S_{particle}} \quad (5.6)$$

where $S_{coverage}$ is the GOx surface coverage (ng/mm²), I_{GOx} is the total amount of adsorbed GOx at a given pH (ng/g), $P_{loading}$ is the particle loading in the fiber (wt. %, eq. 5.1) and $S_{particle}$ is the surface area as calculated after the particle milling (mm²/g).

From the dynamic immobilization measurements and using equation 5.6, the GOx surface coverage can be estimated. The results are shown in table 5.5.

The calculated GOx surface coverage is in all cases superior to the P_{ideal} value of 2.23 ng/mm². This means that in all situations formation of GOx multilayers is to be expected, with a minimum of 4 GOx layers being formed.

Table 5.5 – Gox surface coverage at different pH's. The particle loading is 50 wt. %

pH	Adsorbed GOx		Surface coverage (ng/mm ²)	Number of GOx layers
	mg _{GOx} /g _{fiber}	ng _{GOx} /g _{particle}		
4.0	33.9	67.8 × 10 ⁶	27.1	12
4.5	17.0	34.0 × 10 ⁶	13.6	6
5.0	15.3	30.6 × 10 ⁶	12.2	5
5.5	15.7	31.4 × 10 ⁶	12.5	5
6.0	12.9	25.8 × 10 ⁶	10.3	4
6.5	11.0	22.0 × 10 ⁶	8.8	4
7.0	13.7	27.4 × 10 ⁶	10.9	4

5.3.4 Dynamic activities

The aim of this work is to assess the enzyme immobilization effectiveness, which can only be done by evaluating the enzymatic activity of immobilized enzymes. For this purpose, fibers containing immobilized GOx were used for glucose conversion into hydrogen peroxide. The enzymatic activity was determined by measuring the absorbance at 505 nm of quinoneimine dye, which is a reaction product of a fast secondary reaction using the produced hydrogen peroxide, phenol and 4-amino-antipyrene (4-AAP), catalyzed by horse radish peroxidase (HRP). By applying different buffers and different pH's, the reaction mixture was permeated through the fiber wall, with the quinoneimine production being monitored inline using a spectrophotometer. By varying the flow rate, different contact times of the reaction mixture with the immobilized enzyme were obtained, resulting in different conversion rates.

The activity was normalized to the total fiber weight and calculated for the pH range of 4.0 to 7.0. The results are shown in figure 5.11.

The results presented in figure 5.11 show a clear maximum in the enzymatic activity of adsorbed GOx at pH 5.0, with a minimum at pH 4.0. The reason for the low activity value at pH 4.0 is attributed to the lower part of the pH range (4-7). The enzymatic activity abruptly increases at pH 4.5 and reaches a maximum at pH 5.0, after which point it steadily decreases with increasing pH. The pH optimum for the free enzymatic activity is 5.5, which is close to the maximum in the activity of adsorbed GOx. This suggests that GOx mainly retains configuration after immobilization in mixed matrix hollow-

fibers (MMHF's). This is also in accordance to literature, where different maximums for GOx activity ranging from pH 5.0 to 7.0 are published [20, 26, 32-34].

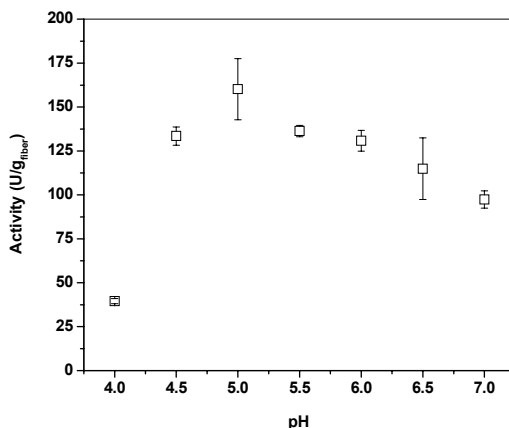


Figure 5.11 – Total enzymatic activity of immobilized GOx in glucose conversion related to dry fiber weight.

In order to better describe the behavior of immobilized GOx, the immobilized enzymatic activity is related to the total amount of adsorbed GOx, as displayed in figure 5.12.

In figure 5.12, the activity related to the amount of immobilized GOx shows a very slight decline in the pH interval between 5.0 and 7.0, similar to that presented in figure 5.11. Considering that the adsorption mechanism, due to hydrophobic interactions, is similar in this pH interval and that the adsorbed GOx amount is comparable for all pH's, this observation is not unexpected.

At pH 4.0, the enzymatic activity is lower. This is clearly due to the presence of enzyme multilayers adsorbed via electrostatic interactions onto the resins (table 5.5). In this adsorption mechanism, the lower adsorbed GOx layers are constricted by the upper ones, which cause a shielding effect in which the upper layers prevent the lower ones to contribute to the overall activity. This takes place due to the fact that the upper layers present an increased resistance to diffusion of substrate to the lower layers. This effect, in turn, increases the contact time of the substrate with the upper layers, causing it to be completely converted, thus removing the contribution of the lower GOx molecule layers due to substrate depletion. This effect, increased by

the bigger molecule size of the GOx molecule, cancels out the increased adsorption capacity the fibers possess at pH 4.0. The relatively low activity value at pH 4.5 is probably due to the also present electrostatic interactions that contribute to a higher GOx adsorption, which increases the shielding effects.

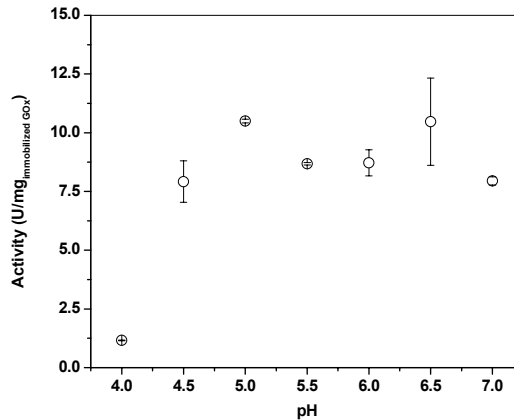


Figure 5.12 – Enzymatic activity of immobilized GOx related to total adsorbed enzyme.

An important observation taken from figures 5.11 and 5.12 is that the higher activity values obtained with the GOx adsorption taking place via hydrophobic interactions than those obtained when the adsorption takes place via electrostatic interactions. In this case, the advantage of enzyme immobilization via electrostatic interactions is in the support regeneration after enzyme inactivation, since enzyme desorption takes place by using a simple pH swing. In the case of enzyme immobilization via hydrophobic interactions, desorption takes place using hydrophobic solvents, which are prone to interact with the fiber polymeric matrix.

5.4 CONCLUSIONS

In this chapter, a new approach for enzyme immobilization using the mixed matrix membrane platform is presented. Sized down Lewatit 112WS strong cation-exchange resins are incorporated in a macroporous hollow-fiber membrane with polyethersulfone as the polymeric matrix. The prepared hollow-fibers are open and present a high interconnectivity with easy access to the embedded resins. Static adsorption tests using glucose oxidase (GOx) as model enzyme with an isoelectric point of 4.2, show an adsorption following

a Langmuir-type adsorption isotherm for low concentrations at pH's 3.5, 4.0 and 4.5. This behavior is consistent with data published for protein adsorption in cation-exchange supports at pH's lower or in the vicinity of the pI. At higher pH's, from 5.0 to 7.0, the adsorption takes place via hydrophobic interactions due to the hydrophobic nature of the ion-exchange resins.

Dynamic adsorption measurements were performed in a pH range of 4.0 to 7.0, the stability range of GOx. The highest adsorption capacity was found at pH 4.0, with a reduction in adsorption capacity at pH 4.5 and stabilization in adsorption capacity at pH's 5.0 to 7.0, due to the pH independent hydrophobic interactions governing the adsorption process.

Performance studies were carried out after the adsorption to assess the activity of adsorbed glucose oxidase and the pH influence. Results show a maximum in overall fiber activity at pH 5.0 and generally higher activities for fibers containing GOx adsorbed via hydrophobic interactions. The difference is explained by the highest intrinsic activity GOx displays in the 5.0 to 7.0 pH range and by the fact that the multilayers formed during electrostatic adsorption cause substrate depletion between the adsorbed enzyme molecules, thus reducing overall activity. These results are confirmed when comparing the activity of adsorbed glucose oxidase at different pH's. The activity increase from pH 4.0 to pH 5.0 is approximately four-fold, due to higher adsorption capacities at pH 4.0 which lead to the formation of thicker GOx layers, thus increasing the shielding effects.

This work proves that the use of mixed matrix hollow-fibers with ion-exchange functionality is viable for enzyme immobilization. Adsorption taking place via hydrophobic interactions between the resins and the enzyme yields lower adsorption but provides an increase in overall fiber activity and specific enzyme activity.

Acknowledgement

The authors acknowledge The Netherlands Organization for Scientific Research (NWO) for the financial support of the project.

REFERENCES

1. Boller, T., C. Meier, and S. Menzler, *EUPERGIT oxirane acrylic beads: How to make enzymes fit for biocatalysis*. Organic Process Research & Development, 2002. **6**(4): p. 509.

2. Tischer, W. and F. Wedekind, *Immobilized enzymes: Methods and applications*, in *Biocatalysis - From Discovery To Application*. 1999. p. 95.
3. Mateo, C., et al., *Improvement of enzyme activity, stability and selectivity via immobilization techniques*. *Enzyme and Microbial Technology*, 2007. **40**(6): p. 1451.
4. Katchalski-Katzir, E., *Immobilized enzymes -- learning from past successes and failures*. *Trends in Biotechnology*, 1993. **11**(11): p. 471.
5. Katchalski-Katzir, E. and D.M. Kraemer, *Eupergit (R) C, a carrier for immobilization of enzymes of industrial potential*. *Journal Of Molecular Catalysis B-Enzymatic*, 2000. **10**(1-3): p. 157.
6. Rao, S.V., K.W. Anderson, and L.G. Bachas, *Oriented immobilization of proteins*. *Mikrochimica Acta*, 1998. **128**(3-4): p. 127.
7. Kiyono, R., et al., *Mixed matrix microporous hollow fibers with ion-exchange functionality*. *Journal of Membrane Science*, 2004. **231**(1-2): p. 109.
8. Lensmeyer, G.L., et al., *Use of particle-loaded membranes to extract steroids for high-performance liquid chromatographic analyses improved analyte stability and detection*. *Journal of Chromatography A*, 1995. **691**(1-2): p. 239.
9. Lingeman, H. and S.J.F. Hoekstra-Oussoren, *Particle-loaded membranes for sample concentration and/or clean-up in bioanalysis*. *Journal of Chromatography B: Biomedical Sciences and Applications*, 1997. **689**(1): p. 221.
10. Avramescu, M.E., Z. Borneman, and M. Wessling, *Mixed-matrix membrane adsorbers for protein separation*. *Journal Of Chromatography A*, 2003. **1006**(1-2): p. 171.
11. Avramescu, M.E., et al., *Preparation of mixed matrix adsorber membranes for protein recovery*. *Journal Of Membrane Science*, 2003. **218**(1-2): p. 219.
12. Avramescu, M.E., et al., *Adsorptive membranes for bilirubin removal*. *Journal Of Chromatography B-Analytical Technologies In The Biomedical And Life Sciences*, 2004. **803**(2): p. 215.
13. Saiful, Z. Borneman, and M. Wessling, *Enzyme capturing and concentration with mixed matrix membrane adsorbers*. *Journal of Membrane Science*, 2006. **280**(1-2): p. 406.
14. Barsan, M.M., et al., *Design and application of a flow cell for carbon-film based electrochemical enzyme biosensors*. *Talanta*, 2007. **71**(5): p. 1893.

15. Bidan, G., *Electroconducting conjugated polymers: New sensitive matrices to build up chemical or electrochemical sensors. A review*. Sensors and Actuators B: Chemical, 1992. **6**(1-3): p. 45.
16. Cosnier, S., *Biomolecule immobilization on electrode surfaces by entrapment or attachment to electrochemically polymerized films. A review*. Biosensors and Bioelectronics, 1999. **14**(5): p. 443.
17. Pauliukaite, R., et al., *Characterisation of poly(neutral red) modified carbon film electrodes; application as a redox mediator for biosensors*. Journal of Solid State Electrochemistry, 2007. **11**(7): p. 899.
18. Garke, G., et al., *The Influence of Protein Size on Adsorption Kinetics and Equilibria in Ion-Exchange Chromatography*. Separation Science and Technology, 1999. **34**(13): p. 2521.
19. Sun, H., et al., *A study of human γ -globulin adsorption capacity of PVDF hollow fiber affinity membranes containing different amino acid ligands*. Separation and Purification Technology, 2006. **48**(3): p. 215.
20. Rauf, S., et al., *Glucose oxidase immobilization on a novel cellulose acetate-polymethylmethacrylate membrane*. Journal of Biotechnology, 2006. **121**(3): p. 351.
21. Vinu, A., et al., *Adsorption of cytochrome c on mesoporous molecular sieves: Influence of pH, pore diameter, and aluminum incorporation*. Chemistry of Materials, 2004. **16**(16): p. 3056.
22. Arica, M.Y., et al., *Dye derived and metal incorporated affinity poly(2-hydroxyethyl methacrylate) membranes for use in enzyme immobilization*. Polymer International, 1998. **46**(4): p. 345.
23. Arica, M.Y., H.N. Testereci, and A. Denizli, *Dye-ligand and metal chelate poly(2-hydroxyethylmethacrylate) membranes for affinity separation of proteins*. Journal of Chromatography A, 1998. **799**(1-2): p. 83.
24. Sarfert, F.T. and M.R. Etzel, *Mass transfer limitations in protein separations using ion-exchange membranes*. Journal of Chromatography A, 1997. **764**(1): p. 3.
25. Smuleac, V., D.A. Butterfield, and D. Bhattacharyya, *Layer-by-Layer-Assembled Microfiltration Membranes for Biomolecule Immobilization and Enzymatic Catalysis*. Langmuir, 2006. **22**(24): p. 10118.
26. Pekel, N., B. Salih, and O. Guven, *Activity studies of glucose oxidase immobilized onto poly(N-vinylimidazole) and metal ion-chelated poly(N-vinylimidazole) hydrogels*. Journal of Molecular Catalysis B: Enzymatic, 2003. **21**(4-6): p. 273.

27. Kusakari, A., M. Izumi, and H. Ohnuki, *Preparation of an enzymatic glucose sensor based on hybrid organic-inorganic Langmuir-Blodgett films: Adsorption of glucose oxidase into positively charged molecular layers*. *Colloids and Surfaces A: Physicochemical and Engineering Aspects*, 2008. **321**(1-3): p. 47.
28. Kalisz, H.M., J. Hendle, and R.D. Schmid, *Structural and biochemical properties of glycosylated and deglycosylated glucose oxidase from *Penicillium amagasakiense**. *Applied Microbiology and Biotechnology*, 1997. **47**(5): p. 502.
29. Simonian, A.L., et al., *Characterization of oxidoreductase-redox polymer electrostatic film assembly on gold by surface plasmon resonance spectroscopy and Fourier transform infrared-external reflection spectroscopy*. *Analytica Chimica Acta*, 2002. **466**(2): p. 201.
30. Lahiri, J., et al., *Biospecific Binding of Carbonic Anhydrase to Mixed SAMs Presenting Benzenesulfonamide Ligands: A Model System for Studying Lateral Steric Effects*. *Langmuir*, 1999. **15**(21): p. 7186.
31. Vianello, F., et al., *Determination of glucose oxidase immobilised as monolayer onto a flat surface*. *Journal of Biochemical and Biophysical Methods*, 2002. **51**(3): p. 263.
32. Hou, X., et al., *Covalent immobilization of glucose oxidase onto poly(styrene-co-glycidyl methacrylate) monodisperse fluorescent microspheres synthesized by dispersion polymerization*. *Analytical Biochemistry*, 2007. **368**(1): p. 100.
33. Onda, M., K. Ariga, and T. Kunitake, *Activity and stability of glucose oxidase in molecular films assembled alternately with polyions*. *Journal of Bioscience and Bioengineering*, 1999. **87**(1): p. 69.
34. Dumont, J. and G. Fortier, *Behavior of glucose oxidase immobilized in various electropolymerized thin films*. *Biotechnology and Bioengineering*, 1996. **49**(5): p. 544.

6

Glucose oxidase immobilization in covalent mixed matrix hollow-fibers

ABSTRACT

Glucose oxidase (GOx) was covalently bound onto Eupergit® C particles embedded in mixed matrix hollow fiber membranes prepared using polyethylene vinyl alcohol (EVAL) as the polymeric macroporous matrix. The Eupergit® C particles were chemically modified with ethylenediamine and activated with glutaraldehyde, ground and fractionated into 20-40 and < 20 µm size classes. GOx was immobilized in the fibers in dynamic mode. Fibers containing the smallest particles show the highest immobilization capacity due to the increased external particle surface area. The activity of immobilized enzyme was evaluated by dynamic conversion of glucose. The results proved that the enzyme retains enzymatic activity after immobilization. The highest glucose conversion yields are obtained with fibers which contain the bigger particles, which is attributed to a better fiber wall morphology leading to an improved flow distribution. The results further showed that GOx covalently immobilized in EVAL/Eupergit® fibers has a lower enzymatic activity than GOx that is physically immobilized in polyether sulfone (PES) fibers containing strong cation exchange (SCIEX) resins. The reduced activity is explained by the differences in the materials used, immobilization methods, fiber morphologies and applied pH's in each case.

6.1 INTRODUCTION

Mixed matrix membranes (MMM's) are materials in which small functional particles are embedded in a polymeric matrix. These materials present a synergistic match between classical membrane and chromatography materials. MMM's are characterized by high fluxes and low pressure drop across the membrane wall, with the fluid transport being predominantly convectively controlled, as typical for pressure driven membrane systems. The active sites are provided by functionalized particles embedded in the membrane wall, which permit to obtain high capacities and selectivities as typical of chromatography media. MMM's present therefore the typical advantages of both techniques, showing the high capacities of chromatographic media and the hydrodynamic characteristics of membranes. The main advantages of the MMM platform technology when compared to packed bed columns are the low manufacturing costs and the flexibility in geometry [1, 2], which permit tailoring of the material to the desired application. Mixed matrix membranes are prepared according to the same procedure as common micro- and ultrafiltration membranes. A homogeneous solution containing polymer, solvent and additives is prepared and thereafter particles with the desired functionality and size are dispersed. The dispersion can then be either cast into a flat-sheet or spun as a hollow-fiber membrane using a phase inversion process, typically using water as a non-solvent.

Although initially developed for improving pervaporation and gas permeation transport using polymeric films containing zeolites as the active material [3-6], mixed matrix membranes started more recently to be applied in micro- and ultrafiltration as a pre-treatment for solute concentration before chromatography processes [7, 8]. This technique has also been applied in processes involving the adsorption and capturing of peptides from multi-component mixtures [9-11], protein adsorption [12], toxin removal [13] and enzyme capturing and concentration [14] by using embedded particles with different functionalities.

Enzymes have been used for decades for biocatalytic processes to obtain improved purities and yields due to their high specificity and selectivity while maintaining the processes environmentally friendly [15]. The need for enzyme removal after the conversion process and the interest in enzyme reutilization has driven the interest in enzyme immobilization [15]. Further advantages of enzyme immobilization are long-term stability and increased

chemical and thermal resistance, which add to the economic benefits [16-18].

In this work we covalently immobilize the enzyme glucose oxidase (GOx) in a mixed matrix hollow-fiber (MMHF) in order to perform dynamic enzymatic conversions. The covalent immobilization in supports generally provides stronger enzyme-support bonds, which increases the enzyme stability when compared to other enzyme-support binding mechanisms. The coupling can take place between any readily available functional group on the surface of the support with compatible groups in the aminoacid residues present in the enzyme [19]. This chapter describes the dynamic GOx immobilization onto epoxy functionalized Eupergit® C particles embedded in a MMHF. The enzymatic activity of immobilized GOx was evaluated by dynamic glucose conversion. In order to study the particle size influence, fibers containing two different particle size classes (20-40 μm and $< 20 \mu\text{m}$) were used. The enzymatic performance was compared with the results presented in chapter 5, for fibers containing physically bound GOx.

6.2 EXPERIMENTAL

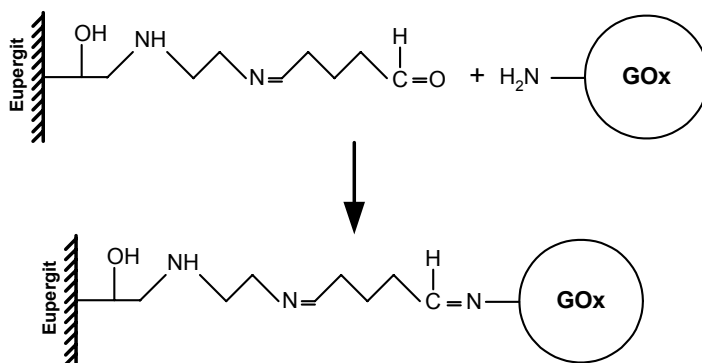
The experimental section follows the same procedures as presented in chapter 4 for the chemical modification, milling and sieving of the two Eupergit® C particle size classes (20-40 and $< 20 \mu\text{m}$). Also the spinning of EVAL fibers containing the prepared Eupergit® C particles and the preparation of a lab scale module are described in chapter 4.

6.2.1 Materials

Potassium phosphates (mono- and dibasic, Acros) were used for preparing the buffer solutions. Glucose Oxidase from *aspergillus niger* (Fluka, the main characteristics are presented in table 6.1) was used as the immobilized enzyme (figure 6.1). Glucose (Merck) was used as substrate for determining the glucose oxidase enzymatic activity. Phenol (Acros Organics), 4-amino antipyrine (Acros Organics) and horseradish peroxidase (Sigma) were employed in the secondary conversion reaction. Ultrapure water was prepared using a Millipore purification unit Milli-Q plus.

Table 6.1 – Relevant data of glucose oxidase as provided by the supplier.

Property	Data
Isoelectric point (pI)	4.2
Molecular weight	186×10^3 g/mol
pH activity range	4-7
pH optimum	5.5
Enzymatic activity	159 U/mg

**Figure 6.1** – Coupling chemistry of glucose immobilization in chemically modified Eupergit® C particles.

6.2.2 Dynamic immobilization

The dynamic GOx immobilization capacity of the fibers was determined by evaluating the breakthrough curves. A solution of 0.25 mg/ml of GOx in 50 mM phosphate buffer at pH 7.0 was eluted through the fiber in dead-end mode at a 0.15 ml/min flow-rate using an Äkta Purifier chromatographic system. The breakthrough curve was determined by measuring the GOx depletion at 280 nm using the in-line spectrophotometer. The immobilization of GOx in the fiber was calculated according to the following equation.

$$I = \sum i_j \quad (6.1)$$

$$i = \frac{\left(1 - \frac{C'}{C_0}\right) \times C_0 \times V'}{W} \quad (6.2)$$

with I the total amount of immobilized GOx in the membrane (mg/g), i as the fraction of GOx immobilized in the membrane (mg/g), C' the fractional concentration in the permeate side (mg/ml), C_0 the initial concentration (mg/ml), V' the fraction volume (ml) and W as the dry weight of membrane (g).

6.2.3 Enzymatic activity

GOx activity was calculated for the free and the covalently bound enzyme. The method was based on the work by Rauf *et al* [20], using glucose as substrate. Glucose is converted in the presence of water and oxygen to hydrogen peroxide and gluconic acid. In a fast secondary reaction, the produced hydrogen peroxide reacts with phenol and 4-Amino-Antipyrine (4-AAP) in the presence of horseradish peroxidase (HRP) to water and quinoneimine. The activity of GOx was measured by recording the production of quinoneimine in time, by measuring the light absorbance of the solution at 505 nm. The two-step reaction is depicted in figure 6.2.



Figure 6.2 – Two-step reaction used for GOx activity measurements. The second reaction, which produces the quinoneimine, is much faster than the first reaction and is therefore used to measure the GOx activity.

Static activity

The activity of free GOx in static mode was measured using solutions of 8.5 mM of glucose, 41.5 mM phenol, 0.06 mM 4-AAP and 0.08 U/ml of HRP in buffers at different pH's. 3 ml of the solution were placed in a 10 mm quartz cuvette, to which 20 μ l of a 200 U/ml GOx solution were added. After homogenization, the increase in signal at 505 nm in time was recorded using a Varian Cary 300 spectrophotometer. The obtained values were plotted against time and the activity was taken from the linear portion of the curve and related to the dry weight of enzyme.

Dynamic activity

Dynamic activity of the covalently bound GOx was evaluated by adapting the static method. After the GOx binding, the fiber was washed with buffer to remove the unbound enzyme molecules. A solution of 50 mM glucose, 50 mM phenol, 0.08 mM 4-AAP and 0.1 U/ml HRP was permeated through the fiber walls with different flow rates. The permeate absorbance was monitored at 505 nm to evaluate the quinoneimine production. For each flow rate, the reaction was given time to reach steady-state conditions, at which the absorbance value was registered. By using different flow rates it was possible to achieve different absorbance values for different residence times [21]. The values were plotted against the different residence times and the enzymatic activity was calculated from the linear portion of the curve and related to the dry weight of used fiber or to the dry weight of adsorbed enzyme. In order to keep the experiments in neutral conditions, a pH of 7.0 was used in all situations.

6.3 RESULTS AND DISCUSSION

6.3.1 Membrane morphology

The morphology of the applied fibers is presented in chapter 4. Figures 4.6 and 4.7 illustrate the results from the scanning electron microscopic (SEM) analysis.

6.3.2 Dynamic immobilization

GOx was immobilized by permeating a solution of 0.25 mg/ml through the fiber at a flow rate of 0.15 ml/min, corresponding to a residence time of 1.9 minutes for FCm₂₀ fibers and 1.6 minutes for FCm₄₀ fibers. The breakthrough curves for the dynamic immobilization performed both on FCm₂₀ and FCm₄₀ fibers are presented in figure 6.3. The results are average values of at least two experiments with good reproducibility.

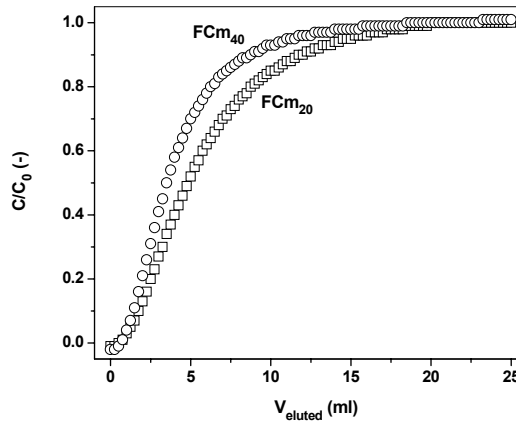


Figure 6.3 – GOx breakthrough curves for FCM₂₀ and FCM₄₀ fibers. A flow rate of 0.15 ml/min and a GOx concentration of 0.25 mg/ml were used in the experiments.

The results depicted in figure 6.3 clearly show a faster breakthrough of GOx when permeated through FCM₄₀ fibers when compared to permeation through FCM₂₀ fibers. This is due to the fact that FCM₄₀ fibers contain bigger sized particles (particle size 20-40 μm) than the FCM₂₀ fibers (particle sizes < 20 μm). This means that for FCM₄₀ fibers a smaller active surface area is available for GOx immobilization, when compared to the FCM₂₀ fibers. Due to the high molecular weight of GOx (160 kDa), the molecules do not have access to the complete interior pore structure of the Eupergit® C particles, which possess a fine porous structure with an average pore size of 10 nm. For this reason, the GOx immobilization is mainly controlled by the external particle surface area. It is therefore to expect that the total immobilization capacity for FCM₂₀ fibers is higher than that for FCM₄₀. This hypothesis is configured by figure 6.4 and table 6.2.

It is important to notice that, at these low flow rates, the fiber structure has little influence on the immobilization capacity, since the linear speed of permeation across the membrane wall is very low, which greatly increases the GOx residence time in the fibers and allows the GOx molecules to diffuse from the permeating bulk solution to the surface of the embedded particles. This means that preferential flow paths across the fiber wall do not dictate the immobilization process. This discussion is further developed in chapter 4.

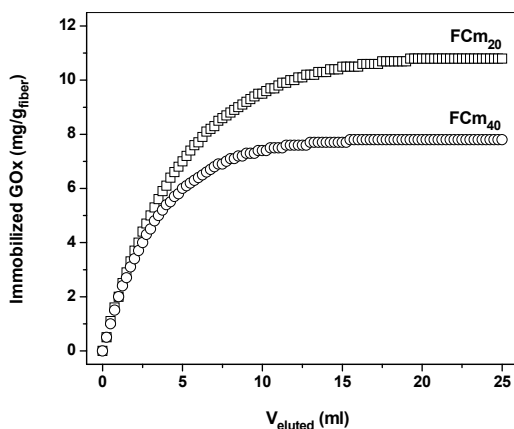


Figure 6.4 – Dynamic immobilization curves for FCm₂₀ and FCm₄₀ fibers as calculated using equations 6.1 and 6.2. The eluted solution has a GOx concentration of 0.25 mg/ml.

6.3.3 Dynamic activity measurements

The activity of immobilized glucose oxidase was evaluated by permeating a glucose solution through the fiber wall at different flow rates. The reaction product hydrogen peroxide reacts subsequently with phenol and 4-aminoantipyrine (4-AAP) in the presence of horseradish peroxidase (HRP) to quinoneimine, a dye with an absorbance maximum at 505 nm. The quinoneimine production is therefore linked to the glucose conversion rate which means that in the presence of excess phenol, 4-AAP and HRP, the activity of immobilized GOx determines the kinetics of the reaction. By applying different flow rates, different residence times in the fiber wall and therefore different reaction times can be obtained. The results of the activity measurements are summarized in table 6.2.

Table 6.2 – Fiber immobilization capacity and enzymatic activity of immobilized GOx.

Fiber	Immobilized GOx (mg/g_{fiber})	Activity (U/g_{fiber})
FCm ₂₀	10.8 ± 2.1	20.1 ± 2.2
FCm ₄₀	7.8 ± 0.4	30.1 ± 1.9

The activity results presented in table 6.2 show a considerable higher activity for GOx immobilized in FCm₄₀ fibers (containing particles in the size class of 20-40 μm) over that of GOx immobilized in FCm₂₀ fibers (containing particles with sizes < 20 μm). These results are in contradiction with the immobilization results, which show a higher immobilization capacity for FCm₂₀ than for FCm₄₀. This discrepancy can be explained by the difference in fiber structure and the nature of the experiments for the dynamic immobilization and the dynamic activity measurements. In the dynamic immobilization process, the applied flow rate is very low, 0.15 ml/min, permitting the big GOx molecules a long time interval to diffuse towards the surface of the embedded particles that are located in diffusive regions in the fiber wall. In the case of dynamic activity measurements, the applied flow rate ranges from 0.5 to 5.0 ml/min, thus greatly reducing the residence time of the substrate solution in the fiber wall. This means that in the dynamic immobilization process the transport of GOx to the active sites located on the particle surface is more diffusively controlled, while in the dynamic activity measurements the transport of substrate molecules is dominated predominantly by convective mechanisms. Furthermore, SEM images show that the morphology of FCm₂₀ and FCm₄₀ fibers is different. The FCm₂₀ fibers contain voids in the fiber wall, whereas in the FCm₄₀ fibers voids are hardly present. The result is that the preferential flow in the FCm₂₀ fibers causes passage of substrate molecules which have almost no interaction with the immobilized GOx molecules. As consequence, the “effective” enzymatic activity in the FCm₂₀ fibers is lower than in FCm₄₀ fibers.

6.3.4 Comparison with MMF with cation-exchange functionality

In order to provide a better insight into the effectiveness of covalently immobilized glucose oxidase in FCm₂₀ and FCm₄₀ fibers, the enzymatic activity was compared with glucose oxidase immobilized in mixed matrix hollow fibers via physical interaction using strong cation-exchange resins (SCIEX). The results are present in chapter 5. The comparison was made in terms of the activity normalized by the amount of immobilized GOx.

The enzymatic activity of GOx in fibers containing SCIEX resins is significantly higher than in the fibers containing modified Eupergit® C. In SCIEX resins, the immobilization takes place via electrostatic interaction at pH's lower than the isoelectric point (pI) of GOx, where the enzyme molecules are in the cationic form. For glucose oxidase, the supplier provided a pI of 4.2.

At higher pH's, the molecules increasingly assume anionic form, which means that electrostatic interaction no longer plays a role in the immobilization of GOx. Since the divinylbenzene/polystyrene based resins embedded in the fibers present also hydrophobic domains [22], enzyme immobilization at pH's above the pI takes place via hydrophobic interactions.

The dynamic activity of GOx immobilized in fibers containing strong cation-exchange resins is considerably higher for pH's over 4.0 than that of FC_{m20} (over three times higher) and FC_{m40} (two times higher). The difference can be explained by the contribution of several factors that differ in each case.

- polymeric matrix: the applied polymers are different. In the covalent experiments, ethylene vinyl alcohol is used as polymer and Eupergit® is used as the particulate material. In experiments with physically bound enzymes, polyether sulfone is used as polymer and SCIEX as the particulate material. The applied polymers present different properties which reflects on the different morphology of both fibers. PES/SCIEX fibers present a much more homogeneous fiber structure than FC_{m40} and FC_{m20} fibers, which present more irregularities. This contributes to a better flow profile along the fiber wall, thus reducing possible instabilities that can reduce the overall enzymatic activity;
- particle size: in the PES/SCIEX fibers, the particle size is considerably lower than in the case of the Eupergit® particles. Since the particle size has been shown to have an influence in the amount and on the enzymatic activity of immobilized GOx, it is reasonable to consider that the particle size difference, even when the particles have a different nature, influences the overall enzymatic activity;
- immobilization mechanism: in FC_{m40} and FC_{m20} fibers, the immobilization takes place by covalently binding the GOx molecules to the surface of the particles embedded in the fiber wall. In PES/SCIEX fibers, the physical immobilization, at pH's below the pI, takes place via electrostatic interactions, while at pH above the pI, binding takes place via hydrophobic interactions. In covalent immobilization, the bond is much stronger than in both electrostatic and hydrophobic interactions, but also promotes multi-point attachment (figure 6.5), which contributes to the reduction in enzymatic activity [23]. Multi-point attachment is further enhanced in the case of Eupergit® particles, which present an initial high density of oxirane functionalized groups that can be used for enzyme immobilization;

At pH 4.0, where the GOx immobilization in the PES/SCIEX fibers takes place via strong electrostatic interactions, formation of GOx multi-layers occurs. Due to this fact, GOx molecules immobilized in the lower layers do not come into contact with substrate molecules, which are depleted by conversion in the upper GOx layers. In addition to the possibilities presented above, this also explains the lower enzymatic activity per amount of immobilized glucose oxidase. A more complete discussion can be found in chapter 5.

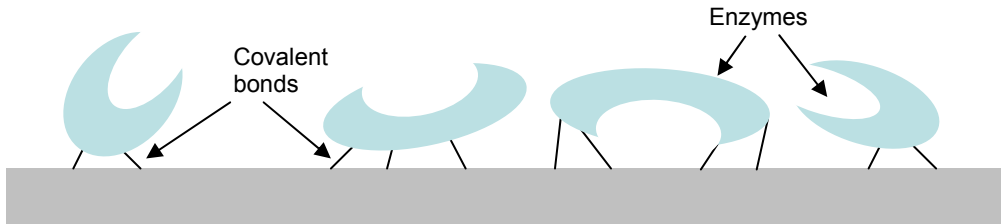


Figure 6.5 – Schematic representation of covalent immobilization via multi-point covalent attachment. The high density of active sites on the carrier surface promotes covalent binding to several available groups in the enzyme structure and changes the conformation of the enzyme molecules. This reduces access of substrate to the conversion sites and thus overall activity.

The lower enzymatic activity obtained by the covalent immobilization in comparison to that of the physically immobilized enzymes can be attributed to a combination of factors. Based on the current results, it is not possible to indicate which factor plays the most determinant role. A more detailed discussion of the different immobilization methods can be found in chapter 2 and the influence of fiber morphology and particle size for FCM₄₀ and FCM₂₀ fibers can be found in chapter 4.

6.4 CONCLUSIONS

In this chapter glucose oxidase (GOx) was covalently immobilized on modified Eupergit® C particles (in two different particle size classes, 20-40 μm and < 20 μm) embedded in mixed matrix hollow fibers (MMHF). Dynamic immobilization tests showed that the amount of covalently bound GOx in Eupergit® C-functionalized MMHF's depends on the size of the Eupergit® C particles. Fibers containing smaller particles are able to bind more GOx to the matrix. This is due to the high molecular size of GOx (7×5.5×8 nm [24])

and the low pore size of Eupergit® C particles (10 nm). Therefore GOx binding takes place only on the external particle surface area.

MMHF's containing bigger particles show a higher enzymatic activity, which is due to the more homogeneous fiber wall structure which reduces the possibility of preferential flow through the fiber wall when compared to fibers containing smaller particles, which present more voids in the wall structure. Preferential flow is an important factor in dynamic conversion experiments, since the applied permeation flow rates (0.5 to 5.0 ml/min) are much higher than in the case of the dynamic immobilization (0.15 ml/min). Dynamic immobilization, in contrast, uses longer permeation times during the elution through the fiber wall and is, therefore, less dependent on irregularities in fiber morphology.

The enzymatic activity of GOx covalently bound in Eupergit® C-containing fibers was considerably lower than that of GOx immobilized in PES/SCIEX fibers. The difference between the enzymatic activities of immobilized GOx in each fiber type is explained by a conjugation of different factors which reflect the different fiber properties and each immobilization method. Further statements about the differences can only be made after a more thorough evaluation of the influence of the polymeric matrix, particle size and the different immobilization mechanisms, studies which fall out of the scope of this work.

The work presented in this chapter shows that mixed matrix membranes present a flexible platform for enzyme immobilization by immobilizing enzymes on embedded particles with different functionalities. Furthermore, flexibility is enhanced by the fact that different supports can be used according to the desired application.

Acknowledgement

The authors acknowledge The Netherlands Organization for Scientific Research (NWO) for the financial support of this project.

REFERENCES

1. Vu, D.Q., W.J. Koros, and S.J. Miller, *Mixed matrix membranes using carbon molecular sieves: I. Preparation and experimental results*. Journal of Membrane Science, 2003. **211**(2): p. 311.

2. Vu, D.Q., W.J. Koros, and S.J. Miller, *Mixed matrix membranes using carbon molecular sieves: II. Modeling permeation behavior*. Journal of Membrane Science, 2003. **211**(2): p. 335.
3. Duval, J.M., et al., *Adsorbent filled membranes for gas separation. Part 1. Improvement of the gas separation properties of polymeric membranes by incorporation of microporous adsorbents*. Journal of Membrane Science, 1993. **80**(1): p. 189.
4. Li, Y., et al., *The effects of polymer chain rigidification, zeolite pore size and pore blockage on polyethersulfone (PES)-zeolite A mixed matrix membranes*. Journal of Membrane Science, 2005. **260**(1-2): p. 45.
5. Pechar, T.W., et al., *Preparation and characterization of a glassy fluorinated polyimide zeolite-mixed matrix membrane*. Desalination, 2002. **146**(1-3): p. 3.
6. te Hennepe, H.J.C., et al., *Zeolite-filled silicone rubber membranes: Part 1. Membrane preparation and pervaporation results*. Journal of Membrane Science, 1987. **35**(1): p. 39.
7. Lensmeyer, G.L., et al., *Use of particle-loaded membranes to extract steroids for high-performance liquid chromatographic analyses improved analyte stability and detection*. Journal of Chromatography A, 1995. **691**(1-2): p. 239.
8. Lingeman, H. and S.J.F. Hoekstra-Oussoren, *Particle-loaded membranes for sample concentration and/or clean-up in bioanalysis*. Journal of Chromatography B: Biomedical Sciences and Applications, 1997. **689**(1): p. 221.
9. Baxter-International, *Composite membranes and methods to make such membranes*. 1999, Patent WO0002638. p. 58.
10. Millipore, *Cast membrane structures for sample preparation*. 2000, Patent US6048457.
11. Tokuyama-Soda-Kabushiki-Kaisha, *Microporous shaped article and process for preparation thereof*. 1993, Patent US5238735.
12. Avramescu, M.-E., et al., *Preparation of mixed matrix adsorber membranes for protein recovery*. Journal of Membrane Science, 2003. **218**(1-2): p. 219.
13. Avramescu, M.E., et al., *Adsorptive membranes for bilirubin removal*. Journal of Chromatography B, 2004. **803**(2): p. 215.
14. Saiful, Z. Borneman, and M. Wessling, *Enzyme capturing and concentration with mixed matrix membrane adsorbents*. Journal of Membrane Science, 2006. **280**(1-2): p. 406.

15. Boller, T., C. Meier, and S. Menzler, *EUPERGIT oxirane acrylic beads: How to make enzymes fit for biocatalysis*. Organic Process Research & Development, 2002. **6**(4): p. 509-519.
16. Katchalski-Katzir, E., *Immobilized enzymes -- learning from past successes and failures*. Trends in Biotechnology, 1993. **11**(11): p. 471.
17. Katchalski-Katzir, E. and D.M. Kraemer, *Eupergit (R) C, a carrier for immobilization of enzymes of industrial potential*. Journal Of Molecular Catalysis B-Enzymatic, 2000. **10**(1-3): p. 157-176.
18. Mateo, C., et al., *Improvement of enzyme activity, stability and selectivity via immobilization techniques*. Enzyme and Microbial Technology, 2007. **40**(6): p. 1451.
19. Bickerstaff, G.F., ed. *Immobilization of Enzymes and Cells*. Methods in Biotechnology. Vol. 1. 1997, Humana Press: Totowa, New Jersey.
20. Rauf, S., et al., *Glucose oxidase immobilization on a novel cellulose acetate-polymethylmethacrylate membrane*. Journal of Biotechnology, 2006. **121**(3): p. 351.
21. Bencina, K., et al., *Enzyme immobilization on epoxy- and 1,1'-carbonyldiimidazole-activated methacrylate-based monoliths*. Journal Of Separation Science, 2004. **27**(10-11): p. 811-818.
22. Sanagi, M.M., et al., *Development and Application of New Modified Poly(styrene-divinylbenzene) Adsorbents and Chromatography Stationary Phases. Volume 1: PS-DVB Heptadecyl Ketone, Chloromethyl PS-DVB, and Octadecoxy Methyl PS-DVB*. 1996, University Teknologi Malaysia.
23. Mateo, C., et al., *Increase in conformational stability of enzymes immobilized on epoxy-activated supports by favoring additional multi-point covalent attachment*. Enzyme and Microbial Technology, 2000. **26**(7): p. 509-515.
24. Vianello, F., et al., *Determination of glucose oxidase immobilised as monolayer onto a flat surface*. Journal of Biochemical and Biophysical Methods, 2002. **51**(3): p. 263.

SUMMARY

Chemical reactors are one of the main focus points for optimization within process engineering. There is a permanent search for new methods which can improve yields and reduce costs, thus making the processes more effective and affordable. In this search, process optimization can be performed to equipment, materials, reactants, conditions or in the dynamics of the process itself. An approach which has been consistently growing concerns the merge of different platforms, where the best characteristics of each technology are used in order to overcome the possible individual shortcomings. Examples of this approach are membrane reactors, where the separation effects and operation advantages of membranes are used to improve the reaction taking place.

This thesis focuses on the development of new types of membrane reactors based on mixed matrix membranes (MMM) where the basic membrane structure is used as a support matrix for embedded particles which act as catalysts, either as a carrier for immobilized enzymes or as catalysts themselves. This concept takes advantage of the excellent flow properties of membranes, such as high throughput or low pressure drop, and the inherent characteristics of chromatographic particles, such as the high diversity of chemical affinities or the high density of functional groups.

In chapter 2, an introduction over the different types of enzyme immobilization is given. The discussion focuses mainly on the different methods for immobilization and the different types of carrier which can be used. In the end, a short history about mixed matrix membranes is presented.

In chapter 3, a flat-sheet MMM was prepared and optimized for the immobilization of trypsin. The MMM is prepared using a phase inversion process using ethylene vinyl alcohol (EVAL) as the polymeric matrix and Eupergit® as the chromatographic particles. The embedding is achieved by dispersing Eupergit® particles, milled to sizes of 20 to 40 μm , in the polymer dope. Two types of Eupergit® particles, Eupergit® C and Eupergit® C250L, with different densities of functional groups and pore sizes, employed for covalent immobilization of enzymes, are used. The influence of the embedding process in the particle functionality was evaluated. The immobilization capacity

and the enzymatic activity were tested for trypsin immobilized in suspended Eupergit® particles (milled and non-milled) and in Eupergit® in a packed bed. The same tests were performed using the prepared MMM. In order to improve the enzymatic activity of immobilized trypsin, the Eupergit® particles are chemically modified with ethylenediamine and glutaraldehyde prior to milling. Eupergit® C particles show an overall better performance than Eupergit® C250L particles in terms of enzymatic activity of trypsin for all situations. The enzymatic activity is proved to improve by embedding the particles in a mixed matrix membrane comparatively to particles in packed beds. The chemical modification proves also to be advantageous, causing at least a nine fold increase in enzymatic activity for trypsin immobilized in MMM containing chemically modified Eupergit® C comparatively to the other supports.

Chapter 4 describes the preparation of mixed matrix hollow-fibers (MMHF) using EVAL and chemically modified Eupergit® C particles. The fibers were prepared by phase inversion using wet-spinning technique. The best polymer dope compositions were developed in order to optimize the fiber morphology. Two different size classes were used, 20-40 μm and $< 20 \mu\text{m}$. The fibers are used in trypsin immobilization and the fiber performance was evaluated in terms of the enzymatic activity of immobilized trypsin. MMHF proves to be better than flat-sheet MMM due to a better flow distribution through the membrane wall. The comparison between MMHF containing 20-40 μm and $< 20 \mu\text{m}$ particles yields no significant differences, implying that the advantages of particle size reduction do not extend to particles smaller than 20 μm .

The preparation of MMHF containing strong cation-exchange Lewatit resins as chromatographic particles is the focus of chapter 5. The MMHF were prepared using polyether sulfone (PES) as a polymeric matrix. The prepared fibers were used for the static immobilization of glucose oxidase (GOx) at different pH values. At pH's below the isoelectric point (pI) of the enzyme, the immobilization takes place via electrostatic interactions and follows a Langmuir-type adsorption isotherm. At pH values above the pI, the adsorption takes place via hydrophobic interactions and yields lower adsorption capacities. Dynamic immobilization tests show adsorption capacities close to those of static measurements. The activity of the immobilized GOx was evaluated by glucose conversion. The results show that higher adsorption capacities do not correspond to higher enzymatic activities normalized for the amount of adsorbed glucose oxidase. The reason for this behavior is attributed to the formation of GOx multi-layers in which the top layers deplete the substrate (glucose) and the lower layers do not contribute to the overall enzymatic activity.

The flexibility of the mixed matrix membrane platform is evaluated in chapter 6. The covalent-based mixed matrix hollow-fibers developed in chapter 4 were used for the immobilization of glucose oxidase. The results show that the covalent-based fibers are adequate for GOx immobilization and that the GOx stays active after immobilization. A comparison between the covalent-based MMHF and the strong cation-exchange based MMHF developed in chapter 5 prove that the latter fibers are more advantageous for this system, with the activity of immobilized GOx being more than doubled comparatively to the ones showed in the case of covalent-based MMHF.

SAMENVATTING

Één van de aandachtspunten binnen het vakgebied chemische technologie is de ontwikkeling van chemische reactoren. Continu wordt er gezocht naar nieuwe methoden die de productiviteit kunnen vergroten en de kosten kunnen verlagen, zodat processen effectiever en economischer bedreven kunnen worden. Binnen deze zoektocht wordt gekeken naar de toegepaste apparatuur, materialen, chemicaliën en procescondities. Daarnaast wordt ook de dynamica van de processen zelf bestudeerd. Een aanpak die aan populariteit wint, is het combineren van verschillende technologieën. Hierbij vullen de goede punten van de ene technologie de zwaktes van de andere aan. Een goed voorbeeld hiervan is de membraanreactor. In deze reactor wordt het scheidend vermogen van een membraan gebruikt om een reactie te verbeteren.

Dit proefschrift richt zich op de ontwikkeling van een nieuw type membraanreactor, gebaseerd op zogenaamde “mixed matrix membranes” (MMM). Dit zijn poreuze membranen waarin deeltjes zijn ingekapseld. Dit concept combineert de goede doorstroombaarheid en lage drukval van membranen met de grote diversiteit aan chemische affiniteit en de hoge dichtheid aan functionele groepen van chromatografische deeltjes. De in dit proefschrift toegepaste chromatografische deeltjes hebben van zichzelf een katalytische werking, of worden gebruikt om enzymen te immobiliseren die als katalysator werken.

In Hoofdstuk 2 wordt een introductie gegeven over immobilisatie van enzymen. De nadruk ligt voornamelijk op de verschillende methodes voor immobilisatie en de verschillende soorten dragermaterialen. Daarnaast wordt een kort overzicht van de geschiedenis van “mixed matrix membranes” gegeven.

Hoofdstuk 3 beschrijft het maken van een vlakke film MMM en het optimaliseren voor immobilisatie van trypsine. Het MMM is gemaakt met behulp van fasescheiding, waarbij ethylene vinyl alcohol (EVAL) als polymere matrix is gebruikt en Eupergit® voor de chromatografische deeltjes. Het inbedden van de deeltjes is bereikt door Eupergit® te malen tot deeltjes van 20-40 µm en te dispergeren in de polymeeroplossing. Twee type

Eupergit® deeltjes zijn gebruikt: Eupergit® C en Eupergit® C250L. Deze deeltjes hebben een verschillende dichtheid aan functionele groepen en een verschillende poriegrootte, maar zijn beide geschikt voor het covalent binden van enzymen. De invloed van de manier van inbedden op de functionaliteit van de deeltjes is bestudeerd. De immobilisatiecapaciteit en enzymatische activiteit zijn bepaald voor trypsine in vrije Eupergit® deeltjes (gemalen en ongemalen), zowel in suspensie als in een gepakte kolom. Vervolgens zijn dezelfde testen herhaald voor het MMM. Om de enzymatische activiteit van geïmmobiliseerd trypsine te verhogen, zijn de Eupergit® deeltjes, al voor het malen, chemisch gemodificeerd met ethyleendiamine en glutaaraldehyde. Op het gebied van trypsine activiteit presteert Eupergit® C in alle gevallen beter dan Eupergit® C250L. Verder is bewezen dat de enzymatische activiteit van de deeltjes ten opzichte van een gepakt bed verbetert door deze in een mixed matrix membraan in te bedden. Daarnaast blijkt de chemische modificatie voordelig te zijn; in een MMM met chemisch gemodificeerd Eupergit® C kan een enzymatische activiteit van trypsine bereikt worden die minstens een factor 9 hoger ligt dan bij de andere dragers.

Hoofdstuk 4 beschrijft mixed matrix membranen in holle vezel vorm (MMHV), op basis van EVAL en chemisch gemodificeerde Eupergit® C deeltjes. Deze holle vezels zijn door middel van fasescheiding gesponnen in een nat spinproces. De samenstelling van de gebruikte polymeeroplossingen is gevarieerd om tot een optimale vezelmorfologie te komen. Er is met 2 fracties van het gemalen Eupergit® C gewerkt: deeltjes van 20-40 µm en deeltjes kleiner dan 20 µm. De geproduceerde vezels zijn gebruikt voor immobilisatie van trypsine, en vervolgens is de enzymatische activiteit geëvalueerd. Daarbij is gebleken dat een MMHV beter presteert dan een vlakke film MMM, wat verklaard wordt door een verbeterde stromingsverdeling over de membraanwand. Wat betreft de grootte van de deeltjes is geen significant verschil gevonden tussen de fracties van 20-40 µm en <20 µm. Dit impliceert dat het voordeel van verlaging van deeltjesgrootte niet meer geldt voor deeltjes kleiner dan 20 µm.

Het onderwerp van hoofdstuk 5 is het maken van MMHV's waarin het sterke kation-uitwisselend resin Lewatit® als chromatografisch medium is ingebed. Het polymeer Polyethersulfon (PES) is hierbij gebruikt als matrix materiaal. De gesponnen vezels zijn gebruikt voor de statische immobilisatie van glucose oxidase (GOx) bij verschillende zuurgraad (pH). Voor pH waarden beneden het iso-electrisch punt van dit enzym (pI) verloopt de immobilisatie via electrostatische interacties volgens een adsorptie isotherm van het Langmuir type. Voor pH waarden boven de pI verloopt immobilisatie via hydrofobe interacties. Onder deze laatste omstandigheid wordt een

lagere adsorptiecapaciteit gevonden. De adsorptiecapaciteit in dynamische adsorptietesten ligt vlakbij die van statische metingen. De activiteit van geïmmobiliseerd GOx is geëvalueerd op basis van de conversie van glucose. De resultaten laten zien dat een hogere adsorptiecapaciteit niet overeenkomt met een hogere enzymatische activiteit, wanneer genormeerd wordt op de hoeveelheid geadsorbeerd GOx. Dit gedrag wordt toegekend aan de formatie van GOx multilagen, waarbij de toplaag al het aangevoerde substraat (glucose) omzet, en de onderlagen niet bijdragen aan de enzymatische activiteit.

Tot slot wordt in Hoofdstuk 6 de flexibiliteit van het “mixed matrix membrane” platform geëvalueerd. Met behulp van de in Hoofdstuk 4 ontwikkelde holle vezels is getracht om glucose oxidase covalent te binden. De resultaten laten zien dat deze aanpak mogelijk is en dat het GOx achteraf nog steeds actief is. Wanneer de twee principes voor enzymebinding –covalent binden of immobilisatie met behulp van een sterke kation-uitwisselend resin– vergeleken worden voor de MMHV's, blijkt de laatste aanpak gunstiger voor dit systeem, met een twee maal zo hoge activiteit van het GOx.

ACKNOWLEDGMENTS

After almost five years since I first arrived to Enschede to start my Ph.D., the time has come to (literally) close the book on this research. The moment warrants a sense of accomplishment, but it cannot be completely attributed to me. Many people were fundamental in this personal achievement, whether through direct help and contribution to my work or simply by the indispensable support such a project demands. Here, it is finally the moment to thank those who helped me to reach this point.

First and foremost, I have to thank Matthias Wessling, my promoter, not only for giving me the chance to do this work and having trusted in me, but also for the nudges and pushes that were important for me not to lose track of the fundamental things in the work. Thank you very much Matthias, for the patience and faith you have shown. Without those, it would have been much harder to finished this work.

The second word has to go to Zandrie Borneman, my daily supervisor who, even though still busy with his own Ph.D. at the time of my start, always could find time for discussing some points, give me his precious insights about mechanisms and apply a critical eye to my findings. Zandrie, our many discussions gave a very strong contribution for this thesis, something for which I can only be grateful.

Before I joined the Membrane Technology Group (MTO) in Twente, there were two people who were also important on my course to reach this point. The first was Prof. Dr. Maria Helena Gil, my Polymer Materials professor at the University of Coimbra, who first introduced me to the scientific world of polymers and later gave me the chance to perform my first research with membranes. The second person was Dr. Karl Pflanz, my boss and friend at Sartorius AG (now Sartorius Stedim Biotech), who welcomed me in Göttingen and through whom I ended up discovering the MTO.

As can be read all over this thesis, the materials I used in my work were Mixed Matrix Membranes. I am the latest to use this technology, but for a while the MMM-family was somewhat more extended. Besides Zandrie, there was also Magda Avramescu, who was the “mother” of the MMM concept, did a post-doc within my project and was fundamental in my work.

Magda, without your help, support and suggestions, it is very likely that this thesis would never had been. I cannot thank you enough for your help and am extremely grateful that you accepted to be my paranimf. Another person from whom I learned a great deal, both scientifically and personally, was Saiful. It was my great honor to be one of your paranimfs, and your courage, determination and dedication will always be an example to me. Also Ana Urmenyi was important for my work, especially in the understanding of the behavior of biomolecules at a time when my knowledge of biochemistry was still tangent to zero.

I had two students during this period, Eef and Jelle. It was a pleasure being mentor in your final master assignments. Your work did not feature in the thesis, but it did contribute to a better understanding of the MMM system, fact for which I am grateful. Another person to have contributed with work for the thesis was Erik van de Ven, who performed a few measurements and reduced the experimental load on my last stretch.

I already mentioned one of my paranimfs, but not the other. Maik, it was a pleasure to share the office with you these last years. True, the chicken box might not have been the ideal environment, but it was always nice and fun and you have been (and still are) the ideal office-mate for me. Thank you for being there with me on this day.

Speaking of office mates, I had a few more. First, the occupants of the other chicken-box which, with such thin walls, were as if next to us. First, Jörg and Miriam. Then Matías and Ikenna. Later, still in the Langezijds, also Gor for a couple of months. In the Meander I had Zeynep and Al-Hadidi in my office. Thank you all for putting up with me.

In the group, mention should be made to those who make our lives easier. The first is to Greet, who was always available for any questions concerning bureaucracies and procedures. Also John was always ready to help with any set-up or piece of equipment. Thanks to all the other technicians, Herman (I didn't do it!), Erik R., Lydia (Boe!), Ineke, Marcel, Wika and Jutta (knöbelen?).

Many people in the group contributed for the great atmosphere. Jens, (Professor) Hakan, Can, Matias, Katja and the others who also tended to show up at the sound of "Rauchen!". Dana, it was a pleasure and an honor to be your friend and paranimf. Alisia (hey boss), Jorrit (thanks a lot for the translation of the summary), Bernke, Wilbert, Tymen, Hylke, et al, dank je wel voor de gezellige tijden. One of the nice things in the group were the activities, including the Friday afternoon borrels, Picture of the Month at de

Geus, Bike Tours, Christmas Dinners or sport activities (volleyball, football, swimming, etc).

My life in Enschede took also place outside the group. A good deal of my time was with Arriba, the basketball club of the UT. Thank you all for the nice times (despite two dislocated shoulders and a range of other injuries) I had. Dank jullie wel voor een fantastische tijd.

Also other friends made the time enjoyable. Davide, thanks for having been a great housemate and a good friend. Maybe we could have spent some more time together, but the time we did was always (at the very least) pleasant. Grazie mille per tutti. Staying with italians, also my thanks to Francesca and Cristiano, for the great fun we had together. Some other people with whom I enjoyed nice times: Bas, Monique, Fernando, Socorro, Lourdes, Sandra, Laura, Meritzell, Nina, (both) Hugo, Ana, Miguel, Sigrid, etc, etc, etc. Now, in Maastricht, also to Raša and Mara. Thank you for the support. A very special thank you has to go to Dorota. Thank you very much for having let me into your life and for having been such a good friend during this time. I still miss our coffees.

The support of my friends from Portugal has to appear in here. All the support and faith in me, even from far away, always kept me going and cheerful. Obrigado a todos pelo apoio. I cannot be mentioning all, but I can mention two: Carmen, obrigado por tudo, mais alguma coisa e seja lá o que for mais. Não tenho forma de te agradecer aquilo que tens sido para mim. Mónica, o teu exemplo deu-me sempre um alento extra. Ser teu amigo é um prazer enorme. Ser teu padrinho um orgulho imenso. Muito obrigado às duas e à(s) vossa(s) famílias.

Now, finally, my family. My aunt and my cousins: tia Gabriela, Gó, Célia, Zê, Francisco e Guilherme. Não se escolhe a família, mas eu não escolheria outra se o pudesse. Obrigado por tantas coisas.

To my mother and my sister: Mãe, Ana. O dia chegou e vocês estão aqui. Nada mais poderia pedir. Este livro é vosso e nada mais posso dizer que expresse o que sinto por vocês. Palavras não chegam. Fica só um obrigado do tamanho do mundo pelo vosso amor.

Каћа, волим те највише на свету. Сад и заувек.

